An investigation into the induction of non-associative long-term synaptic depression in the CA1 region of the rat hippocampus *in vitro*.

by

Michael Francis Barry

A thesis submitted for the degree of Doctor of Philosophy
in the University of London
Faculty of Science

Department of Physiology
University College London

March 1997

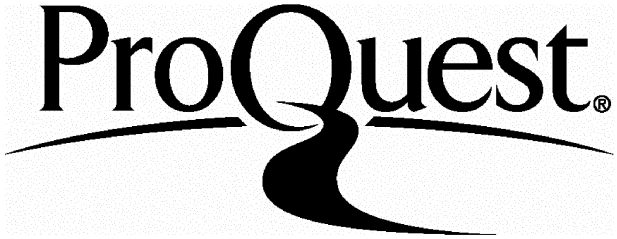

ABSTRACT

Non-associative long-term depression (LTD) is a long-term reduction in the strength of synaptic transmission that occurs at inactive synapses following a period of postsynaptic depolarization. I have investigated the importance of intracellular Ca^{2+} levels in the induction of non-associative LTD in single pyramidal cells in the CA1 region of the rat hippocampus *in vitro*.

Postsynaptic Ca^{2+} entry on depolarization was manipulated by changing the amount of Ca^{2+} in the bathing medium ($[Ca^{2+}]_o$). Following unpaired postsynaptic depolarization, a significant non-associative LTD could be induced in about half of the cells tested when slices were bathed in a lower $[Ca^{2+}]_o$ than normal but not when they were bathed in a higher $[Ca^{2+}]_o$. Postsynaptic depolarization in the presence of the $GABA_A$ receptor antagonist bicuculline, which also affects intracellular Ca^{2+} concentration ($[Ca^{2+}]_i$), failed to induce non-associative LTD in the naïve slice. However postsynaptic depolarization in bicuculline could produce significant non-associative depotentiation of previously potentiated synapses in about half of the cells tested.

To directly measure the rise in $[Ca^{2+}]_i$ following postsynaptic depolarization, cells were filled with the calcium indicator Fura-2. Postsynaptic depolarization applied to cells in bathing media designed to lower postsynaptic calcium entry, resulted in a reduction in the rise of dendritic and somatic $[Ca^{2+}]_i$ compared to in the normal bathing medium in most cases. In many but not all of these cells LTD was also observed.

Although LTD induction occurred with a higher probability when the rise in $[Ca^{2+}]_i$ was experimentally reduced, there was no direct correlation found between the amount of synaptic depression and the magnitude of the $[Ca^{2+}]_i$ rise in the apical dendrite, or the soma ($r^2 = 0{\cdot}18$ and $0{\cdot}02$ respectively). Further experimentation is needed to measure the $[Ca^{2+}]_i$ in the close vicinity of the test synapses in order to clarify the influence $[Ca^{2+}]_i$ has on non-associative LTD induction.

DEDICATION

To Mum and Dad

ACKNOWLEDGMENTS

First and foremost I would like to thank my supervisor Dr Lynn Bindman for her help and patience during my studies. I would also like to thank Dr Richard Vickery for his support and his knowledge of bad Australian music, I had fun! Thanks must also go to the following people in U.C.L.; Professor Mike Spyer, Dr Peter Mobbs, Dr Steven Bolsover and the Dean of Students Mrs Jackie Dyson.

For financial support during my time at U.C.L., I thank the M.R.C., the Graduate School of U.C.L., Mr Martin Butcher (I'm still in the dark as to where that money actually came from), and Dr Sally Page for her unexpected application for an Elliot-Blake Studentship in Physiology on my behalf. Thanks also Lynn for those lab meals, they were much appreciated!

I also owe a great debt to both Dr Tony O'Sullivan and Janice Bell for putting up with my problems for those many hours, and my parents for all the hassle, thanks.

Lynn, for all of the problems we have encountered, I have throughly enjoyed my time in your lab, I could not imagine myself doing anything other than confronting those problems head on and continuing in research, I know you feel the same, thanks again.

TABLE OF CONTENTS

LIST OF FIGURES

LIST OF TABLES

List Of Abbreviations

AA	Arachidonic acid
ABS	Artola, Bröcher & Singer (model of synaptic modification)
ACPD	1S,3R-aminocyclopentate dicarboxylate
ACSF	Artificial cerebrospinal fluid
Ag/AgCl	Silver/silver chloride
AMPA	α-amino-3-hydroxy-5-methyl-4-isoxazolepropionate
ANOVA	Analysis of variance
D-APV	D-2-amino-5-phosphonovalerate
BAPTA	1,2-bis(2-Aminophenoxy)ethane-*N,N,N',N'*-tetraacetic acid
BCM	Bienenstock, Cooper & Munroe (model of synaptic modification)
Bic	Bicuculline
°C	Degrees celsius
$[Ca^{2+}]_i$	Intracellular calcium concentration
$[Ca^{2+}]_o$	Extracellular calcium concentration
CaM-KII	Ca^{2+}/calmodulin-dependent protein kinase II
cAMP	Cyclic adenosine monophosphate
cm	Centimetres
CNQX	6-cyano-2,3-dihydroxy-7-nitroquinoxaline
CsAc	Cæsium acetate
dc	Direct current
EEG	Electroencephalogram
EGTA	Ethylene glycol-bis(aminoethylether) *N,N,N',N'*-tetraacetic acid
EPSP	Excitatory postsynaptic potential
F	Fluorescence
ΔF	Change in fluorescence
g	Gram
GABA	γ-amino-butyric acid
$GABA_A$	γ-amino-butyric acid type A receptor
$GABA_B$	γ-amino-butyric acid type B receptor
Hz	Hertz
IC	Intracellular conditioning
IP_3	Inositol triphosphate
IPSP	Inhibitory postsynaptic potential
KAc	Potassium acetate
KHz	Kilohertz
LFS	Low frequency stimulation
LTD	Long-term depression
LTP	Long-term potentiation
M	Molar
MCPG	(R,S)-α-methyl-4-carboxphenylglycine
mm	Millimetres
μm	Micrometres
nm	Nanometres
ml	Millilitres
mGluRs	Metabotropic glutamate receptors
min	Minutes
mM	Millimolar
μM	Micromolar
mV	Millivolts

MΩ	Megaohms
nA	Nanoampere
NMDA	*N*-methyl-D-aspartate
NO	Nitric oxide
P	Probability
PAF	Platelet-activating factor
PKA	cAMP-dependent protein kinase A
PKC	Protein kinase C
PLA_2	Phospholipase A_2
PLC	Phospholipase C
PP1	Protein phosphatase 1
PP2A	Protein phosphatase 2A
PPF	Paired pulse facilitation
PSP	Postsynaptic potential
R_{in}	Apparent input resistance
rpm	Revolutions per minute
s	Seconds
SEM	Standard error of the mean
STP	Short-term potentiation
TBS	Theta burst stimulation
TEA	Tetraethylammonium
V	Volts
VDCC	Voltage dependent calcium channel
VDCCLTP	Voltage dependent calcium channel dependent long-term potentiation
V_m	Membrane potential
%	Percent

CHAPTER 1

INTRODUCTION

1.1 Long-term changes in synaptic strength.

In the late nineteenth century, biologists had discovered that most mature neurones have lost the capacity to divide. This discovery ruled out models of learning and memory based on the production of new neurones. As a result a new connectionist theory of learning and memory was independently proposed by Tanzi (1893) and Ramon y Cajal (1894) whereby learning involved a strengthening of connections amongst neurons. Since at this time there was no method of directly testing this hypothesis, theoretical advances in the connectionist hypothesis were made following scrutiny of anatomical data. Such an advance was the suggestion that plastic changes occurred at the synapse (Konorski 1948).

The most famous advancement of the connectionist hypothesis was made by the psychologist Donald Hebb (1949) when he suggested that the synaptic modifications involved in learning occurred as a consequence of coincidence between presynaptic and postsynaptic activity. What is now known as Hebb's postulate reads: "When an axon of cell A is near enough to excite cell B and repeatedly or persistently takes part in firing it, some growth process or metabolic change takes place in one or both cells such that A's efficiency as one of the cells firing B, is increased."

Modern neurophysiological investigation into the cellular mechanisms involved in learning and memory stem from the studies of Bliss & Lømo (1973) and Bliss & Gardner-Medwin (1973). Using *in vivo* electrophysiological recording techniques, synaptic strength was measured by field recording electrodes placed in the dentate gyrus of the anaesthetized and the awake rabbit respectively in response to stimulation of the perforant path. The response to test stimulation was shown to increase for hours in the anaesthetized, and days in the awake animal in response to brief high frequency (tetanic) stimulation of the test pathway. This has been subsequently been called long-term potentiation (LTP).

Although LTP has been reported in many brain areas including the rat cerebral cortex (Bindman et al., 1988), the majority of LTP studies has focused on the mammalian hippocampus. The hippocampus is important in memory processing; this has been evident since the discovery that lesions in, or the removal of parts of the hippocampal formation in man severely impairs the ability to lay down new memories

(see Dudai 1989 for review). In addition the transverse hippocampal slice formation is favoured for *in vitro* studies due to its regular laminar axonal and synaptic structure. In the hippocampus LTP has been reported at synapses between the perforant path and dentate gyrus (Bliss & Lømo, 1973; McNaughton et al., 1978), the mossy fibre and CA3 (Alger & Teyler, 1976), and the Schaffer collateral and CA1 (Schwartzkroin & Wester, 1975).

Long-term changes in synaptic strength are not exclusive to mammals or the central nervous system. LTP has been reported in the sympathetic ganglia of the rat (Brown & McAfee, 1982), and bullfrog (Koyano et al., 1985) and in the sensorimotor pathways in aplysia (Walter & Byrne, 1985). A persistent potentiation of synaptic activity has also been described in the intermediate medial hyperstriatum ventrale of birds (Bradley et al., 1991).

Further investigation into this phenomenon, originally termed long-lasting potentiation but now well known as long-term potentiation (LTP), has revealed that in most cases, both pre- and postsynaptic activity are necessary for its induction. This association between the activity of the pre- and postsynaptic elements of the synapse fit well with the theoretical Hebbian synapse.

1.2 The induction of LTP.

The Hebbian nature of LTP induction has been demonstrated in the CA1 region of the hippocampal slice preparation using the intracellular recording technique. Kelso et al., (1986) reported that both pre- and postsynaptic activity in conjunction was necessary for LTP induction. Postsynaptic depolarization alone, achieved by intracellular current injection, did not alter the strength of synaptic transmission, nor did the application of tetanic afferent stimulation during hyperpolarization of the postsynaptic neurone. Only afferent tetanic stimulation paired with postsynaptic depolarization led to LTP induction. LTP induction has now been characterized by three basic properties, that of cooperativity, associativity and input-specificity. The cooperative nature of LTP describes the existence of an induction threshold where tetanic afferent fibre activation at weak intensities fails to induce LTP but the activation of a greater number of afferent fibres with strong tetanic stimulation, results in LTP.
Associativity is analogous to classical conditioning where a weak input can be potentiated when paired with strong tetanic activation to a separate but convergent input. Finally, input-specificity describes the fact that other inputs not active at the time of the tetanus do not express the increase in synaptic strength.

Further investigation has revealed the importance of postsynaptic neurotransmitter receptor subtypes in the induction of LTP. Collingridge et al., (1983) reported the importance of the *N*-methyl-D-aspartate (NMDA) receptor in LTP induction, where addition of the NMDA receptor antagonist DL-2-amino-5-phosphonovalerate (APV) prevented tetanus induced LTP. The NMDA receptor-channel was in turn postulated to underlie the Hebbian nature of LTP induction where, acting as a molecular coincidence detector, the channel opens only in response to presynaptic release of glutamate together with postsynaptic depolarization, which relieves a voltage-dependent Mg^{2+} block (Nowak et al., 1984; Ascher & Nowak, 1988). This facet of NMDA receptor activation can explain the three basic properties of LTP induction (see Bliss & Collingridge, 1993 for review). Weak tetanic stimuli would fail to depolarize the target neurone(s) sufficiently to relieve the voltage dependent Mg^{2+} block of the receptor, hence explaining the cooperative nature of LTP induction. Strong tetanic stimulation at an independent but convergent pathway to a weak stimulus would cause sufficient depolarization to lead to NMDA receptor activation in the weaker pathway, thus explaining associativity. Input specificity is explained since presynaptic activity is needed to release an adequate amount of glutamate to activate NMDA receptors since depolarization alone is insufficient.

In the CA1 region of the hippocampus, low frequency stimulation of the Schaffer collateral-commissural pathway evokes an excitatory postsynaptic potential (EPSP) which is mediated via the activation of the non-NMDA receptors (Neuman et al., 1988; Hestrin et al., 1990). This receptor subtype known as AMPA receptors after the selective ligand for these receptors, α-amino-3-hydroxy-5-methyl-4-isoxazolepropionate (AMPA), is permeable to Na^+ and mediates EPSPs in response to glutamate binding. Following low frequency stimulation of the Schaffer collateral-commissural pathway feed-back and feed-forward inhibitory interneurones are also activated. Interneurones, activated via glutamatergic synapses, release the inhibitory neurotransmitter γ-amino-butyric acid (GABA). Release of GABA from these interneurones triggers inhibitory postsynaptic potentials (IPSPs) via activation of the Cl^- permeable $GABA_A$ receptors on the target cells which in turn repolarize the neurone. During tetanic stimulation these inhibitory circuits are depressed because GABA depresses its own release by an action on $GABA_B$ autoreceptors. This reduction in IPSP activity permits sufficient depolarization to relieve the voltage-dependent Mg^{2+} block and allow sufficient NMDA

receptor activation for the induction of LTP (Davies et al., 1991; Mott & Lewis, 1991). Indeed the addition of $GABA_A$ receptor antagonists has been shown to facilitate LTP induction (Wigström & Gustafsson, 1983).

Theta burst stimulation (TBS) has been reported to induce stable LTP in both the *in vitro* (Larson & Lynch, 1986; Larson et al., 1986) and the *in vivo* preparation (Staubli & Lynch, 1987). TBS consists of short bursts (4 or 5 pulses at 100 Hz) repeated at a 'theta' rhythm (5 Hz) which corresponds to the electroencephalogram (EEG) frequency found in exploring rats (Vanderwolf, 1969; Otto et al., 1991). The stimulation frequencies used during TBS are designed to promote NMDA receptor activation by reducing the effects of inhibitory events in a manner which is thought to occur physiologically. TBS induced LTP has been reported to occlude tetanus-induced LTP (Diamond et al., 1988) and is also blocked by NMDA receptor antagonists (Diamond et al., 1988; Larson & Lynch, 1988).

1.3 The importance of Ca^{2+} in LTP induction.

What is the signal passing through the NMDA channel that triggers LTP induction? Lynch et al. (1983) reported that the induction of LTP could be blocked by the intracellular injection of the Ca^{2+} chelator ethylene glycol-bis(aminoethylether) *N,N,N',N'*-tetraacetic acid (EGTA). This result strongly suggested a role for Ca^{2+} in LTP induction and the NMDA receptor has since been shown to be permeable to Ca^{2+} (Jahr & Stevens, 1987; Mayer & Westbrook 1987; Ascher & Nowak, 1988). Calcium imaging studies in cultured spinal cord neurons and in the CA1 region of the hippocampus have both shown that activation of the NMDA channel can cause significant elevations of intracellular Ca^{2+} (MacDermott et al., 1986 and Regehr & Tank, 1990 respectively). An important finding presented by Malenka et al., (1988) was that elevation of intracellular Ca^{2+} by the photolysis of caged Ca^{2+} induced a form of LTP. Although this first suggested that elevation of postsynaptic Ca^{2+} alone was necessary for LTP induction, low frequency stimulation had continued during the release of intracellular Ca^{2+} therefore the possibility of other factors contributing to LTP induction could not be ruled out. Further evidence was provided by Kullmann et al., (1992) where they showed that a large Ca^{2+} entry which was achieved by postsynaptic depolarization with Cs^+ present in the cell (activating only voltage dependent calcium channels; VDCCs; in the presence of *D*-APV) resulted in short term potentiation (STP) and was only transformed into LTP when test presynaptic activity was applied.

1.4 Calcium-dependent activation of second messengers in LTP induction.

Phosphorylation of ligand-gated ion channels has been suggested by many groups as a possible mechanism for increasing the strength of synaptic plasticity (see Swope et al., 1992 for review). Several serine/threonine protein kinases have been proposed to play a role in regulating the phosphorylation state of these channels. Among these protein kinases, one of the first to be implicated in LTP was protein kinase C, a phospholipid and calcium-dependent kinase. Malenka et al. (1986a) reported that PKC activation by phorbol esters produced a long-lasting enhancement of synaptic responses that prevented further potentiation by high-frequency stimulation. In addition, postsynaptic injection of H-7, a potent, but non-specific blocker of PKC, prevented the induction of LTP in the CA1 region of the hippocampus (Malenka et al., 1989). Further evidence however, has shown that activation of PKC does not modify the sensitivity of the postsynaptic response to iontophoretically applied glutamate (Malenka et al., 1986b) and that PKC activity is not necessary during LTP maintenance (Denny et al., 1990; see reviews by Muller et al., 1992 and Ben-Ari et al., 1992).

The best biochemical candidate to date for the storage mechanism involved in LTP is Ca^{2+}/calmodulin-dependent protein kinase II (CaM-KII), as it is localized at synapses and its known autophosphorylation properties enable it to undergo long-term modification (for review see Lisman, 1994). Ca^{2+}-dependent phosphorylation of this kinase switches the enzyme into a state in which autophosphorylation occurs in a Ca^{2+}-independent manner. This mechanism would maintain CaM-KII activity for long periods after the initial Ca^{2+} signal had subsided. Indeed the activity of CaM-KII has been reported to be enhanced for long periods of time following LTP induction in a calcium independent manner (Fukunaga et al., 1993). CaM-KII has also been shown to be sufficient in enhancing the activity of the AMPA channels involved in synaptic transmission (McGlade-McCulloch et al., 1993) and knockout mice lacking α-CaM-KII have deficient hippocampal LTP and have inhibited spatial learning (Silva et al., 1992a and 1992b).

Other Ca^{2+}-dependent enzymes that have been shown to play a role in LTP induction include tyrosine kinases (O'Dell et al., 1991a), the protease calpain (Oliver et al., 1989), and phosphatases such as calcineurin (Halpain & Greengard, 1990). There is also evidence suggesting that activation of cAMP-dependent protein kinase A (PKA), enhances the responses mediated by AMPA receptors (Greengard et al., 1991; Lu-Yang et al., 1991).

1.5 The role of metabotropic glutamate receptors in LTP induction.

Glutamate acts on both ionotropic and metabotropic glutamate receptors (mGluRs). A fundamental role for mGluRs in LTP induction in the CA1 region of the hippocampus was suggested by the finding that the application of the specific mGluR agonist *trans*-ACPD (1S,3R-aminocyclopentate dicarboxylate) induces a slowly developing synaptic enhancement which occludes subsequent LTP induction (Bortolotto & Collingridge, 1993). ACPD has also been shown to augment tetanus induced LTP (McGuinness et al., 1991) and convert STP into LTP (Otani & Ben-Ari, 1991). Metabotropic glutamate receptors are coupled through G-proteins to phosphoinositide specific phospholipase C (PLC), phospholipase A_2 (PLA_2) and adenylate cyclase (AC). Activation of PLC can produce inositol triphosphate (IP_3) which will induce Ca^{2+} release from intracellular stores. Bortolotto & Collingridge (1993) suggested that this Ca^{2+} rise along with the additional activation of protein kinases by adenosine monophosphate (cAMP) via AC, could be responsible for the enhancement in synaptic strength.

Use of the specific mGluR antagonist (R,S)-α-methyl-4-carboxphenylglycine (MCPG) has also been shown to prevent LTP induction in the CA1 (Bashir et al., 1993; O'Connor et al., 1994). In addition experiments performed in the CA1 region of slices removed from mutant mice lacking the gene encoding mGluR1 show LTP to be substantially reduced although basal synaptic transmission was normal (Aiba et al., 1994). The finding that mGluR activation is necessary for LTP induction is not universal. Several groups have reported MCPG to be ineffective preventing both tetanus induced LTP (Chinestra et al., 1993; Manzoni et al., 1994; Selig et al., 1995b) and TBS induced LTP (Selig et al., 1995b; Brown et al., 1994).

These discrepancies have been proposed (see review by Bear & Malenka, 1994) to be as a result of the ability of mGluRs to act as a molecular switch (Bortolotto et al., 1994). In the report by Bortolotto et al., (1994) the need for mGluR activation was shown to be necessary for LTP induction in the naïve slice, but was not necessary for subsequent LTP induction. The failure of MCPG to block the induction of LTP during the second tetanus could be reversed by the application of low frequency (1 Hz) stimulation between tetani. Although this novel behaviour of mGluRs could explain the differences in results from some laboratories, Selig et al., (1995b) reported MCPG to have no effect on LTP induction even after low frequency stimulation.

1.6 The locus of LTP expression.

An increase in the postsynaptic response occurring at potentiated synapses could be due to a number of possibilities. There could be a postsynaptic change, where there is for example an increase in the number or sensitivity of postsynaptic glutamate receptors. An alternative is that there is an increase in the amount of glutamate release, a presynaptic change. It is also possible that there is a combination of both pre- and postsynaptic changes. Additionally there may be either a morphological change in the synapse or an alteration in the characteristics of glutamate uptake. Most of the research to date has focused on the pre- versus postsynaptic locus of synaptic strengthening.

Evidence for a postsynaptic change that occurs during LTP, include experiments in which the postsynaptic responsiveness to iontophoresed quisqualate, a glutamate analogue, was increased following LTP induction (Davies et al., 1989). If it is assumed both AMPA and NMDA receptor responses are present postsynaptically, a similar increase in both responses to their respective agonist following LTP induction, would favour a preseynaptic locus of LTP, but an increase in only AMPA or NMDA responses would suggest a postsynaptic site of change. This latter scenario has been reported by both Kauer et al., (1988) and Muller & Lynch (1988) but has been somewhat undermined by the finding that NMDA receptor mediated synaptic transmission can also exhibit LTP (Bashir et al., 1991; Xie et al., 1992). More recently, evidence of the existence of silent synapses has added weight to a postsynaptic locus for LTP expression. Liao et al., (1995) followed by Isaac et al., (1995) reported that using minimal stimulation, NMDA responses could be induced in the absence of AMPA-mediated synaptic responses. These synapses would therefore be silent during synaptic transmission at normal resting potentials. Following the induction of LTP, new AMPA mediated responses were detected at these synapses. These studies suggest that following LTP induction, either new AMPA receptors are inserted into the postsynaptic membrane, or that there is a modification of AMPA receptors that were electrophysiologically silent prior to LTP induction.

The possibility that there is an increase in presynaptic glutamate release following LTP induction was first proposed by Skrede & Malthe-Sorenssen (1981) and Dolphin et al., (1982), from experiments in which they observed an increase in the overflow of radiolabelled L-glutamate measured following LTP induction *in vivo*. An increase in endogenous glutamate collected via a push-pull cannula after LTP induction in the dentate region of the hippocampus *in vivo* has also been reported by Bliss et al., (1986). In addition, in a recent study by Kullmann et al. (1996), evidence was presented that

tetanic LTP is associated with an increased rate of decay of the NMDA receptor-mediated signal in the presence of the use-dependent blocker MK-801, implying an increase in glutamate release.

Other methods of investigating presynaptic changes in LTP expression have included observing changes in paired pulse facilitation (PPF). PPF in the CA1 region of the hippocampus is seen as a facilitation of the second response elicited by weak paired stimuli separated by intervals of approximately 50 ms. Evidence suggests that PPF is mediated via presynaptic mechanisms, since manoeuvres that increase the probability of transmitter release such as raised Ca^{2+} in the bathing medium, cause a decrease in PPF whereas antagonism of postsynaptic receptors has no effect (Manabe et al., 1993). Many investigators have reported PPF to be unaffected following LTP induction (for example see Manabe et al., 1993). However this has been explained by other groups to be the effect of averaging across many experiments since larger stimulus strengths can result in paired pulse depression due to the increasing involvement of inhibitory interneurones. Schulz et al., (1994) reported that a large PPF prior to LTP induction was reduced following synaptic strengthening and vice versa, therefore implicating presynaptic mechanisms in the maintenance of LTP.

Many studies investigating the locus of synaptic change have used quantal analysis. This form of investigation utilizes the quantal hypothesis proposed by del Castillo & Katz (1954) for the synapses at the neuromuscular junction. The quantal theory states that the mean postsynaptic current (**M**) is a function of the amplitude of the postsynaptic potential (**a**), the number of presynaptic release sites (**N**) and the probability of release from a release site (**p**). Assuming that **a** is the same for any one of N quanta, and since the fluctuations in release follow binomial statistics, it is possible to calculate the relationship between $\mathbf{M}^2$ and its coefficient of variance (σ^2) which is dependent upon only **N** and **p** which are presynaptic in origin. Unfortunately, using this technique a clear picture has failed to emerge. There have been reports of a purely presynaptic locus (Voronin, 1983; Bekkers & Stevens, 1990), some groups finding a purely postsynaptic locus (Foster & McNaughton, 1991) and yet other investigators finding a combination of both pre- and postsynaptic changes responsible for LTP expression (Kullmann & Nicoll, 1992; Larkman et al., 1992). There may be a number of reasons for the discrepancies in the conclusions following the use of quantal analysis including varying experimental techniques and different assumptions being applied when adapting a simple quantal release system to complex central nervous neurons. Edwards (1995) has

attempted to explain some of the diferences by theorizing that LTP may produce a gradual developing division of synapses.

1.7 Retrograde signals.

As induction of LTP has been shown to be postsynaptic in origin, a retrograde signal has been proposed to trigger increased transmitter release from the presynaptic terminal (Bliss et al., 1986). For a messenger to accomplish this task it must be either permeable to, or released from postsynaptic neurons, diffuse across synapses, and either permeate presynaptic membranes or interact with presynaptic receptors in order to activate biochemical changes that alter the release characteristics of the presynaptic terminal. A prime candidate for a retrograde messenger in LTP is nitric oxide (NO). NO is a freely diffusible, membrane permeable gas that is highly reactive with a half-life of several seconds (for review see Moncada et al., 1991).

Since the discovery that NMDA receptor activation induced the release of a factor that has the characteristics of NO (Garthwaite et al., 1988), several groups have shown LTP in the CA1 to be blocked by the application of various NO synthase inhibitors and by haemoglobin which avidly binds free NO (O'Dell et al., 1991b; Bohme et al., 1991; Schuman & Madison, 1991; Haley et al; 1992). The reports that NO increases the frequency of miniature EPSCs (O'Dell et al., 1991b) is blocked by haemoglobin (O'Dell et al., 1991b; Schuman & Madison, 1991; Haley et al; 1992), which would be restricted to the extracellular space, and is blocked by postsynaptic application of NO synthase inhibitors (O'Dell et al., 1991b; Schuman & Madison, 1991) all add weight to the argument that NO is released from the postsynaptic cell and is acting presynaptically. In a report by Schuman & Madison (1994), induction of LTP in one cell by repeated pairing of low frequency stimulation with postsynaptic depolarization resulted in potentiated responses in that cell as well as a nearby cell whose dendritic arbors overlapped the paired cell. In contrast, recording from a second cell that was a greater distance away and had no detectable dendritic overlap, no LTP was seen. Postsynaptic injection of a NO synthase inhibitor into the paired cell blocked LTP induction in that and the nearby cell.

The role that NO plays in synaptic transmission and synaptic plasticity is by no means clear, indeed several investigators have found that NO synthase inhibitors block LTP under some circumstances but not others (see Hawkins et al., 1994 for review).

Both Gribkoff & Lum-ragan (1992) and Chetkovitch et al., (1993) report that NO synthase inhibitors block LTP by weak but not strong tetanic stimulation. In contrast Kato & Zorumski (1993) reported that sub-threshold tetani induced LTP in the presence of NO synthase inhibitors due to an decrease in NMDA responses by NO.

Another candidate for the role of a retrograde messenger in LTP is the membrane permeable compound arachidonic acid (AA). Inhibitors of lipoxygenase and PLA_2, enzymes involved in the production of AA have been shown to block LTP in both the CA1 (O' Dell et al., 1991b) and dentate gyrus region of the hippocampus (Lynch et al., 1989). Although AA in itself has been reported by some groups to have no effect on synaptic transmission (O'Dell et al., 1991b), others have reported that AA causes a synaptic enhancement that is slow to develop (Williams et al., 1989; Drapeau et al., 1990). Since AA only produces a delayed enhancement of synaptic strength, interest has waned over its role as a fast retrograde messenger. There have however been reports of another PLA_2 metabolite, platelet-activating factor (PAF) fulfilling this role. Kato et al. (1994) reported that presynaptic activity paired with the application of the PAF analogue MC-PAF, induced a synaptic enhancement within 5 min in the presence of NMDA receptor antagonists, in addition to blocking LTP induction by inhibitors of PAF receptors.

1.8 Other methods of LTP induction.

There have been many different methods used to induce LTP in the mammalian brain which have shed some light on the nature of LTP. At least two papers have suggested that presynaptic activity is not necessary for LTP induction. Cormier et al. (1993) reported that LTP could be induced in the CA1 region of the hippocampus by the iontophoretic application of glutamate in the absence of evoked presynaptic activity. LTP induced in this manner partly occluded tetanus induced LTP and was NMDA receptor-dependent. As well as being blocked by the intracellular application of the Ca^{2+} chelator EGTA, the potentiation was also induced following glutamate application in the presence of adenosine which reversibly reduces presynaptic release. These results imply that although glutamate action on postsynaptic receptors is necessary for LTP, presynaptic activity is not required. This finding may be important in interpreting the results of experiments investigating the role of retrograde messengers, where unpaired postsynaptic activation can lead to LTP at inactive presynaptic terminals (Kuhnt et al., 1994; Volgushev et al., 1994).

In a separate study by Neveu & Zucker (1996), LTP (and LTD) was induced in the absence of presynaptic activity by the photolytic release of Ca^{2+} from the caged Ca^{2+} compound Nitr-5. Prior tetanic induction of LTP (or LTD) was shown to occlude the potentiation (and depression) induced by the intracellular release of Ca^{2+}. This work suggests that under certain experimental conditions, LTP can be induced solely by a postsynaptic rise in $[Ca^{2+}]_i$, without the activation of postsynaptic receptors. The induction of LTP under the conditions set by Neveu & Zucker (1996) and Cormier et al. (1993) is in contrast to other studies in which activation of postsynaptic receptors was necessary for LTP induction. In particular Kullmann et al., (1992) reported that unpaired postsynaptic depolarization and activation of VDCCs (in the presence of D-APV) was insufficient for LTP induction. Only when paired with presynaptic test shocks and NMDA receptor activation did postsynaptic depolarization result in LTP.

As we have discussed (see Section 1.2), the role of the NMDA receptor is that of a molecular coincidence detector which underlies the Hebbian nature of LTP in the hippocampus. However, NMDA receptor-independent LTP has been described, particularly at the mossy fibre-CA3 synapse (see Johnston et al., 1992; Nicoll & Malenka, 1995 for review) but also in the CA1 region. Grover & Teyler (1990; 1992) have shown that high frequency stimulation of the Schaffer collateral-commisural pathway (200 as opposed to 100 Hz) results in LTP even in the presence of the NMDA receptor-antagonist D-APV. This form of LTP was blocked by nifedipine, a blocker of L-type VDCCs and has been termed VDCCLTP (see Teyler et al., 1994 for review). There are reported differences between LTP and VDCCLTP, which include differences in the kinetics of the expression of the potentiated response (VDCCLTP requires 20-30 min to peak), and the fact that once expression of VDCCLTP is established in one pathway, potentiation in a second independent pathway is blocked (termed preclusion).

The ability to induce LTP via activation of VDCCs has also been reported in experiments when applying the drug tetraethylammonium (TEA) to the bathing medium (Aniksztejn & Ben-Ari, 1991). TEA block of K^+ conductances causes a reversible increase in presynaptic activity, broadening of action potentials and Ca^{2+} entry through VDCCs. The potentiation seen following TEA application is VDCC-dependent (Huber et al., 1995; Huang & Malenka 1993), and has been shown to be partially (Huber et al., 1995) or totally NMDA receptor independent (Aniksztejn & Ben-Ari, 1991; Huang & Malenka 1993).

All of the experimental manoeuvres described above have demonstrated that the critical step in LTP induction is a rise of [Ca^{2+}] within the postsynaptic cell. Although NMDA receptor activation is normally very important in this process, these studies suggest that the entry of Ca^{2+} through the NMDA receptor is not critical. Indeed in a recent study in the dorsal horn of the spinal cord preparation, LTP of miniature EPSCs has been reported by activation of Ca^{2+}-permeable AMPA receptors (Gu et al., 1996).

1.9 Long-term depression.

To date there have been several types of long-term depression (LTD) described in the mammalian brain. Figure 1.9i illustrates schematically the main forms of LTD studied today along with the two most common forms of LTP already described, that of homosynaptic (tetanus induced) and associative LTP.

Cerebellar LTD is analogous to associative LTP since it is induced by a pairing protocol. First described by Ito et al., (1982) it can be induced by repetitively stimulating parallel and climbing fibre inputs onto cerebellar Purkinje neurones at low frequency (1-4 Hz) for a period of 4-6 min. This procedure results in a long-term reduction of the parallel fibre-Purkinje cell response. This form of plasticity, which has been extensively studied (reviewed by Linden, 1994 and Linden & Connor, 1995), requires an increase in postsynaptic calcium, induced by climbing fibre activation and activation of VDCCs, and the activation of postsynaptic mGluRs via parallel fibre activation. There has now been research that suggests that parallel fibre activation is necessary for the production of nitric oxide, which acting in an anterograde manner is necessary for cerebellar LTD induction (Lev-Ram et al., 1995).

In the CA1 region of the hippocampus, an associative form of LTD has been reported following an anti-correlation procedure where a strong conditioning input is applied out of phase with a weak test input, which is then subject to synaptic depression (Stanton & Sejnowski, 1989). This type of LTD was shown to be NMDA receptor-independent and was reproduced by the pairing of intracellular hyperpolarization with the application of the test stimulus (Stanton & Sejnowski, 1989). To date several groups have failed to reproduce the results of Stanton & Sejnowski, (1989), and have questioned the existence of this form of synaptic plasticity in the hippocampus (Paulsen et al., 1993; Kerr & Abraham, 1993). Stanton (1996), explains the differences in results by the fact that prior to conditioning, in the initial study by Stanton & Sejnowski, (1989), there was a period of low frequency afferent stimulation which may have altered the

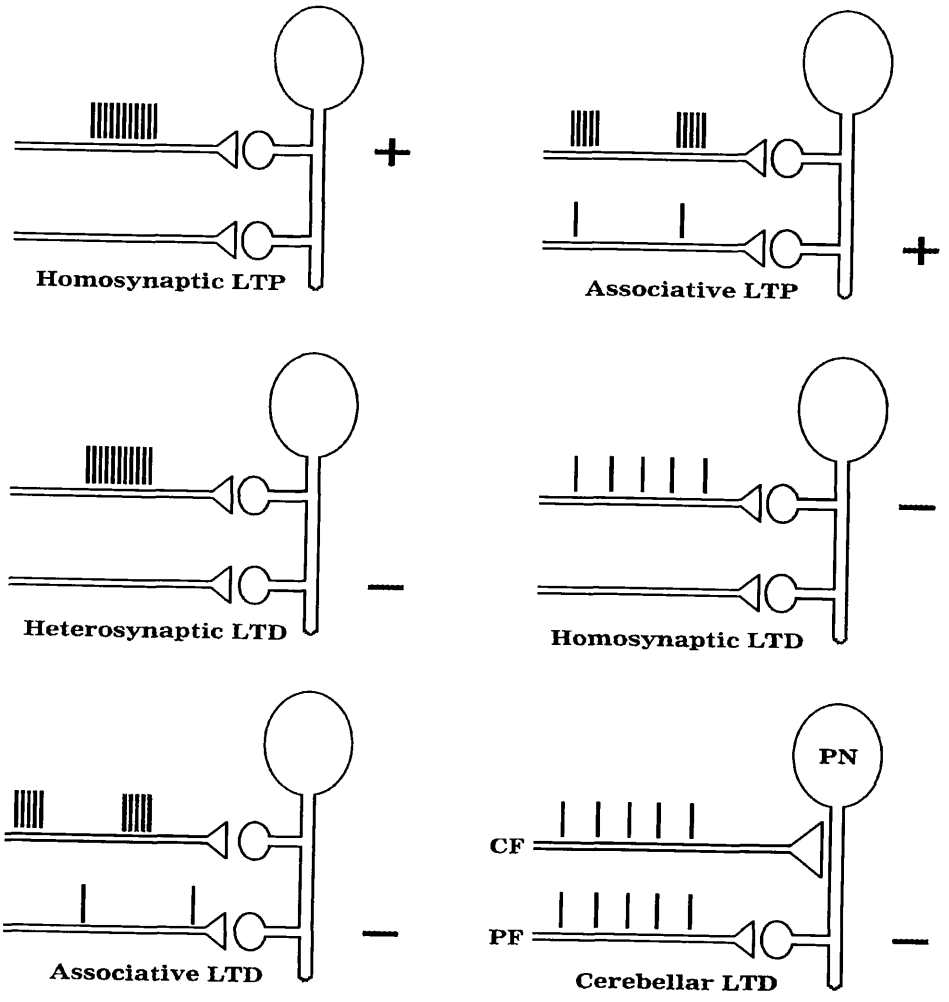

FIGURE 1.9i: The multiple forms of synaptic plasticity in the mammalian brain.

Schematic of the various types of synaptic plasticity in the brain and how they are induced. Vertical bars indicate applied afferent stimulation at either high (a group of bars) or low (single bars) frequency. + and – signs indicate the direction and location of the relevant alteration in synaptic strength. All are representative of the Schaffer commisural-collateral to CA1 synapse except in the case of cerebellar LTD where CF indicates climbing fibres, PF indicates parallel fibres, and PN indicates a Purkinje Neurone.

Figure taken from Linden & Connor (1995).

threshold for the induction of associative LTD in this preparation. This ability of prior synaptic stimulation to alter the threshold for subsequent LTD (or LTP) induction is known as priming, and has been reported to occur in the CA1 (Wexler & Stanton 1993)

In a separate study, Debanne et al. (1994) reported the induction of associative LTD in the CA1 by the asynchronous pairing of presynaptic activity and postsynaptic depolarization. This form of associative LTD was NMDA receptor-dependent and was also dependent on the interval between postsynaptic depolarization and presynaptic activity, such that with a 400 ms delay, LTD was seen, but increasing the interval to 800 ms prevented LTD induction. Debanne et al., (1994) also failed to induce LTD when pairing presynaptic activity with postsynaptic hyperpolarization. In a review of associative LTD in the hippocampus by Debanne & Thompson (1996), it is suggested that the association between pre- and postsynaptic activity which gives rise to LTD probably results in the additive interaction between a VDCC influx of Ca^{2+} and a synaptically activated NMDA receptor-mediated Ca^{2+} influx. This Ca^{2+} influx is below that which would be achieved by directly pairing pre- and postsynaptic activity (which would induce LTP), and is at a level sufficient for LTD induction.

1.10 The induction of homosynaptic LTD.

Homosynaptic LTD is induced by prolonged low frequency stimulation (usually 1 Hz for 10 min) of afferent fibres and results in a depression that is confined to that set of fibres. This form of depression was first witnessed by Dunwiddie & Lynch (1978), following the application of 100 pulses given at 1 Hz (low frequency stimulation: LFS) to the Schaffer collateral fibres in the hippocampal slice preparation, although the depression was only monitored for minutes following conditioning. Recent investigations of homosynaptic LTD stem from the studies by Dudek & Bear (1992) and Mulkey & Malenka (1992), who demonstrated that the administration of 900 pulses at 1 Hz reliably induced a persistent and input specific LTD. This form of depression was shown by these investigators to be saturable, reversible following high frequency stimulation and NMDA receptor-dependent. In addition, homosynaptic LTD was blocked by postsynaptic hyperpolarization, and by the postsynaptic application of Ca^{2+} chelators.

Homosynaptic LTD is thought to be induced as a consequence of a postsynaptic increase in $[Ca^{2+}]$, but at a lower level than when high frequency stimulation is applied (see Artola & Singer 1993). This has been demonstrated experimentally by the

application of high frequency stimulation (50 to 100 Hz) in conjunction with some treatment that limits, but does not eliminate postsynaptic depolarization (see Malenka & Nicoll 1993, for review). Artola et al., (1990) recording from cells in the visual cortex reported that the application of tetanic stimulation (50 Hz) to cells with a hyperpolarized membrane potential resulted in no change in synaptic strength. Following increasing amounts of depolarizing current through the recording electrode during the conditioning period, tetanic stimulation was shown to induce first LTD and then LTP. Why should the extent of postsynaptic depolarization affect the direction of synaptic plasticity? Since there are voltage-dependent ion channels in the postsynaptic membrane, and homosynaptic LTP and LTD are Ca^{2+} dependent, it is thought that increasing postsynaptic hyperpolarization may be limiting the entry of Ca^{2+} into the postsynaptic cell on afferent stimulation. This has been shown to be the case by several groups in various brain regions whereby tetanic stimulation which gave rise to LTP would produce LTD with the partial block of NMDA receptors by D-APV (Cummings et al. 1996 in the CA1; Kato 1993 in the visual cortex; Hirsch & Crepel 1991 in the prefrontal cortex).

The induction of homosynaptic LTD has been reported to require the activation of L-type VDCCs in combination with mGluR activation (Bolshakov & Siegelbaum, 1994). In a separate report, pharmacological activation of mGluRs have been shown to induce homosynaptic LTD independently of postsynaptic depolarization in the dentate gyrus (O'Mara et al., 1995). Kato (1993) also describes how homosynaptic LTD can be induced in the visual cortex by the application of a mGluR agonist, and further reported how mGluR activation resulted in Ca^{2+} release from intracellular stores via the intracellular second messenger IP_3.

The induction of homosynaptic LTD has not been without some controversy as several groups have failed to reproduce the phenomenon. Errington et al., (1995), showed in the *in vivo* preparation that LFS failed to induce LTD in the dentate gyrus of both young and mature rats, but is seen in the CA1 in very young animals only. This age dependency of homosynaptic LTD has also been reported in the *in vitro* preparation where LTD in slices from older animals is either small (Dudek & Bear 1993) or absent (Wagner & Alger 1995) following LFS. Indeed young animals were used in the initial studies investigating homosynaptic LTD (Dudek & Bear 1992; Mulkey & Malenka 1992). The finding that induction of homosynaptic LTD was possible in slices from mature animals when in presence of the $GABA_A$ receptor antagonist bicuculline, may

explain these results since it is known that inhibitory connections in the hippocampus develop later than excitatory ones (Wagner & Alger 1995).

1.11 The induction of heterosynaptic LTD.

Heterosynaptic LTD was the first form of LTD described in the mammalian brain. It is expressed in a test pathway following an LTP-inducing afferent tetanization of a pathway independent of the inactive test pathway, both synapsing on the same population of cells. Heterosynaptic LTD has been observed in CA1 (Lynch et al., 1977; Dunwiddie & Lynch, 1978; Abraham & Wickens, 1991; Scanziani et al., 1996), CA3 (Bradler & Barrionuevo, 1989), and the dentate gyrus (Levy & Steward, 1979; Abraham & Goddard, 1983; Christie & Abraham, 1992).

However, in the CA1 region of the hippocampus, many groups used the same induction protocol but failed to elicit heterosynaptic LTD (Schwartzkroin & Wester 1975; Andersen et al., 1977) or found only short term depression (Alger et al., 1978; Sastry et al., 1984; Bashir & Collingridge 1992; Grover & Teyler 1992; Paulsen et al., 1993). Heterosynaptic LTD has been more extensively researched in the perforant path-dentate gyrus synapse in the hippocampus where the phenomenon has been shown to be long lasting (weeks in the *in vivo* preparation, Krug et al., 1985), was saturable upon repeated stimulation (Levy & Steward 1983) and was reversed by LTP induction (Abraham & Goddard 1983; Levy & Steward 1983). In a report by Scanziani et al., (1996) heterosynaptic LTD in the CA1 region of the hippocampus was shown to be blocked by bath application of the NMDA receptor antagonist D-APV, but was not blocked by the use dependent block of NMDA receptors in the test pathway by the antagonist MK-801. This result shows that heterosynaptic LTD induction does not require any presynaptic activity at the test synapses. Scanziani et al. (1996) also show heterosynaptic LTD to be independent of L-type VDCC activation and to be enhanced by the intracellular application of the Ca^{2+} chelator 1,2-bis(2-Aminophenoxy)ethane-*N,N,N',N'*-tetraacetic acid (BAPTA). This last finding is somewhat at odds with the observation, also by Scanziani et al. (1996), that prior induction of homosynaptic LTD occludes heterosynaptic LTD induction since the induction of homosynaptic LTD is blocked by postsynaptic BAPTA application (Mulkey & Malenka 1992). Scanziani et al., (1996) suggest the presence of an intercellular messenger as a trigger for heterosynaptic LTD induction, but do not rule out a role for calcium. This is perhaps wise since in the dentate gyrus *in vivo*, heterosynaptic LTD has been shown to be

blocked by L-type VDCCs and enhanced by the L-type VDCC agonist BAY-K8644 (Christie & Abraham 1994).

1.12 Postsynaptic induction of non-associative LTD.

As described above, heterosynaptic LTD may be expressed at synapses that are inactive while postsynaptic activity is produced by tetanization of a separate but convergent pathway. Replacing tetanization of an afferent pathway with antidromic stimulation or by direct postsynaptic depolarization can mimic heterosynaptic LTD and is known as non-associative LTD. Induction of non-associative LTD by antidromic tetanization was first reported by Pockett & Lippold (1986). In these experiments field EPSPs recorded from the CA1 region of the hippocampal slice preparation were transiently blocked with the application of a bathing medium containing a high concentration of Mg^{2+}. Without antidromic stimulation, washout of the medium containing a raised [Mg^{2+}] led to a return of the test response to control levels. However, following washout of the medium after an antidromic tetanus, the test response did not fully recover and plateaued at a new depressed level. This form of conditioning was repeated by Pockett et al. (1990), recording from individual CA1 neurons. Pockett et al. (1990) also reported the induction of non-associative LTD in some cells following antidromic tetanization (without afferent stimulation) in a normal bathing medium, although LTP was seen in other cells following this procedure.

The involvement of VDCCs in non-associative LTD has been demonstrated by Wickens & Abraham (1991). As with the induction of heterosynaptic LTD by afferent tetanization of a separate pathway in the dentate gyrus, non-associative LTD induced by antidromic stimulation in the CA1 is blocked by L-type VDCC antagonists and is enhanced by VDCC agonists. In addition non-associative LTD induced by voltage pulses applied to CA1 pyramidal neurons is blocked by L-type VDCC antagonists and by the postsynaptic application of BAPTA (Cummings et al., 1996).

In the experiments described in this thesis postsynaptic activity was achieved by the injection of positive current through the recording electrode which was impaled in a single CA1 pyramidal neurone. Action potentials elicited by somatic depolarization have been shown to back-propagate along the apical dendrite and activate VDCCs triggering dendritic calcium transients (Markram et al., 1995; Spruston et al., 1995). In my study, experimental manoeuvres were designed to increase or decrease calcium influx on postsynaptic depolarization in order to investigate the conditions in which non-

associative LTD could be induced. Some of the findings included in this study, including the observation that non-associative LTD can be induced by postsynaptic depolarization under conditions designed to limit postsynaptic Ca^{2+} entry have been published (Barry et al., 1996a and c).

1.13 The role of calcium in LTD induction.

With the exception of the results of Scanziani et al., (1996) in which postsynaptic injection of BAPTA did not block heterosynaptic LTD, most other investigations into long-term depression in the CA1 region of the hippocampus have reported a requirement for postsynaptic calcium in its induction. Experimental evidence as we have already discussed suggest that the induction of homosynaptic LTD is facilitated by experimental protocols designed to limit postsynaptic calcium entry. This has been achieved by either lowering the frequency of afferent stimulation (LFS; Dudek & Bear 1992) or by a partial block of NMDA receptors during an afferent tetanus (Cummings et al., 1996; see Artola & Singer, 1993 and Teyler et al., 1994 for review).

The concept that it is the magnitude of the rise in postsynaptic $[Ca^{2+}]$ on conditioning that determines whether synaptic strength is increased or decreased was originally proposed by Lisman (1989). Large Ca^{2+} rises through the NMDA receptor channels during a high frequency afferent stimulation would preferentially activate kinases, leading to LTP (see Section 1.4), whereas moderate rises in Ca^{2+} would activate phosphatases that lead to contribute to LTD. Lisman (1989) proposed that the dephosphorylation of CaM-KII by protein phosphatase 1 (PP1) and protein phosphatase 2A (PP2A) is a requirement for the reduction of synaptic strength. Mulkey et al. (1993) reported that the extracellular application of okadaic acid or calyculin A, two inhibitors of PP1 and PP2A did indeed prevent induction of homosynaptic LTD. PP1 and PP2A are not directly influenced by calcium concentration, but PP1 has been reported to be activated via a biochemical cascade which is triggered by low postsynaptic levels of calcium. Mulkey et al. (1994), reported that inhibitors of calcineurin blocked the induction of LTD but not LTP. Calcineurin has a much higher affinity for calcium-calmodulin than CaM-KII, and may be activated by lower postsynaptic calcium concentrations (see Lisman 1989). Also, activation of calcineurin will dephosphorylate inhibitor-1, which when phosphorylated binds to PP1 rendering the phosphatase inactive. Indeed Mulkey et al. (1994) also demonstrated that loading cells with phosphorylated inhibitor-1 via a patch pipette blocked the induction of homosynaptic LTD by LFS.

1.14 LTD expression.

In contrast to the many reports investigating the locus of LTP expression, there have been relatively few studies examining the locus of LTD expression. In common with the studies on LTP expression, is the evidence for both pre- and postsynaptic mechanisms involved in the expression of LTD.

Bolshakov & Siegelbaum (1994) using a quantal analysis technique (see Section 1.6) reported that the induction of homosynaptic LTD was accompanied by a large change in M^2/σ^2 without any significant change in the amplitude of spontaneous EPSCs, which strongly suggested a presynaptic locus for LTD expression. Evidence has also been provided which suggests that the activation of NO may have a role in the induction of LTD. Both the application of NO synthase inhibitors and haemoglobin have been shown to significantly reduce the extent of synaptic depression following the application of LFS (Izumi & Zorumski 1993).

Selig et al. (1995a) using a quantal analysis technique similar to that used by Bolshakov & Siegelbaum (1994) reported that LFS induced LTD of responses mediated by AMPA receptors was accompanied by a change in M^2/σ^2, but that LTD of responses mediated by NMDA receptors was not. Selig et al. (1995a) also reported that the application of brief bursts of afferent stimulationation (10 Hz for 10 sec applied 6 times) can depress NMDA receptor responses without affecting AMPA mediated responses. On the basis of these findings, Selig et al. (1995a) conclude that there are different mechanisms that underlie the depression of both the NMDA and AMPA receptor mediated responses which are most probably postsynaptic in nature. In a study by Vickery & Bindman (1997), a long-lasting decrease in the response to iontophoretically applied AMPA was observed following non-associative postsynaptic activity in single CA1 neurones. Although the depression of AMPA responses were not accompanied by a change in the size of intracellularly recorded EPSPs, unpaired postsynaptic depolarization, similar to that used by Vickery & Bindman (1997) has been reported to induce a non-associative depotentiation of synaptic strength in the CA1 under some conditions (Barry et al., 1996b). The results of Vickery & Bindman do therefore suggest a postsynaptic locus for the phenomenon of non-associative LTD.

1.15 Depotentiation.

An activity dependent down regulation of potentiated synaptic responses has been put forward as a mechanism that would prevent saturation of potentiated synapses, since

saturation would prevent further increases. Barrionuevo et al. (1980) were the first group to witness a long-term depotentiation in the hippocampus *in vivo*, induced by repetitive LFS (1 Hz), a stimulus which they found was ineffective at depressing naïve synapses. The ability of LFS to induce depotentiation but not homosynaptic LTD has also been reported by Fujii et al., (1991) and can be explained by the inability of LFS to induce LTD in preparations from older animals (Dudek & Bear, 1993; Wagner & Alger, 1995).

The inability of LFS to induce LTD in older animals might suggest that LTD and depotentiation are distinct phenomena, or alternatively, that in older animals the synapses are in a maximally depressed state. This second alternative is argued against by the work of Wagner & Alger (1995) who reported that repeated LFS following LTP induction will eventually lower the synaptic strength below that of pre-LTP levels, where LFS in the naïve slice has no effect.

A number of laboratories using LFS (1 to 5 Hz) have since reported that depotentiation is synapse specific (Staubli & Lynch, 1990), reversible, and long-lasting (Staubli & Lynch, 1990; Dudek & Bear, 1993; Bashir & Collingridge, 1994; O'Dell & Kandel, 1994; Staubli & Chun, 1996). There is some discrepancy as to whether the phenomenon is NMDA receptor-dependent (Fujii et al., 1991; Wexler & Stanton, 1993; O'Dell & Kandel, 1994; Selig et al., 1995b), or NMDA receptor-independent (Bashir & Collingridge, 1994; Staubli & Chun, 1996), but the discrepancy could be due to slightly different induction protocols. Apart from one report (Bashir & Collingridge, 1994), most laboratories have observed a consolidation of LTP with time, such that the magnitude of the depotentiation is reduced the greater the interval between LTP induction and the depotentiation stimulus (Fujii et al., 1991; O'Dell & Kandel, 1994; Staubli & Chun, 1996).

1.16 Models of synaptic plasticity.

Since Hebb's postulate of learning (Hebb, 1949) several groups have proposed models of synaptic plasticity. Figure 1.16iA presents a graphical representation of two such models including that presented by Hebb. Sejnowski (1977) proposed an extension of Hebb's postulate called the covariance rule in which decreases in synaptic gain are also taken into account which would prevent saturation of LTP at all synapses. In this model, the change in synaptic strength is a linear function of postsynaptic activity, where a greater amount of postsynaptic activity would result in LTP, and a lesser amount of

FIGURE 1.16i: Synaptic modification rules.

A A graphical representation of three major synaptic modification rules: a) Hebb's postulate of learning; the synaptic gain is a linear function of Φ, which is a product of the association of pre- and postsynaptic activity. b) The covariance rule; the synaptic gain change is a linear function of Φ (postsynaptic activity) that crosses the x axis at a given threshold. Depending on how the postsynaptic activity compares with this threshold either LTD or LTP will be produced. c) The BCM rule; the direction of synaptic gain change is a non-linear function of Φ (postsynaptic activity), where the threshold for LTP may change. The threshold for LTD induction in the BCM rule is when $\Phi=0$, which implies that any postsynaptic activity below the LTP threshold will cause a decrease in synaptic strength.

Figure adapted from Frégnac (1991).

B The original Artola, Bröcher & Singer (ABS) rule, where the direction of synaptic change, LTP ($\oplus$), or LTD ($\ominus$) depends on the membrane potential (E_m) of the postsynaptic cell or in mechanistic terms, on the amplitude of the surge of $[Ca^{2+}]_i$. If the first threshold Θ^- is reached, a mechanism is reached that leads to LTD. If the second threshold Θ^+ is reached, another process is triggered that leads to LTP (see inset).

Figure taken from Artola & Singer (1993).

A

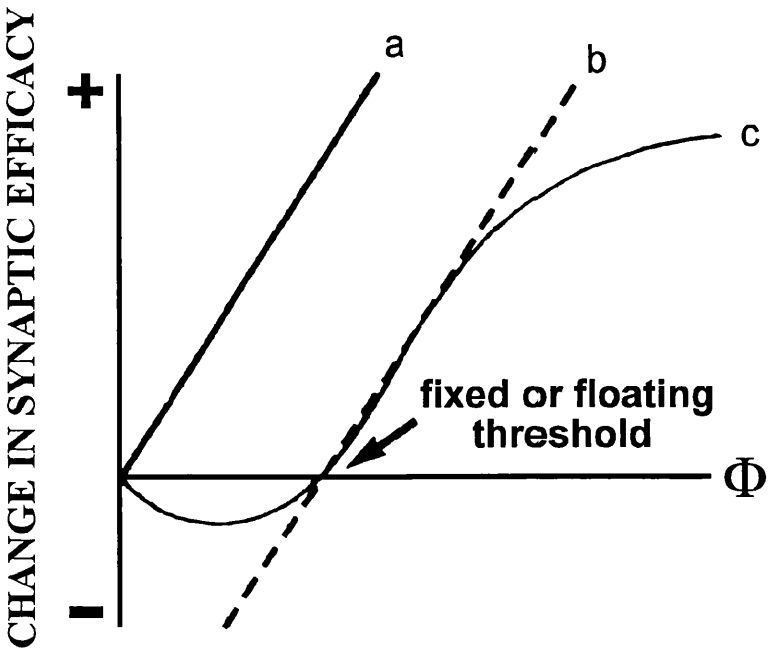
CHANGE IN SYNAPTIC EFFICACY
+
−
a
b
c
fixed or floating
threshold
Φ

B

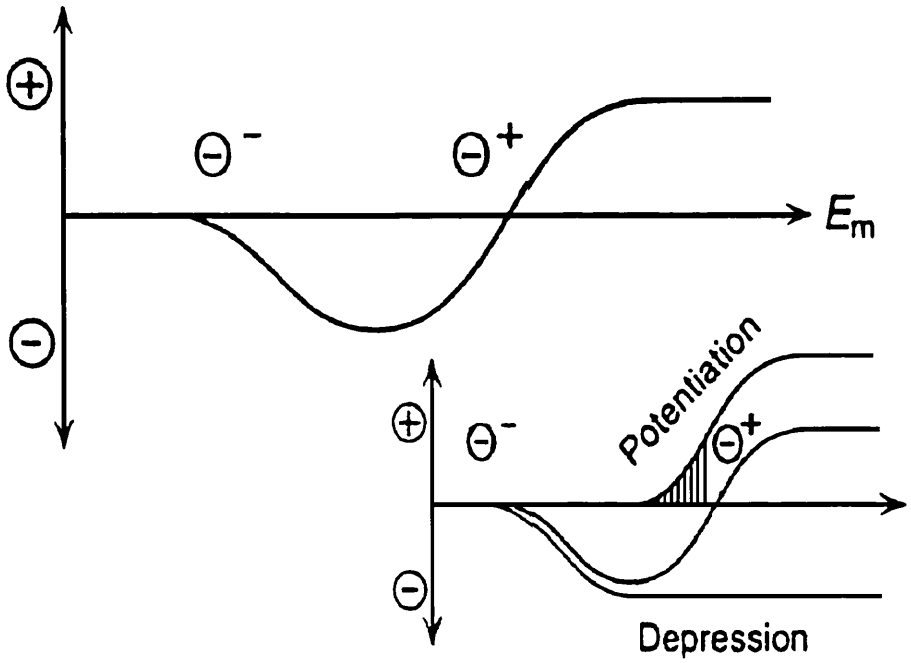
⊕
⊖
⊖⁻
⊖⁺
Em
⊕
⊖
⊖⁻
Potentiation
⊖x
⊖
Depression

postsynaptic activity, LTD. The Bienenstock, Cooper & Munroe (BCM) rule of synaptic modification, based on experiments performed in the visual cortex (Bienenstock et al., 1982), differs from the covarience rule in several aspects. In the BCM rule the direction of synaptic gain change is a non-linear function of postsynaptic activity, where the threshold for LTP may change. This floating threshold for LTP would shift rightwards following a history of increased synaptic activity which would make it less likely for an input to elicit LTP and more likely to elicit LTD. Conversely, low levels of synaptic activity would result in a leftward shift in the LTP threshold and therefore more likey for an input to elicit LTP. The non-linearity of the BCM rule has been reproduced experimentally by several groups including Artola et al., (1990) in the visual cortex, and Cummings et al. (1996) in the CA1. There have also been several reports suggesting the threshold for LTP (and LTD) is not fixed, where prior synaptic activity can influence the ability of a given input to elicit LTP and LTD (see Abraham & Bear, 1996 for review).

A synaptic modification rule which claims to account for both homosynaptic and heterosynaptic modification is the Artola, Bröcher & Singer (ABS) rule (Artola & Singer, 1993; Figure 1.16iB). Like the BCM rule the change in synaptic plasticity is a non-linear function of postsynaptic activity, defined by the authors as a change in either membrane potential or in the amplitude of the surge of intracellular Ca^{2+} concentration ($[Ca^{2+}]_i$). This rule, unlike the BCM rule has two threshold levels, including a threshold of LTD induction, such that a surge in $[Ca^{2+}]_i$ which falls below this threshold will have no effect on synaptic strength. The ABS rule also suggests that a rise in $[Ca^{2+}]_i$ which exceeds the threshold for LTP at inactive test synapses, caused by activity at separate but convergent synapses, will result in heterosynaptic, or non-asociative LTP.

1.17 Aims of this study.

In this study an attempt was made to reliably induce non-associative LTD by unpaired postsynaptic depolarization. Using indirect methods of lowering and raising Ca^{2+} entry on postsynaptic depolarization, the ABS model of synaptic plasticity was tested to observe if the rule applied to non-associative as well as heterosynaptic changes in synaptic strength. The application of the ABS rule to non-associative synaptic plasticity was further tested by combining electrophysiological and direct Ca^{2+} measurements using the ratiometric Ca^{2+} indicator Fura-2.

CHAPTER 2

MATERIALS AND METHODS

2.1 The hippocampal slice preparation.

Male 60 to 200 g Sprague-Dawley rats were killed by cervical dislocation and decapitated. The outer pelt covering the skull was cut along the midline with a scalpel blade and separated to expose the dorsal surface of the skull. The point of a pair of dissecting scissors was carefully inserted into the magnum foramen and the skull was cut laterally to the border of the parietal and squamosal bones. Keeping the point of the scissors upwards to prevent damage to the brain a cut was made along the dorsolateral border rostrally to the level of the olfactory bulb, and then laterally across the frontal bones. A pair of rongeurs was then inserted under the skull to carefully peel away the bone. The dura matter often adhered to the skull and was torn. Any remaining dura on the exposed brain was removed with a pair of fine forceps. Using a small spatula the brain was lifted out of the skull and immediately submerged in cold artificial cerebrospinal fluid (ACSF; 1 to 3°C) previously saturated with 95% O_2/5% CO_2. The operation of killing the animal, removing the brain and submerging it in ACSF took about 45 to 60 s.

After a period of at least 3 min, the brain was placed on filter paper in a petri dish containing cold ACSF. The immediate chilling of the tissue, and refrigeration throughout the slice preparation, minimized anoxic damage and hardened the tissue during sectioning. The brain was bisected along the midline and one half was resubmerged in fresh cold ACSF. On the petri dish the cerebellum and brainstem were removed. The remaining tissue was then lifted free with filter paper and the medial surface was dried. The medial side was then stuck to the nylon stage of a Vibroslice tissue slicer (Campden Instruments Ltd.) with cyanoacrylate adhesive (RS Components). The Vibroslice cutting chamber had previously been part-filled with ACSF to a level below the nylon stage, and frozen. Another frozen chamber was employed for the slicing of the second half of the brain. After the adhesive had dried (3 to 5 s) oxygenated ice-cold ACSF was poured into the Vibroslice cutting chamber, fully submerging the brain. Slices were prepared by slowly moving the cutting chamber, now secured to the Vibroslice, towards the vibrating blade. Initially a ~1·5 mm slice was cut and discarded,

this was followed by slicing at a thickness of 300 μm until the classical features of the transverse hippocampus was visible within the slice (Cajal, 1911; Skrede & Westgaard, 1971; see Figure 2.1i). The hippocampal slice was then dissected out of the brain slice while stationary on the Vibroslice blade using the tips of two hypodermic needles (21 gauge, Sabre) as cutting tools. If the experimental protocol required the addition of the $GABA_A$ receptor antagonist bicuculline to the ACSF during recording, the CA3 portion of the slice was removed while on the blade. This manoeuvre would prevent epileptiform activity and the appearance of paroxysmal depolarizing shifts during recording (Ayala et al., 1973). The hippocampal slice was transferred, using a shortened 5 mm tip diameter, flame-polished Pasteur pipette (Bilbate), onto ACSF moistened filter paper in a petri dish that was resting on ice. About six, 300 μm thick hippocampal slices were prepared. After cutting, the slices were transferred into an incubation chamber. The chamber, a perspex box (17·5 cm high, 16·5 × 16·5 cm width) was filled with ~500 ml tap water (3 cm deep) which covered an airstone through which 95% O_2/5% CO_2 was continually bubbled. The slice chamber was placed on a central pedestal above water level. A perspex sheet covered the gas bubbler to trap condensation, thus preventing the formation of water droplets on the underside of the chamber lid which could then fall onto the slices. The slices remained in this humidified oxygenated atmosphere for at least 1 hour at room temperature before being transferred to the recording chamber. Slices that remained in the incubation chamber were viable for up to 12 hours.

2.2 Artificial cerebrospinal fluid.

ACSF was freshly prepared for each experiment and had the following composition (mM): NaCl 125; KCl 3·2; $NaHCO_3$ 19; NaH_2PO_4 1·2; $MgCl_2$ 1; $CaCl_2$ 2; D-glucose 10 mM (all compounds were obtained from BDH). Under experimental conditions, when bubbled continuously with 95% O_2 and 5% CO_2 at a temperature of 31-32°C, the pH was ~7·3.

2.3 Experimental recording chamber.

Experiments were performed in a standard slice interface chamber (Alger et al., 1984; see Figure 2.3i) to which minor modifications were made to allow recordings from submerged hippocampal slices. A round glass coverslip (diameter 19 mm, BDH), the top of which was coated with Sylgard (10% w/v, Dow Corning), was affixed to the bottom

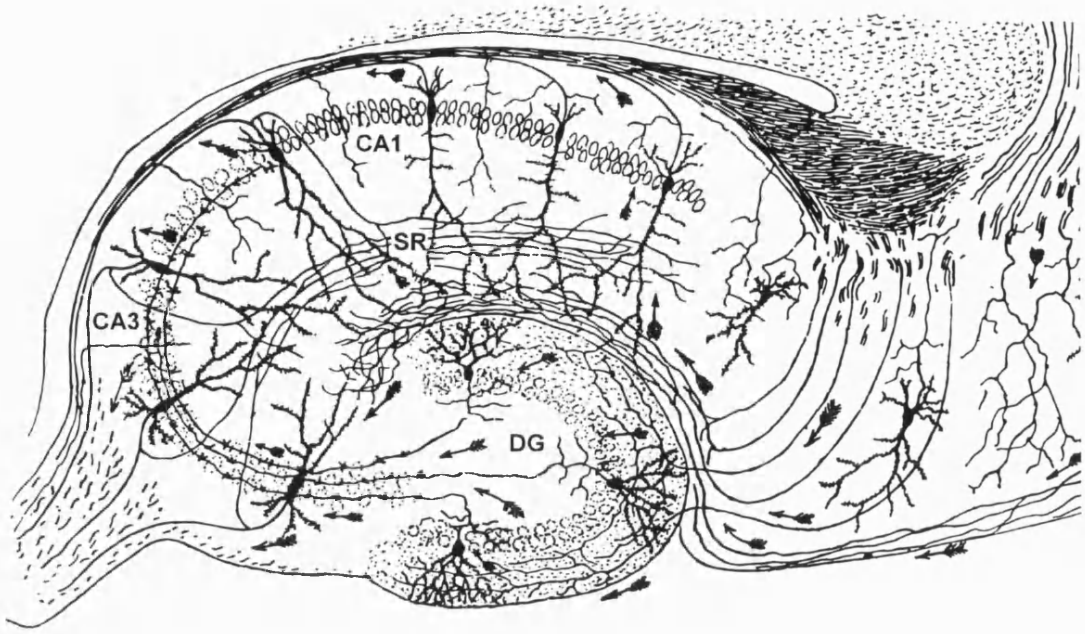

FIGURE 2.1i: Classical features of the transverse hippocampal slice preparation.

Modified from Cajal, (1911), this figure illustrates the major neuronal elements and the basic structure of the hippocampal slice formation. Labelled are the major regions of pyramidal cell bodies namely CA1, CA3 and the dentate gyrus (DG). Also labelled is the stratum radiatum (SR) which contains the major afferent inputs of the Schaffer collateral and commissural pathways to the CA1 region.

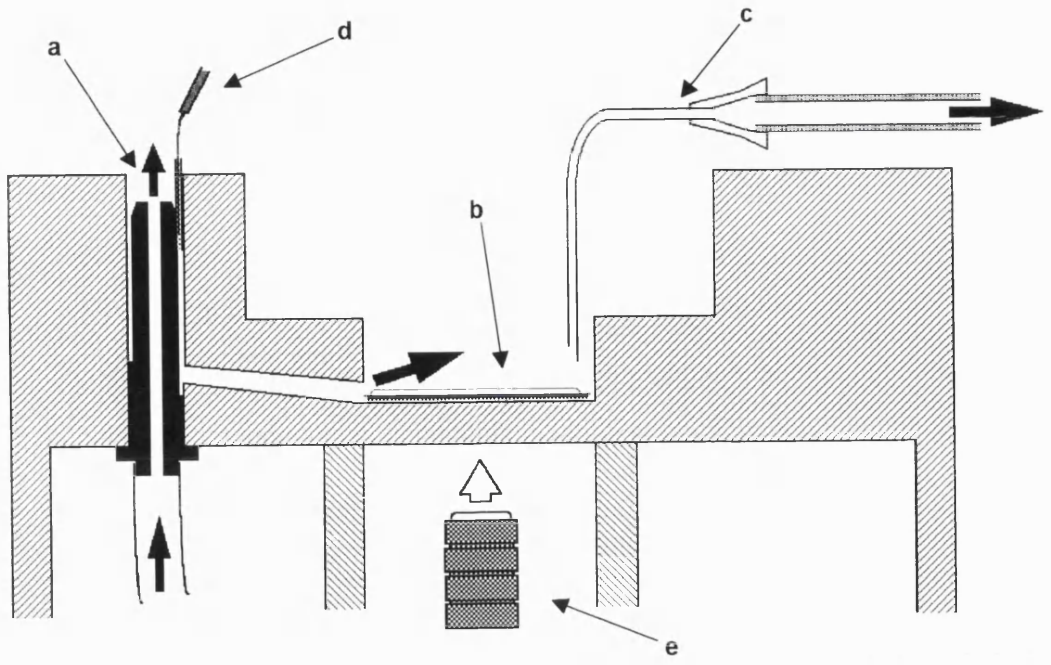

FIGURE 2.3i: The experimental recording chamber.

Above is a diagram of the top half of the experimental recording chamber. Thick black arrows illustrate the direction of ACSF flow throughout the experiment. ACSF is introduced via a peristaltic pump into the lower half of the chamber which contains a water bath at approximately 35°C. ACSF then travels up through a bubble trap (a) in which is also placed the indifferent electrode (d). The ACSF then flows over a Sylgard coated cover slip (b) in the centre of the chamber on which the hippocampal slice is placed. A bent hypodermic syringe needle (c) via another pump clears away excess ACSF. Below the hippocampal slice and cover slip is a cool light source (e) which illuminates the preparation (open arrow).

of the central well with silicon grease (Dow Corning). The fluid volume of the central well was reduced by placing two perspex (medical grade) D-shaped segments (dimensions: length 2·2 cm, width 7 mm, depth 5 mm) on each side of the well above the coverslip, also secured with silicon grease, this also ensured the smooth flow of ACSF across the slice, removing instabilities detrimental to long term recordings. The submerged slices were placed in the central well of the chamber through which ACSF flowed at depth of 2 mm. The slice was firmly held down by nylon threads that were stretched over a platinum frame (termed a "harp"; Edwards et al., 1989). During an experiment, slices were maintained at a constant temperature of 31-32°C by a heating element situated in the base of the chamber which was filled with approximately 350 ml of tap water. The water bath temperature was maintained by a thermistor-current feedback circuit (designed and built in the Department's electronics workshop). Following every experiment the water bath of the chamber was drained and the central well was extensively rinsed. At the end of each week the coverslip was replaced during a thorough cleaning of the chamber with Milton or alcohol.

2.4 ACSF perfusion system.

ACSF was held in a 250 ml conical flask at room temperature and was continuously bubbled with 95% O_2/5% CO_2. The ACSF was delivered to the experimental recording chamber via a variable speed peristaltic pump (Watson-Marlow, 502S pump, 508MC2 pump head), at a constant rate of 1-2 ml min^{-1}. The ACSF from the central well of the slice chamber was removed via a 21 gauge hypodermic needle attached to a 1 ml syringe and Portex tubing, the suction supplied by a three-roller peristaltic pump (Crouzet, 60 rpm). During an experiment, the ACSF could be recirculated. The dead space between the ACSF reservoir and the slice was 3 to 4 ml.

2.5 Harp construction.

The frame of the harp was made by bending a 2·8 cm length of 0·5 mm diameter platinum (Goodfellow Metals) into a U-shape (dimensions: 0·9 cm × 1·0 cm × 0·9 cm), and then flattening it in a vice. The threads stretched across the harp were obtained from fine nylon stocking. The material was laddered to expose the parallel fibres which were then stretched and secured over the mouth of a glass bottle (about 2 cm in diameter). Under a dissecting microscope (Prior S2000) the individual nylon threads were separated

to be parallel and about 0·5 to 0·8 mm apart. The side arms of the platinum U-frame were lightly coated with cyanoacrylate adhesive and placed across the nylon threads so that the side arms of the frame were perpendicular to the threads. A £1 coin was placed on top of the frame as a weight until the adhesive dried overnight. The following morning the £1 coin was reclaimed and the nylon threads either side of the frame were cut. The harp was washed in distilled water. Harps were re-used for about 25 experiments and discarded when the threads were no longer taut. The harp was carefully washed in 10% alcohol and then rinsed with distilled water after each experiment.

2.6 Recording electrodes.

Micropipettes were pulled from borosilicate glass (Clark Electromedical Instruments, GC120F-10) on a Flaming/Brown micropipette puller (P-87, Sutter Instrument Company). The micropipettes were normally filled with 4 M potassium acetate (KAc) solution. Some experimental conditions required the filling of the micropipette with 3 M cæsium acetate (CsAc). Only microelectrodes with d.c. series resistances of 70-120 MΩ were used. Experimentally it was found that microelectrodes with series resistances less than 60 MΩ made poor neuronal penetrations whereas microelectrodes with series resistances greater than 120 MΩ were electrically noisy and restricted the passage of applied current.

2.7 Stimulating electrodes.

The stimulating electrodes used in experiments reported in this study were constructed in the laboratory: Two 5 cm lengths of 55 μm diameter varnish-insulated nickel-chromium wire (termed "nichrome", a gift from G. L. Collingridge, University of Bristol) had the insulation removed at one end, and were placed into a 5 mm length tube of stainless steel, cut from a disposable hypodermic needle (21 gauge, Sabre). Light-weight sleeved wires were placed into the opposite end of the stainless steel tubes which were then crimped to hold the wires in place. Each connection was insulated using heat-shrink tubing. The nichrome wires which were to form the tips of the stimulating electrodes were twisted along their lengths and thinly smeared with epoxy-resin (Araldite, 50% wt/wt, Ciba-Geigy), providing insulation and maintaining a 100 to 150 μm distance between them. The wires were passed through a shortened 100 mm pasteur pipette (from 230 mm, Bilbate) until 2·0 cm of the nichrome wire was exposed at

the tip. Both ends of the pipette were sealed with araldite. Once set, the exposed tips of the nichrome wires were squarely cut to a length of approximately 1·5 to 2·0 cm.

This bipolar electrode was secured to a micromanipulator (Prior), and connected to an isolated stimulator (Devices, MK. IV) via the light-weight sleeved wires. The stimulation parameters used for all experiments consisted of square wave pulses of 0·05 to 0·2 ms duration and 0 to 30 Volts in strength in order to evoke a postsynaptic potential that was just below action potential firing threshold. A digitimer (D4030) was used to generate a trigger pulse of −12 V for the stimulator under the control of pClamp 5.5 software (Axon Instruments) driven by a 486P/33 personal computer (Dell). In later experiments the digitimer was discarded, the pClamp software could generate a −1·0 V current pulse, which following a ten times amplification by a d.c. amplifier (built in the Department's electronics workshop) was adequate to trigger the isolated stimulator box.

2.8 Voltage recording and current injection apparatus.

The microelectrodes were mounted in a holder that contained a Ag/AgCl electrode which directly plugged into the headstage (×0·1) of an Axoclamp 2A pre-amplifier (Axon Instruments). The reference electrode consisted of another Ag/AgCl wire mounted in a 1·5 cm length of Portex tubing (i.d. 1 mm) filled with agar (BDH) made up with ACSF minus $CaCl_2$ and D-glucose. This reference electrode was secured in the bubble trap of the recording chamber where it was in electrical continuity with the ACSF bathing the slice. The agar interface between the silver and the ACSF prevented any noxious interaction between the hippocampal slice and the AgCl. Prior to each experiment the Ag/AgCl wires of the recording and reference electrodes were connected together and placed in 1 M NaCl to form two half-cells and left overnight in order to obtain a stable iso-potential. This minimized d.c. drift between the electrodes during an experiment. The Axoclamp pre-amplifier had a bridge-balance (0 to 1000 MΩ) and current injection (0 to 10 nA) facilities. The voltage signal was amplified ten times by the Axoclamp and a further ten times by a d.c. amplifier (built in the Department's electronics workshop), and displayed on a Gould 1604 digital storage oscilloscope. The signal was also acquired on a 486P/33 personal computer (Dell) via a Tl-1 interface analogue to digital converter (range ±10 V) using pClamp 5.5 software (Axon Instruments). The voltage signal was digitized at 10 KHz and displayed on the computer monitor. The Axoclamp pre-amplifier had an internal voltage calibration and an input

current measurement facility, and calibration signals were periodically recorded and stored on computer.

2.9 Microelectrode support and drive systems.

The headstage holding the microelectrode was mounted on a digital microelectrode drive (Robert Clark Engineering, Roslyn Precision Ltd.). The drive unit was supported on a mild steel arm, which was clamped to a steel bar and could be rotated and tilted. The bar was secured to a lathe-carriage, clamped to a mild steel base plate. The lathe-carriage allowed the calibrated movement of the microelectrode to any position within the slice chamber. The drive unit was driven using a remote control facility allowing advancement or withdrawal of the microelectrode in controlled steps of 2 μm or 10 μm per step at a time.

2.10 Reduction of mechanical vibration and electrical interference.

The aim of the anti-vibration measures was to minimize variations in the position of the microelectrodes relative to the preparation. The recording chamber (supported on four rubber bungs), recording and stimulating electrode assemblies, dissecting microscope (W. Watson & Sons, Ltd.), were secured to a heavy mild steel base plate resting on three inflated car inner tubes. The base plate and inner tubes rested on a wooden table standing on rubber blocks. These anti-vibration measures minimized the loss of cell penetrations due to the effects of incidental vibration.

The whole assembly resting on the wooden table was surrounded from beneath, above and three sides by an electrical shield of aluminium sheeting. The shield, base plate, water bath and the hypodermic needle used for sucking surplus ACSF away from the slice chamber were earthed through a common ground connection.

2.11 Positioning of stimulating and recording electrodes.

A single hippocampal slice was transferred into the central well of the recording chamber where it was illuminated from below by direct light from a fibre-optic source (Micro Instruments, KL1500-T) and viewed under a dissecting microscope (×2·5 phase objective, final magnification ×25; W. Watson & Sons, Ltd.). The stimulating electrodes were lowered over the slice using a micromanipulator (Prior) with coarse and fine control, and placed lightly on the stratum radiatum to stimulate axons of the CA3 Schaffer collateral pathway synapsing on CA1 neurones. Figure 2.11i shows a schematic

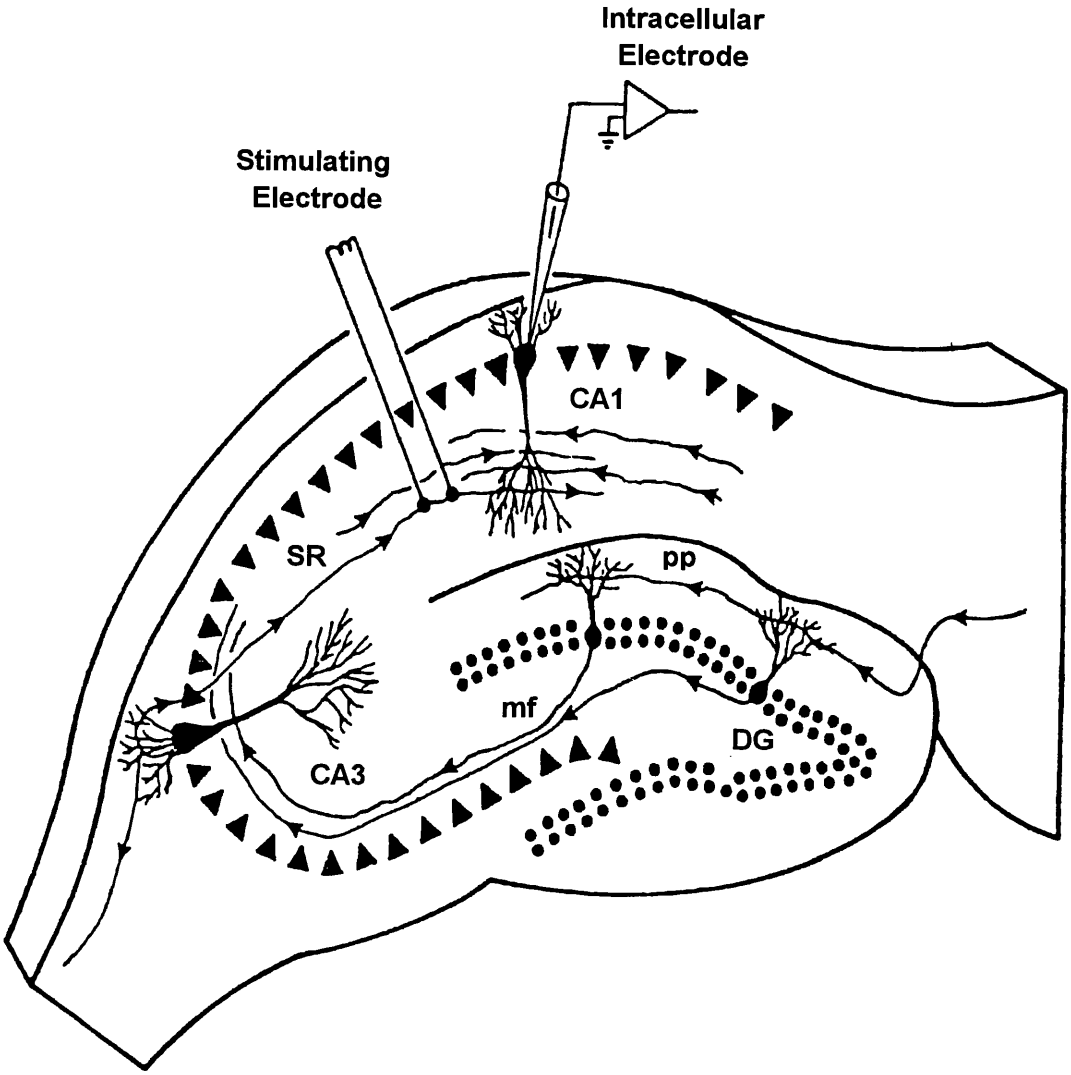

FIGURE 2.11i: Microelectrode placement.

Schematic of the hippocampal slice preparation illustrating the relative positions of the intracellular recording microelectrode, and the stimulating electrode. Labelled are the CA1 and CA3 cell body layers along with the dentate gyrus (DG), perforant path (pp), mossy fibres (mf) and the stratum radiatum (SR).

Adapted from Brown & Zador (1990).

representation of the hippocampal slice and illustrates the relative positions of the stimulating and recording electrodes. An intracellular microelectrode was positioned above the CA1 region of the stratum pyramidale close to the stimulating electrodes (between the same two threads of the harp) using the lathe-carriage.

2.12 Intracellular microelectrode placement.

Once positioned above the CA1 region of the hippocampal slice, the recording microelectrode was lowered into the ACSF. Once the electrode entered the ACSF and the recording circuit was completed, a current pulse of −0·2 nA (30 to 40 ms duration, 1·1 to 2 Hz frequency) was passed through the electrode. Following the application of maximum capacitance neutralization without positive feedback, the bridge circuit on the Axoclamp was balanced and the voltage offset adjusted to +40 mV. The microelectrode was advanced in steps of 10 μm using the stepping microdrive at an angle of 60 to 70° to the plane of the slice until contact, which was marked by a sudden increase in electrode resistance. The microelectrode was advanced in steps of 2 μm, concurrent with brief applied depolarizing current (~60 nA) evoked by momentarily hitting the "clear" switch on the Axoclamp, a procedure that aided cell penetration. The microelectrode was slowly advanced until a cell was penetrated or until ~240 μm below the surface of the slice, at which point it was withdrawn and repositioned for a fresh track through the slice. On passing through the slice the tip of the microelectrode often became blocked with tissue debris, resulting in an increase in electrode resistance. Usually the tip could be unclogged by brief application of negative or positive current via the "clear" switch or by depressing the Axoclamp "buzz" button which resulted in oscillation of the amplifier capacitance neutralization circuit. Microelectrodes were replaced after a maximum of five tracks or on breakage of the microelectrode tip which was marked by a sudden drop in electrode resistance.

On penetration of a neurone there was a sudden negative shift in potential which was usually accompanied by large, fast (1 to 2 ms duration) action potentials. Hyperpolarizing current of up to −1·0 nA was immediately applied via the electrode to prevent action potential firing and depolarization of the cell. After a period of at least 10 min of cell recovery following impalement, the hyperpolarizing current was gradually reduced to zero. Cells were accepted for further experimentation if the membrane potential was more negative than −65 mV, action potentials were more than 60 mV

(threshold to peak) and the apparent input resistance (R_{in}) was ≥20 MΩ. Cells that failed to meet any of the above criteria were abandoned. Occasionally a glial cell was impaled; characteristically these cells had stable membrane potentials of about −80 to −100 mV but did not show membrane charging during the passage of hyperpolarizing or depolarizing current (±0·6 to ±1·0 nA). Again these cells were abandoned. If a slice did not show any signs of neuronal activity it was abandoned and replaced. Dead or hypoxic slices were characteristically granular in appearance when viewed under the dissecting microscope, and no attempt was made to record from them.

2.13 Hippocampal stimulation and recording.

Following the removal of the applied hyperpolarizing current to the cell orthodromic stimulation was applied to evoke PSPs (post synaptic potentials) every 15 or 20 seconds. At the start of each experiment the membrane potential was altered by passing hyperpolarizing and depolarizing (200 ms) current pulses through the recording electrode which preceded and continued during stimulation. The stimulation to evoke PSPs was applied once the cell membrane was fully charged (usually 30 to 50 ms after the onset of the current pulse). This procedure was used to ascertain whether the evoked PSP was an excitatory postsynaptic potential (EPSP), a reversed inhibitory postsynaptic potential (IPSP) or an EPSP-IPSP sequence. If it was the case that an EPSP could not be evoked, or even if the net evoked response was IPSP, an attempt was made to move the stimulating electrodes in order to elicit a net EPSP without losing the impaled cell. The apparent R_{in} of the cell was continually monitored throughout the experiment with the passage of hyperpolarizing current pulses (usually 75 ms duration, −0·1 to −0·3 nA) injected through the recording electrode approximately 280 ms before the onset of each evoked EPSP, the resulting voltage measured at 40 ms into the response. The measurement of voltage deflections following the application a current to calculate R_{in}, was made in respect to a short period after electrode charging was complete (judged by eye), cancelling out any erroneous measurements due to bridge imbalance. Throughout the experiment the threshold and spike height was monitored. If subthreshold, the neurone was made to fire action potentials either synaptically (by increasing the stimulus width) or by the injection of depolarizing current pulses (overriding R_{in} measure). Detailed examination of the current-voltage (I-V) relationship before and after drug perfusion, or a conditioning period, was performed by application

★ The current pulses applied were adjusted in size (sometimes during the conditioning procedure) in an attempt to induce approximately 20 action potentials per pulse.

of depolarizing and hyperpolarizing current pulses (150 ms duration, –0·6 to +0·4 nA) at 0·5 Hz in the absence to evoked PSPs.

The membrane potential (V_m) of the neurone was monitored with the digital voltmeter supplied with the Axoclamp pre-amplifier throughout an experiment. Any d.c. drift occurring between the Ag/AgCl wires during the course of an experiment was determined by V_m and cell firing threshold checks during an experiment (as described above), and observing the change in potential on stepping out of the cell at the end of an experiment.

2.14 Induction of non-associative LTD.

The induction of non-associative LTD was attempted using depolarizing current injection across a bridge circuit via the recording electrode in the absence of evoked postsynaptic potentials (Barry et al., 1996c). Eight depolarizing current pulses (400 or 500 ms duration, +1·0 to 3·5 nA, at 0·1 Hz) were superimposed on steady depolarizing d.c. current used to hold the cell's V_m at or just below action potential firing threshold. This protocol was attempted in the presence of certain ionotropic receptor antagonists or modified ACSF solutions in an attempt to isolate the conditions in which non-associative LTD induction was favoured.

2.15 Induction of hippocampal LTP.

Hippocampal LTP induction was attempted using a theta frequency induction paradigm based upon Larson et al., (1986) in which 10 short high frequency bursts (4 or 5 pulses at 100 Hz) were applied to the Schaffer collateral pathway every 200 ms. This paradigm was repeated 4 times at 60 s intervals. It was usual to double the width of the stimulation pulse during this LTP induction paradigm.

2.16 Drugs and experimental changes to ACSF.

Several ionotropic channel antagonists were used in this study. The $GABA_A$ receptor antagonist bicuculline (Sigma) was used at a concentration of 1 to 20 μM. Stock solutions of bicuculline were prepared at a concentration of 1 mM in distilled water and frozen in aliquots for future use. The required concentration of bicuculline was prepared by thawing out an aliquot and diluting with ACSF. This technique was also employed when using the NMDA receptor antagonist D-APV (10 μM; Sigma). The

★ In this study, LTP was defined as a >15% increase in the size of the postsynaptic response compared with baseline responses, which lasted for greater that 1 hour post-conditioning. In addition, LTD was defined as a >15% decrease in the size of the postsynaptic response compared with baseline responses, which lasted for greater that 1 hour post-conditioning.

AMPA receptor antagonist CNQX (10 μM; Tocris Neuramin), was also prepared as a stock solution in frozen aliquots (10 mM in 0·1% DMSO) but was wrapped in foil due to its light sensitivity.

Several modifications to the ACSF were also employed in this study to investigate the induction of non-associative long-term depression (LTD). The changes to ACSF in these solutions are shown below (mM):

a) ACSF containing 1 mM Ca^{2+}: $MgCl_2$ 2; $CaCl_2$ 1.

b) ACSF containing 4 mM Ca^{2+}: NaCl 123; $MgCl_2$ 1; $CaCl_2$ 4.

c) ACSF containing 25 mM Mg^{2+} and 2 mM Ca^{2+}: NaCl 92; $MgCl_2$ 25; $CaCl_2$ 2.

d) ACSF containing 15 mM Mg^{2+} and 0 mM Ca^{2+}: NaCl 106; $MgCl_2$ 15; $CaCl_2$ 0.

2.17 Analysis of experimental data.

Data records were analyzed off line on computer (Dell) using the pClamp software analysis program Clampfit. Several points in each trace were averaged and stored on file which was incorporated into a spreadsheet (Microsoft Excel) where measurements of V_m, EPSP slope and apparent R_{in} could be calculated. Spike height and threshold measurements were usually measured manually from Clampfit. Graphical representations of experiments were produced using Excel and plotted on a Laserjet printer (Hewlett Packard). ★

2.18 Measurements of intracellular $[Ca^{2+}]$ using Fura-2 microfluorimetry.

Somatic and dendritic cytosolic changes in $[Ca^{2+}]_i$ during non-associative LTD conditioning paradigms were measured using the ratiometric fluorescent Ca^{2+} indicator Fura-2 (Molecular Probes). A 200 μm thick hippocampal slice was placed in a modified chamber on the stage of an inverted Zeiss microscope equipped for xenon epifluorescence and continuously perfused with ACSF as described above. The tip of the recording microelectrode was filled with 20 mM Fura-2 and 2 M KAc. The shaft was then back-filled with 4 M KAc. The series resistances of the Fura-2 filled electrodes were between 90 and 110 MΩ. After impalement of a CA1 neurone situated less than 100 μm from the bottom of the slice, Fura-2 was iontophoresed into the cell with −0·5 to −1·0 nA for about 10 min.

An intensified CCD camera (Extended ISIS, Photonic Science) was used to record the fluorescence intensities following passage through a dichroic mirror (DC400,

Glen Spectra) and a broad band green filter (DF 510/30, Glen Spectra). After 10 min of iontophoresis, the slice was viewed following excitation at 380 nm, in order to check the level of Fura-2 filling and cell resolution. If, following another 5 to 10 min iontophoresis a clear soma could not be distinguished, the cell was abandoned.

During the experiment apparent R_{in}, V_m, threshold and spike height were monitored as previously described although at a lower acquisition rate (5 KHz) and in some but not all experiments orthodromic PSPs were evoked by stimulation of the stratum radiatum (0·1 Hz). During a control period of at least 10 min following cell filling, successive fluorescence intensities were measured while illuminated with ultraviolet light at 350 or 380 nm, using narrow band filters (DF series, Glen Spectra). For each excitation wavelength thirty successive images were acquired over a 3·6 second period and averaged by Vidacq software (Medical Software Services; adapted by Dr K. Boone, Dept. Physiology, U.C.L.) driven by a (Dell 466/ME) personal computer. After this control period, 8 depolarizing current pulses of 500 ms duration and +0·5 to +2·5 nA were injected through the recording electrode in order to induce postsynaptic depolarization and firing in standard ACSF. Evoked test PSPs were switched off during postsynaptic depolarization. Before each period of postsynaptic depolarization (intracellular conditioning) a ratio measurement was obtained which consisted of fluorescent measurements following excitation with ultraviolet light at both 350 and 380 nm. Using this technique resting $[Ca^{2+}]_i$ levels could be calculated using the following equation:

$$[Ca^{2+}] = K_{½}[(I_{350}/I_{380})-R_{min}]/[R_{max}-(I_{350}/I_{380})]$$

Where $K_{½}$ is $K_d(I_{max}/I_{min})$, which is constant for the experimental system, I_{350} is the fluorescence signal at 350 nm, I_{380} is the fluorescence signal at 380 nm, and R_{min} and R_{max} are the ratios measured at saturating and zero calcium levels, again constant for the experimental system. Using the technique as described in Appendix 1 (from Silver et al., 1992), repetitive fluorescence measurements during the steady illumination at 380 nm could be used to calculate rises in $[Ca^{2+}]_i$ during the period of postsynaptic conditioning which greatly increased the time resolution of the system. Associated with each depolarizing current pulse, a series of images were acquired (termed a "spray"). The first image of each spray was acquired before the start of each current pulse followed by seven images separated by 80 ms (1992 experiments) or eight images separated by

120 ms and a ninth after a further second (1994 experiments). Images were averaged across each of the eight sprays and stored on computer for analysis. The test solution or drug was applied for a period of 5 or 20 min respectively during which tine both control and spray images were measured. The bathing medium was then returned to ACSF and the process was repeated.

Measurement of the fluorescence images were made off-line following the completion of an experiment. The fluorescence signal from soma and dendrite were confined within a designated circle and rectangular box. The rectangular box surrounding the dendritic image was divided into five equal segments. Background measurements of fluorescence were made using an equivalent circle and rectangle, placed on a part of the slice containing no cells filled with FURA-2. The measurements were transferred onto computer spreadsheets, and $[Ca^{2+}]_i$ was calculated using the formulae described in Appendix 1.

CHAPTER 3

RESULTS: Electrophysiological experiments.

3.1 Introduction.

Intracellular electrophysiological recording and stimulation were used to investigate the induction of non-associative long-term depression in the CA1 region of the hippocampal slice preparation.

The data arising from these experiments is presented in three parts: **Part 1** describes the electrophysiological and pharmacological properties of CA1 pyramidal neurones in this study. **Part 2** describes experiments in which the induction of long-term changes in synaptic transmission was attempted by non-associative intracellular depolarization. **Part 3** describes the induction of non-associative long-term depotentiation of previously potentiated synapses in the hippocampus.

PART 1: Long-term recordings from CA1 neurones in isolated slices of rat hippocampus - their electrophysiological and pharmacological properties.

3.2 Cell Characteristics.

The experiments were carried out on a total of 50 hippocampal slices from 45 rats. Intracellular recordings were obtained from 50 CA1 neurones under various conditions in an attempt to isolate the circumstances under which a non-associative LTD could be reliably induced. The recordings lasted for at least 20 min and up to 6 hours. The electrophysiological characteristics of cells recorded in each of the conditions used in this study are summarized in Table 3.2i.

Using the analysis of variance (ANOVA) statistical test (single factor), a significant difference ($P < 0{\cdot}05$) in spike height was found among the various conditions, probably due to the lowered $[Na^+]$ in the high Ca^{2+} medium and the K^+ channel block by Cs^+. However further intercomparison between each of the conditions using the Bonferroni test showed no significant differences between spike heights in the different media, which suggests that the original significance obtained using ANOVA was due to chance.

TABLE 3.2i: CA1 cell characteristics under conditions from which recordings were made: Control value ±SEM.

Cell Characteristic:	1 mM $[Ca^{2+}]_o$ (n = 9)	4 mM $[Ca^{2+}]_o$ (n = 6)	Cs^+ (n = 8)	Bicuculline (n = 28)
Apparent R_{in} (MΩ)	32 ± 3·5	31 ± 2·6	25 ± 2·8	26 ± 1·9
Firing threshold (mV)	11 ± 1·0	15 ± 0·9	13 ± 1·2	14 ± 0·5
Action potential (mV)	76 ± 2·0	67 ± 2·1	78 ± 1·8	75 ± 1·5
Total spike height (mV)	87 ± 2·4	82 ± 2·1	92 ± 2·2	88 ± 1·5
V_m on exit (mV)	−72 ± 1·5	−74 ± 1·3	−72 ± 2·0	−73 ± 1·1

Cs^+ values measured with −0·15 to −0·35 nA steady current.
V_m: membrane potential.
Apparent R_{in}: apparent input resistance measured at 40 ms using a −0·2 nA current pulse.
Firing threshold: action potential threshold measured from V_m.
Action potential: action potential measured from firing threshold to peak.
Total spike height: action potential measured from V_m to peak.

3.3 Membrane properties of CA1 pyramidal neurones.

When investigating long-term decreases in synaptic strength, it is important to monitor functional neuronal parameters such as apparent input resistance (R_{in}), membrane potential (V_m), firing threshold and action potential height throughout the recording period, in order to eliminate deterioration of cell recording as a cause of the reduced synaptic response. Any changes in R_{in} that occurred over the recording period could be attributed to the activation or inactivation of voltage-dependent ionic conductances which are seen in the non-linearity of current-voltage (I-V) relationships. The I-V relationship of CA1 neurones was assessed by measuring voltage deflections 40 ms after the onset of postsynaptic injections of square pulses of depolarizing and hyperpolarizing current, at which time membrane charging had reached a maximum. Most cells showed a non-rectifying linear current-voltage relationship over a 5 to 10 mV range negative to the resting potential (Figure 3.3ii) although in some cells this range was much less (Figure 3.3i). Inward rectification was observed at depolarized potentials, at about 10 to 15 mV below action potential firing threshold, (illustrated in Figure 3.3i) which was probably due to the activation of a slow sodium current ($I_{Na(slow)}$) near the threshold for action potential firing (Brown et al., 1990). If the R_{in} rose during the recording period, it was an indication of cell depolarization, which could be confirmed by changes in firing threshold. In addition, the majority of cells exhibited a time- and voltage- dependent inward rectification, an example of which is seen in Figure 3.3ii. This type of rectification, known as anomalous rectification is thought to be due to the

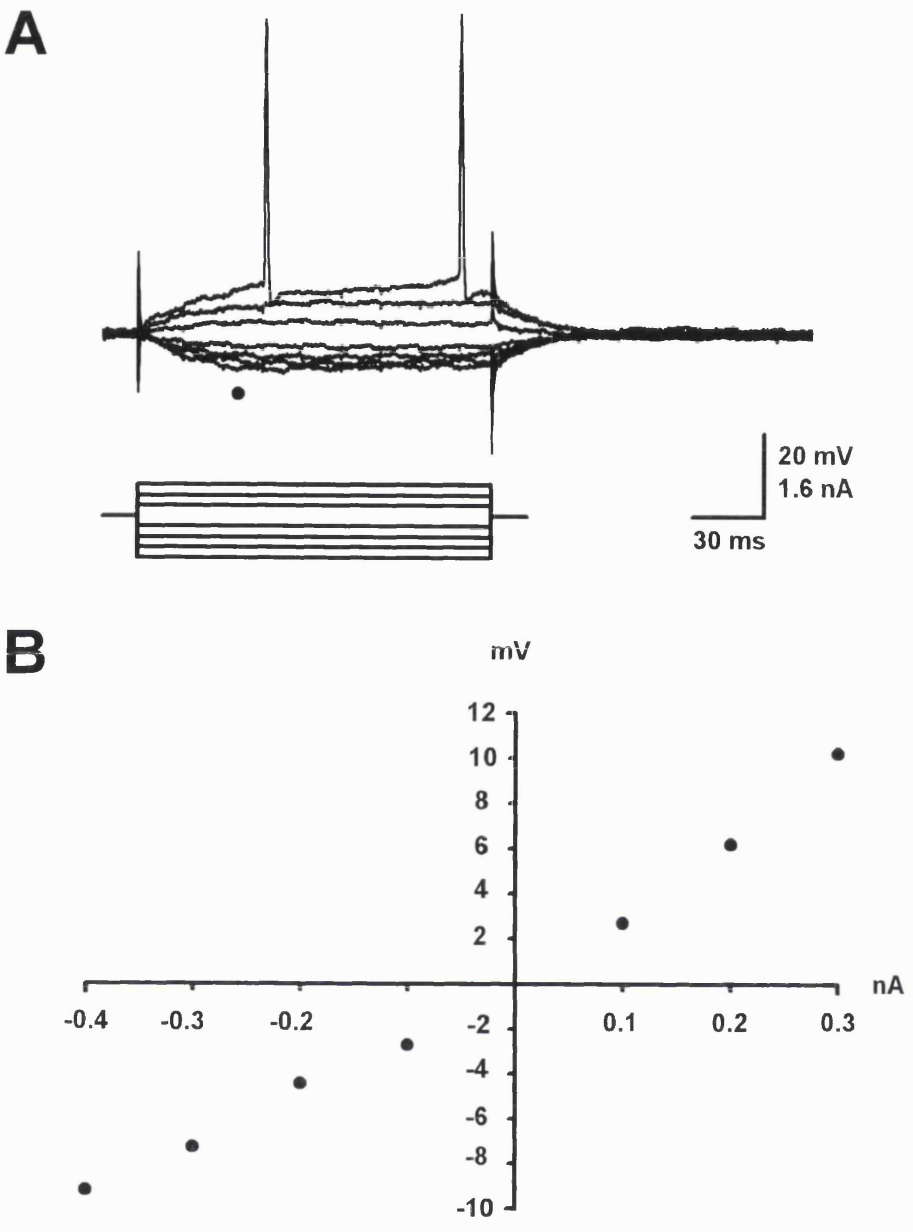

FIGURE 3.3i: Current-voltage relationship of a CA1 neurone showing inward rectification.

A Superimposed postsynaptic responses of a CA1 neurone bathed in normal ACSF to intracellular current injections. Upper traces, voltage; lower traces, current (–0·4 to +0·3 nA) plotted against time. Closed circle below voltage traces indicates time at which measurements were taken (40 ms) to plot the current-voltage relationship shown in B.

B Plot of the change of voltage measured at 40 ms after the onset of current injection for the cell shown in A. Note the inward rectification seen during the larger depolarizations.

Apparent R_{in} 19 MΩ (measured at 40 ms; –0·2 nA current pulse); spike threshold 13 mV; spike amplitude 66 mV (threshold to peak). V_m on exit –70 mV.

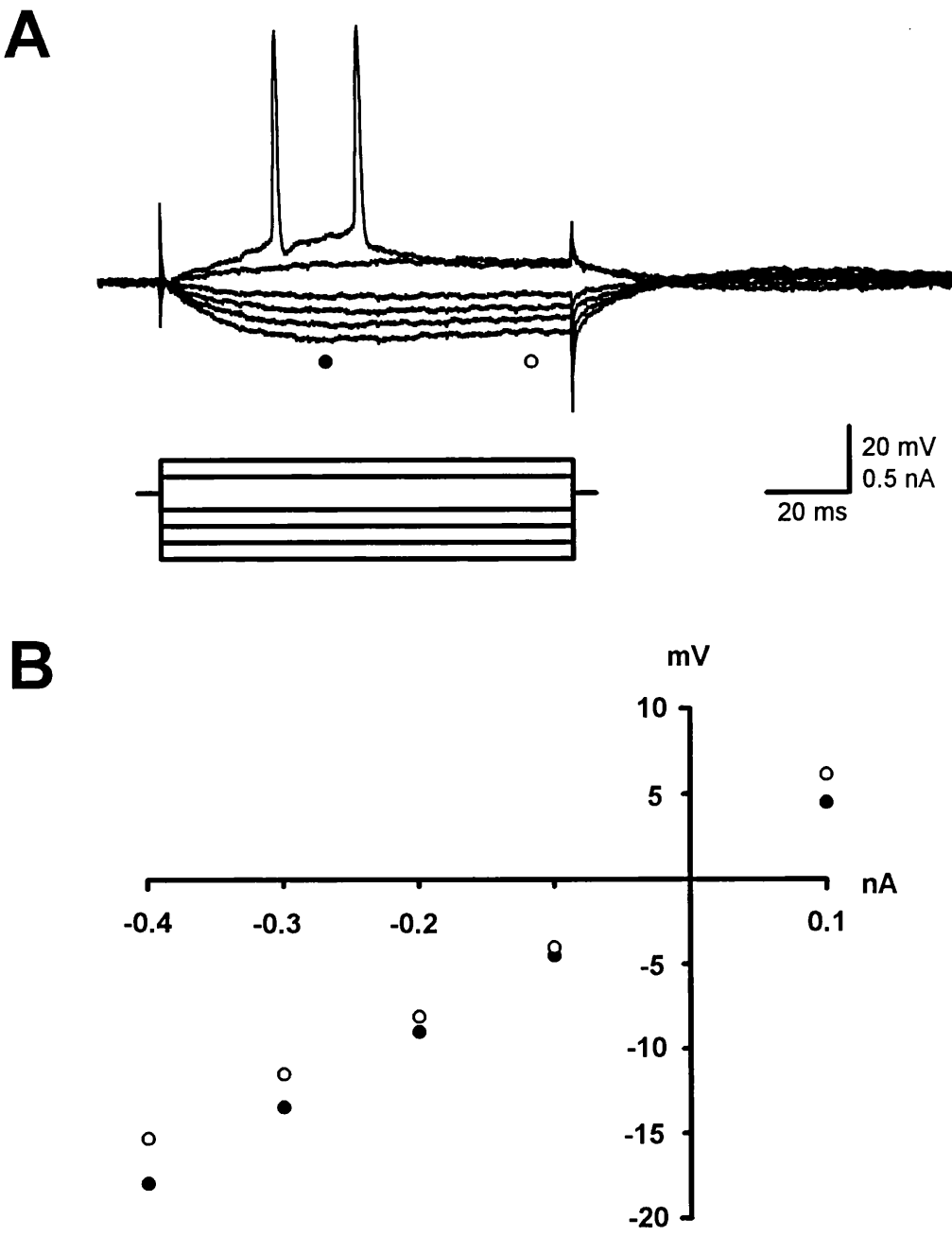

FIGURE 3.3ii: Current-voltage relationship of a CA1 neurone illustrating a delayed inward rectification at hyperpolarized potentials.

A Superimposed postsynaptic responses of a CA1 neurone bathed in normal ACSF to intracellular current injections. Upper traces, voltage; lower traces, current (–0·4 to +0·2 nA) plotted against time. Closed and open circles, below voltage traces, indicate times at which measurements were taken (40 and 90 ms respectively) to plot the graph shown in B.

B Current-voltage relationship for the cell shown in A. Plot of the change of voltage measured at 40 ms (closed circle) and 90 ms (open circle) after the onset of current injection. Note the inward rectification seen during the larger hyperpolarizations for measurements taken at 90 ms.

Apparent R_{in} 43 MΩ (measured at 40 ms; –0·2 nA current pulse); spike threshold 14 mV; spike amplitude 64 mV (threshold to peak), V_m on exit –66 mV.

activation of a time- and voltage-dependent K^+ (or mixed Na^+ and K^+) conductance (Hotson et al., 1979).

Large (> 10 MΩ) decreases in R_{in} during an experiment were often associated with a reduction in action potential height and was attributed to the loss of stable cell recording and these cells were discarded. As changes in V_m could be due to drift in potential difference arising from the Ag/AgCl wire electrode, during experimental analysis changes in R_{in} were compared with action potential height and threshold to assess cell viability.

3.4 Reversed IPSPs.

Occasionally afferent stimulation to the stratum radiatum resulted in what appeared to be an EPSP but which on membrane depolarization was seen to be a reversed $GABA_A$ mediated fast IPSP. This occurred if the resting potential of the cell was more negative than the chloride reversal potential (approximately –75 mV) and if the IPSP was not swamped by excitatory transmission (Alger & Nicoll, 1982a; Newberry & Nicoll, 1985). At depolarized potentials the chloride current flow would reverse and appear as a hyperpolarization of the voltage trace, peaking 20 to 25 ms after the onset of the PSP. In each cell before baseline measurements of EPSPs commenced, orthodromic stimulation was superimposed upon intracellular current injection to test for the presence of EPSPs. An example of a reversed IPSP is seen in Figure 3.4iA, where at depolarized potentials only a very small fraction if any can be attributed to excitatory synaptic transmission. Figure 3.4iB illustrates a classic EPSP superimposed upon hyperpolarizing and depolarizing current pulses. In this cell $GABA_A$ mediated IPSPs have been blocked with 10 μM bicuculline and there is no reversal of the PSP at depolarized potentials. Only cells in which a net EPSP was present were chosen for experimentation, cells were discarded if the majority of the PSP was shown to be IPSP.

3.5 Postsynaptic potentials recorded in CA1 neurones.

PSPs were recorded in response to orthodromic stimulation of afferent fibres located in the stratum radiatum. The size and shape and size of PSPs, although normally variable, show different characteristics depending upon recording conditions. In this study several factors were modified in order to facilitate the induction of long-term changes in synaptic transmission, including lowering or raising the calcium concentration in the bathing medium, introducing Cs^+ into the cell, and the use of a $GABA_A$ receptor

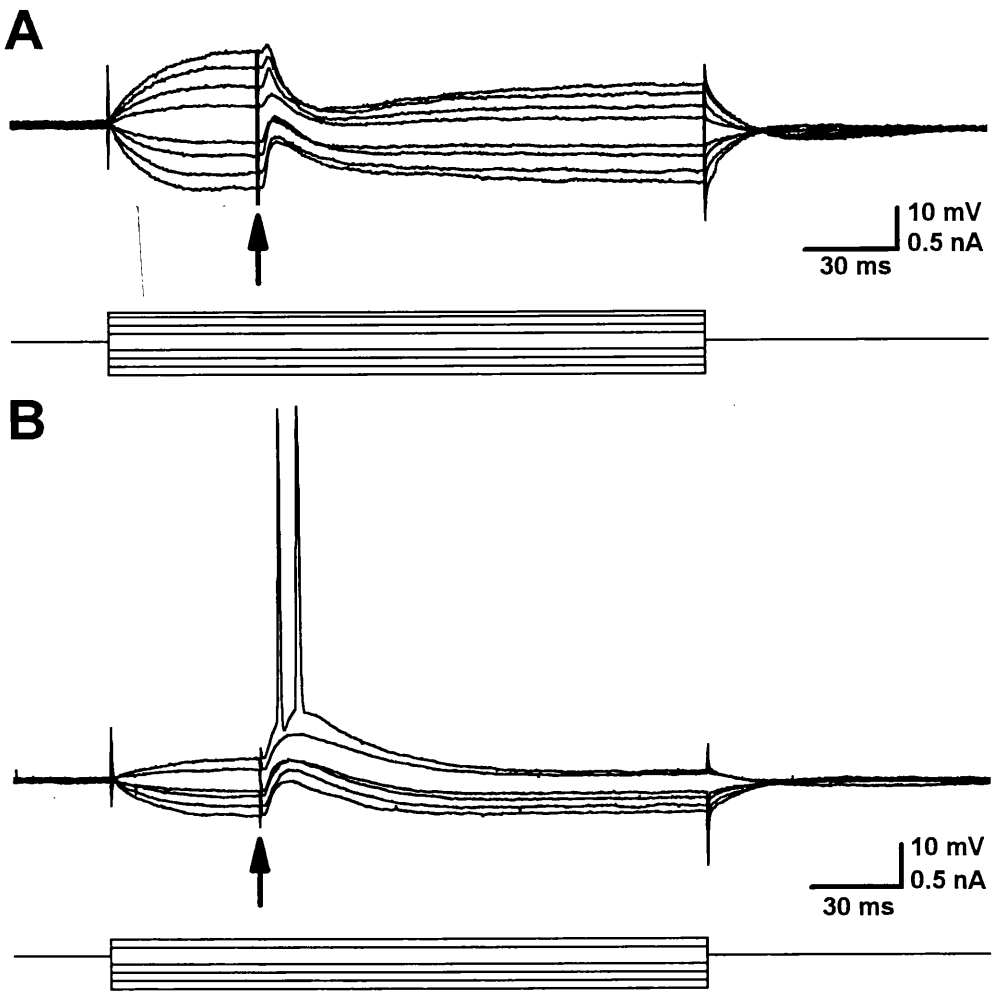

FIGURE 3.4i: Postsynaptic response of CA1 pyramidal cells to electrical stimulation superimposed on intracellular current injection.

A Eight superimposed responses to afferent stimulation occurring 50 ms (filled arrow) after the onset of varying levels on intracellularly injected steady current (–0·40 to +0·35 nA) in a cell bathed in ACSF containing 4 mM Ca^{2+}. Upper traces, voltage; lower traces current. Stimulation of the stratum radiatum at hyperpolarized potentials elicits what appears to be an EPSP. At depolarized potentials the majority of the response reverses revealing the underlying IPSP. Apparent R_{in} 31 MΩ; spike threshold 21 mV; spike amplitude 74 mV. V_m on exit –73 mV.

B Six superimposed responses to afferent stimulation occurring 50 ms (filled arrow) after the onset of varying levels on intracellularly injected steady current (–0·4 to +0·2 nA) in a cell bathed in 10 μM bicuculline. Upper traces, voltage; lower traces current. In this cell the early $GABA_A$ mediated IPSP is blocked. The non-reversal and spike generation at depolarized potentials demonstrates that the postsynaptic potential is in fact an EPSP. Apparent R_{in} 22 MΩ; spike threshold 16 mV; spike amplitude 73 mV. V_m on exit –76 mV.

antagonist. Figure 3.5i illustrates typical, individual PSPs recorded under each of these conditions.

Figure 3.5iA illustrates four consecutively recorded PSPs before and after addition of the $GABA_A$ receptor antagonist bicuculline (1 μM) to the bathing medium (normal ACSF). The loss of the $GABA_A$ mediated IPSP resulted in an increase in EPSP amplitude and cell excitability, but did not markedly change the initial EPSP slope, suggesting that there was a lack of feed-forward inhibition (Alger & Nicoll, 1982a). In most cells action potential generation did not change the initial EPSP slope, although in some cases the depolarizing slope of the late portion of the EPSP prior to spiking was increased. This increase in late EPSP slope before action potential generation is thought to be due to the activation of $I_{Na(slow)}$ (Brown et al., 1990).

Figure 3.5iB illustrates the typically large variability in EPSP amplitude and slope seen when recording from cells bathed in ACSF containing 1 mM Ca^{2+} and 2 mM Mg^{2+}. This occurs despite using larger stimulus intensities to evoke EPSPs which would increase the number of release sites. Both extracellular $[Ca^{2+}]$ and presynaptic calcium current have been shown to be correlated in a supra-linear fashion to the postsynaptic response (Dodge & Rahamimoff, 1967; Charlton et al., 1982; Mintz et al., 1995) such that at low $[Ca^{2+}]_o$ a large increase in the postsynaptic response can be induced by just a small increase in Ca^{2+} entry into the cell during presynaptic depolarization. There is also decreased inhibitory transmission onto cells bathed in low Ca^{2+} ACSF. This decrease in transmitter release probability would lessen the influence of recurrent inhibitory circuits (Lacaille et al., 1987) as can be seen by the lack of clear IPSPs following stimulation in all cells bathed in ACSF containing 1 mM Ca^{2+}.

In contrast to the findings with slices bathed in 1 mM Ca^{2+}, when slices are bathed in ACSF containing 4 mM Ca^{2+}, EPSP variability is far less and IPSPs (presumably $GABA_B$ mediated) were clearly seen (Figure 3.5iC). These slower inhibitory events, for example, $GABA_B$ mediated IPSPs (Dutar & Nicoll, 1988; Soltesz et al., 1988), or Ca^{2+}-dependent K^+ currents activated following action potential generation (Alger & Nicoll, 1980; Hotson & Prince, 1980; Newberry & Nicoll, 1984) are K^+ mediated. These could be distinguished from fast Cl^- mediated events because the responses were seen to drop below resting V_m since K^+ has a reversal potential of approximately –90 mV.

Figure 3.5iD depicts six successive EPSPs recorded in response to afferent stimulation with 3 M CsAc present in the recording electrode and 10 μM D-APV in the bathing medium (normal ACSF). The reduction of the delayed rectifier K^+ current by

FIGURE 3.5i: Postsynaptic responses of CA1 neurones to orthodromic stimulation in various bathing media and conditions used in this study.

A Four successive responses of a CA1 neurone recorded 5 min before and 5 min after addition of 1 μM bicuculline to the bathing medium (normal ACSF). Block of the $GABA_A$ mediated IPSP caused an enhanced depolarization following stimulation, resulting in cell spiking. Calibration bar: 10 mV, 10 ms.

Pre-bicuculline: Apparent R_{in} 17 MΩ; spike threshold 11 mV; spike amplitude 69 mV (threshold to peak). Post-bicuculline (following 10 min application): Apparent R_{in} 19 MΩ; spike threshold 14 mV; spike amplitude 67 mV (threshold to peak); V_m −70 mV.

B Six successive EPSPs recorded in response to afferent stimulation when bathed in ACSF containing 1 mM Ca^{2+}, illustrating high variability of EPSP slope and amplitude. Calibration bar: 5 mV, 10 ms.

Apparent R_{in} 37 MΩ; spike threshold 9 mV; spike amplitude 77 mV; V_m −76 mV.

C Six successive EPSPs recorded in response to afferent stimulation in a cell bathed in ACSF containing 4 mM Ca^{2+}. In contrast to EPSPs recorded in low Ca^{2+} ACSF as illustrated in B, there was little variation in either EPSP slope or amplitude when bathed in a high Ca^{2+} media. In addition a pronounced afterhyperpolarization (presumably $GABA_B$ mediated IPSP) following EPSP generation was seen. Calibration bar: 5 mV, 10 ms.

Apparent R_{in} 30 MΩ; spike threshold 18 mV; spike amplitude 61 mV; V_m −73 mV.

D Six successive EPSPs recorded in response to afferent stimulation with 3 M CsAc present in the recording electrode (normal ACSF; 10 μm D-APV). Experiments were performed with a steady negative current used to prevent leakage of Cs^+ into the postsynaptic cell. This leakage could not always be prevented as can be seen by the transformation of a Na^+ spike into a presumed Ca^{2+} spike, by the blockage of K^+ mediated currents by Cs^+. Calibration bar: 10 mV, 10 ms.

Apparent R_{in} 38 MΩ; spike threshold 8 mV; spike amplitude 73 mV; V_m −82 mV; −0·2 nA steady current.

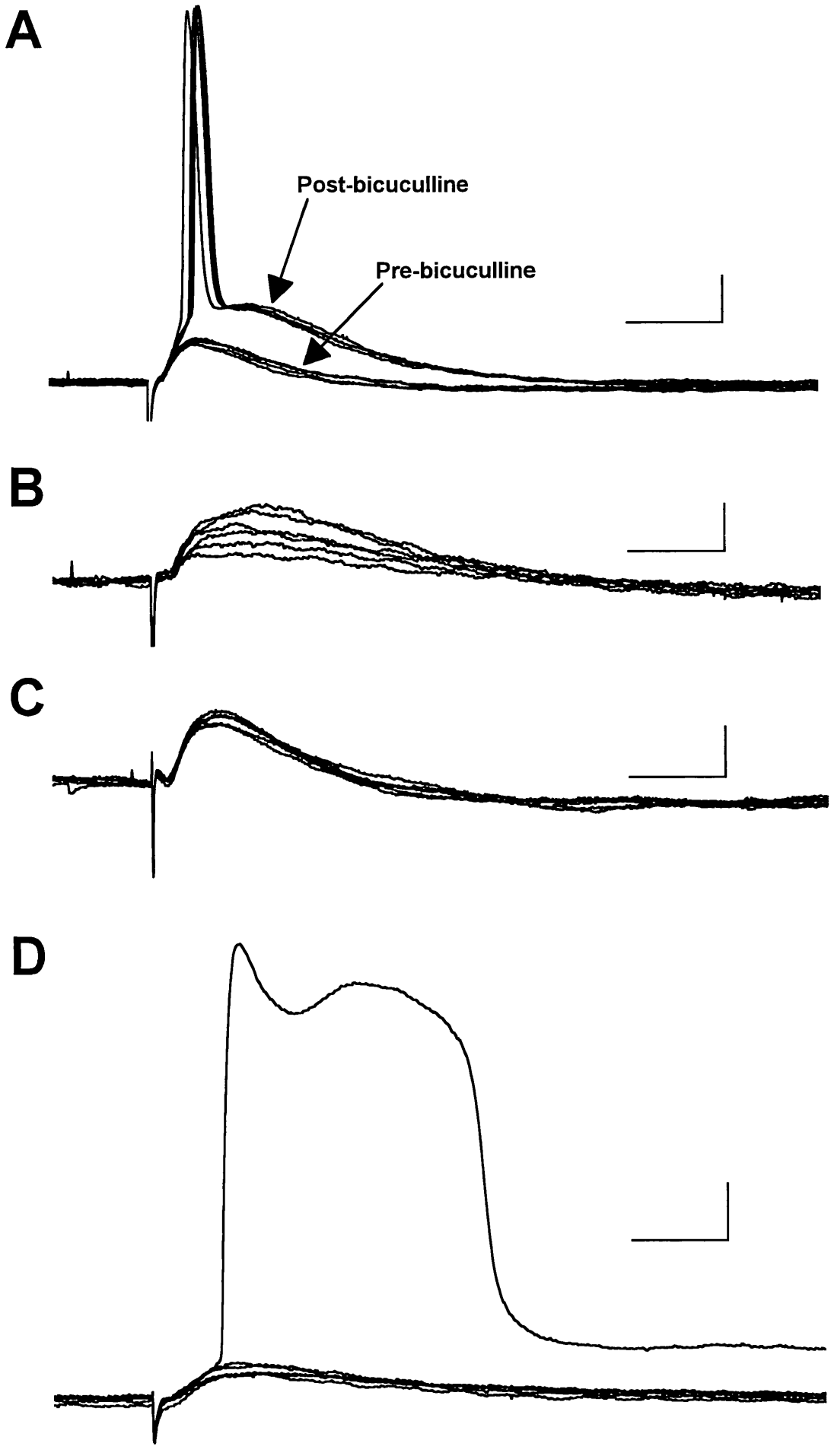
A
Post-bicuculline
Pre-bicuculline
B
C
D

intracellular Cs^+ (Dreyer, 1990) gives rise to activation of VDCCs following spike generation which greatly broadens the action potential following the Na^+ upstroke (Nuñez & Buño, 1992). These presumed Ca^{2+} spikes were rarely seen during synaptic stimulation since negative steady current passing through the recording electrode will hold back Cs^+ leakage into the cell. In the example illustrated, the Ca^{2+} spike was evoked directly following postsynaptic depolarization which introduced large amounts of Cs^+ into the cell.

PART 2: Postsynaptic induction of non-associative LTD.

3.6 Postsynaptic conditioning of neurones bathed in ACSF containing 1 mM Ca^{2+}.

The Ca^{2+} rise caused by conditioning may be an important factor in determining whether LTP, LTD or indeed no change in synaptic strength is produced (Lisman, 1989). Mulkey & Malenka (1992) observed that by lowering the external $[Ca^{2+}]$, a tetanus that previously resulted in LTP now produced LTD. It has been suggested that a small increase of $[Ca^{2+}]_i$ might selectively activate Ca^{2+}-dependent phosphatases resulting in dephosphorylation of membrane proteins, and LTD, whereas an increase to a high level of $[Ca^{2+}]_i$ might activate Ca^{2+}-dependent kinases resulting in protein phosphorylation and LTP (Lisman, 1989; for reviews see Teyler et al., 1994; Artola & Singer, 1993; Malenka, 1993; Christie et al., 1994; Linden, 1994).

Heterosynaptic depression can be seen at inactive synapses following LTP-inducing tetanization of other synapses on the same cell (Lynch et al., 1977; Dunwiddie & Lynch, 1978; Scanziani et al., 1996), although several groups have failed to observe the phenomenon (Schwartzkroin & Wester, 1975; Andersen et al., 1977; Paulsen et al., 1993). Pockett et al., (1990) found a that the probability of inducing non-associative LTD induction by an antidromic tetanus was raised from $P = 0{\cdot}66$ to $P = 1$, if the tetanus was applied during a transient wash in of ACSF containing 25 mM Mg^{2+}, rather than ACSF alone. The high $[Mg^{2+}]_o$ in these experiments was thought to reduce Ca^{2+} entry into the postsynaptic cell, during conditioning, by a partial block of VDCCs (Almers & Palade, 1981). This decrease in Ca^{2+} entry during postsynaptic depolarization in the presence of 25 mM Mg^{2+} compared with normal ACSF was confirmed by measurements of somatic $[Ca^{2+}]_i$ using the Ca^{2+} indicator Fura-2 (Christofi et al., 1993b).

In the experiments described in this and following sections, non-associative LTD induction was attempted by postsynaptic depolarization of the target neurone by injection of depolarizing current (intracellular conditioning) through the recording electrode. Intracellular postsynaptic conditioning in a reduced $[Ca^{2+}]_o$ of 1 mM was designed to mimic the conditions in which Pockett et al., (1990) produced non-associative LTD, but without the need to wash in and wash out the high $[Mg^{2+}]$ solution.

Exposure of slices to 1 mM Ca^{2+} ACSF markedly reduced EPSP size in all cells over a period of approximately 20 min. In the majority of recordings, stimulus intensity was then increased to produce measurable EPSPs. Recordings lasted between 10 and 66 min post-conditioning in 9 cells. A depression of the EPSP slope of > 25%, 8 to 12 min post-conditioning, was seen in 5 of these cells. Figure 3.6i shows the result from one such experiment. Following intracellular conditioning the EPSP slope was depressed and remained so for the remainder of the recording period (> 35 min). The slice was bathed in 1 mM Ca^{2+} ACSF for at least 36 min before control recordings began.

A plot of mean normalized EPSP slope against time for the 5 cells that were depressed at 10 min post-conditioning is shown in Figure 3.6iiA. The duration of the recordings varied, but the depression of the EPSP slope was significant at both 8 to 12 min (52·7 ± 3·01% ±SEM; n = 5) and 28 to 32 min post-conditioning (61·0 ± 7·96% ±SEM; n = 3); both at $P < 0{\cdot}05$ (unpaired *t*-test, 2 tailed), compared with the last 2 min of the control period (n = 4). The number of cells used to construct the graphs presented in Figure 3.6iiA (and B) is plotted below the normalized EPSP slope. The greater n number following conditioning is caused by two cells in which a gap of 10 min occurs at different times during baseline recordings. The duration of exposure to 1 mM Ca^{2+} before conditioning in the 5 cells showing LTD was not significantly different from the other 4 cells in which no depression occurred, suggesting that the decrease in EPSP slope was not due to a general decline following addition of 1 mM Ca^{2+} ACSF.

When the results for all 9 cells were normalized, the depression of the EPSP, slope although smaller than the normalized value for the 5 cells that exibited a depression, was significant at 10 min (67·1 ± 8·83% ±SEM; n = 8) and 30 min (61·2 ± 5·79% ±SEM; n = 5) post-conditioning, compared with the last 2 min average of the control period (n = 8; at $P < 0{\cdot}05$ and $P < 0{\cdot}005$ respectively; unpaired *t*-test, 2 tailed). Figure 3.6iiB shows a normalized plot of EPSP slope against time for all 9 cells. Table 3.6i summarizes the cell characteristics in all 9 experiments before and after postsynaptic conditioning.

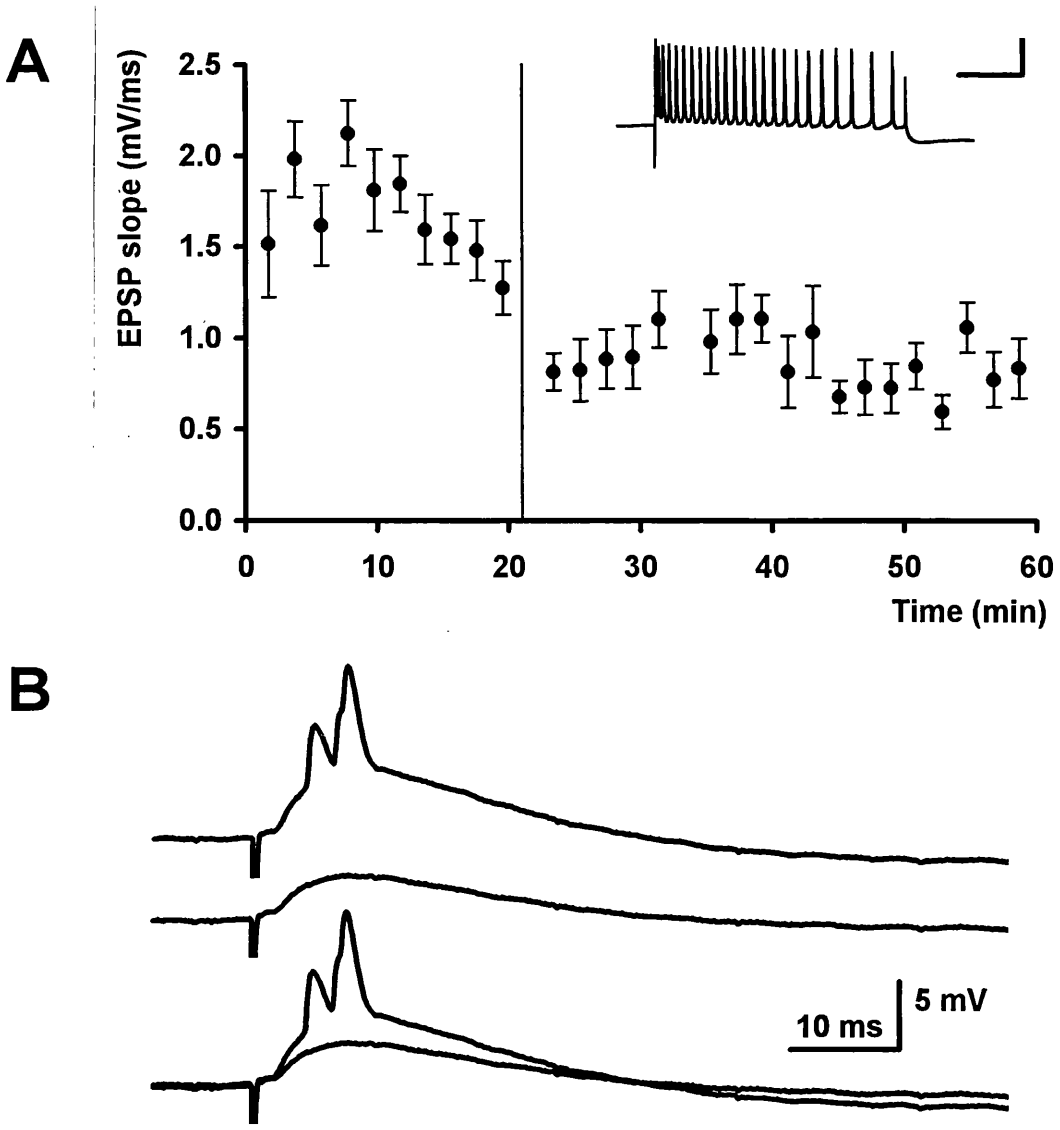

FIGURE 3.6i: Postsynaptic induction of non-associative LTD in a single cell bathed in ACSF containing 1 mM Ca^{2+}.

A Graph of mean EPSP slope against time, each point a 2 min average of 8 consecutive responses. Intracellular conditioning (vertical line on graph), consisted of eight 400 ms depolarizing pulses (each +1·0 nA) at 0·1 Hz, eliciting an average of 25 spikes/pulse. Inset at top right illustrates the result of one of the eight depolarizing current pulses. Calibration bar: 100 ms, 30 mV.

B Representative averaged traces of EPSPs from the cell illustrated in A. Each is an average of 16 successive responses. Responses before conditioning were suprathreshold and spikes were attenuated during averaging. Top: Recorded 4 min before the onset of postsynaptic conditioning. Middle: Recorded 30 min following conditioning. Bottom: Pre- and postconditioning responses superimposed.

Control: Apparent R_{in} 37 MΩ; spike threshold 9 mV; spike amplitude 77 mV (threshold to peak). Thirty minutes post conditioning: Apparent R_{in} 38 MΩ; spike threshold 9 mV; spike amplitude 76 mV. V_m on exit –76 mV.

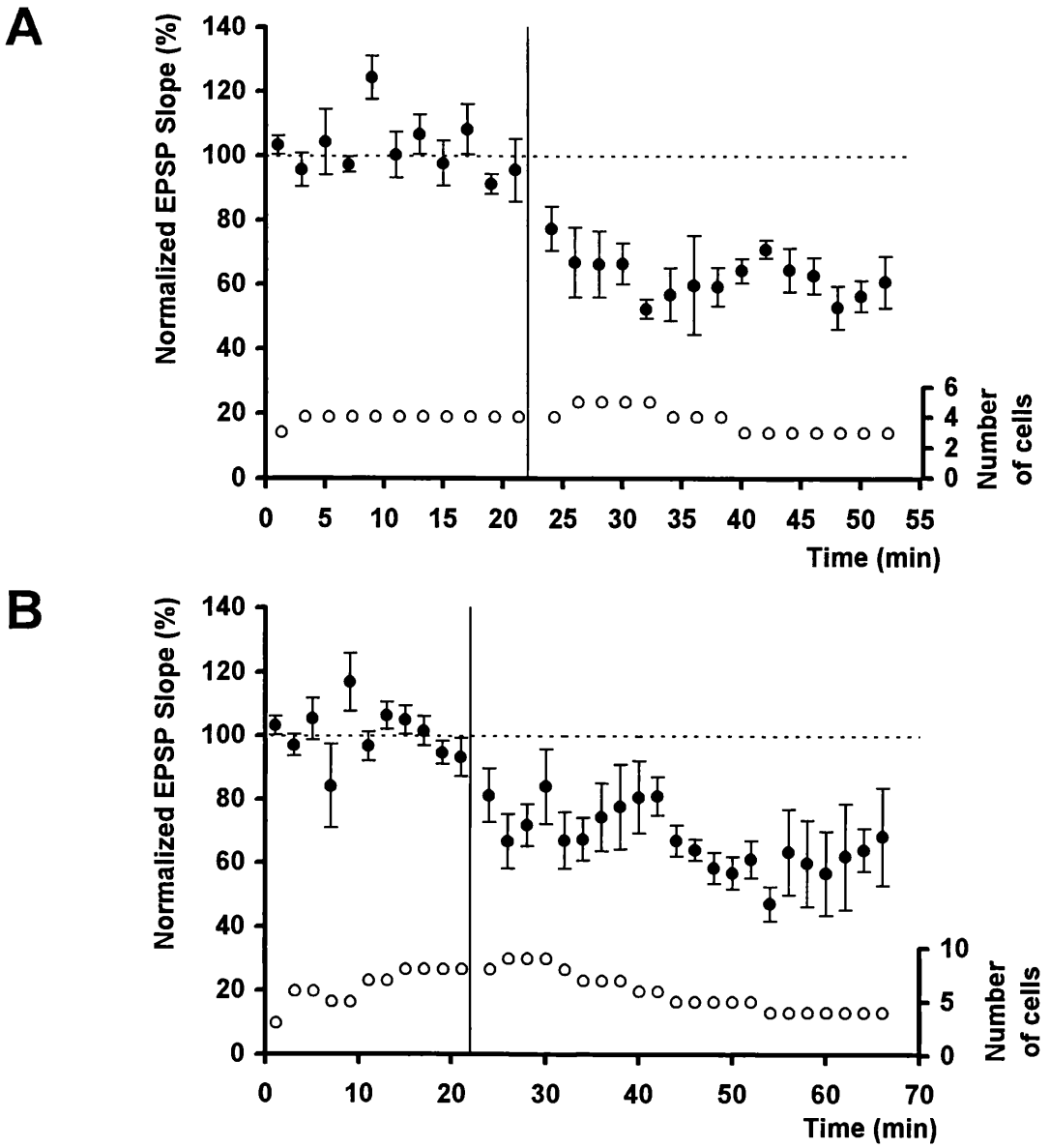

FIGURE 3.6ii: Postsynaptic induction of non-associative LTD in CA1 neurones bathed in ACSF containing 1 mM Ca^{2+}.

A Mean normalized EPSP slope (closed circles) plotted against time for 5 cells in 1 mM Ca^{2+} that exhibited an LTD following intracellular conditioning. Error bars are ±1 SEM. Vertical line on graph indicates end of intracellular conditioning. Also plotted is the number of cells (open circles) over a given time period used to construct the graph of mean normalized EPSP slope. Slices were bathed in ACSF containing 1 mM Ca^{2+} for between 36 and 111 min before baseline recordings began. Broken horizontal line gives the 100% value over the last 10 min of the control.

B Plot of mean normalized EPSP slope (closed circles) against time for all 9 cells subjected to postsynaptic conditioning in 1 mM Ca^{2+} (i.e. depressed and no effect results pooled). Error bars are ±1 SEM. Vertical line on graph indicates end of intracellular conditioning. Slices were bathed in ACSF containing 1 mM Ca^{2+} for between 26 and 172 min before baseline recordings began. As in A the number of cells (open circles) used to construct the mean normalized EPSP graph is also plotted.

TABLE 3.6i: Electrophysiological properties of CA1 neurones bathed in ASCF containing 1 mM Ca^{2+} before and after postsynaptic conditioning.

	Control (n=9)		Post-conditioning (n=9)	
Cell Characteristic:	Mean	±1SEM	Mean	±1SEM
Apparent R_{in} (MΩ)	32·4	3·5	31·0	3·3
Firing threshold (mV)	11·3	1·0	11·4	1·1
Action potential (mV)	75·9	2·0	75·3	2·1
Total spike height (mV)	87·2	2·4	86·7	2·4
V_m on stepping out (mV)			−71·5	1·5

Control values were obtained over the last 10 min of the baseline period. Post-conditioning values were obtained 30 to 40 min post-conditioning, or over the last 10 min of the recording period.

There were no significant differences between mean apparent R_{in}, spike threshold or spike height compared before and after conditioning. The induction of a non-associative LTD by discrete intracellular depolarization in the presence of a reduced $[Ca^{2+}]_o$ appears to suggest that a reduced Ca^{2+} entry during conditioning is important in non-associative LTD induction. The variability of dendritic Ca^{2+} transients and their attenuation with distance from the soma when triggered by trains of backpropagating action potentials (Spruston et al., 1995), could explain why LTD was seen only in a proportion of cells, even though there was no significant difference in the number of spikes elicited during conditioning in cells exhibiting LTD (26 ± 4·0 spikes ±SEM; range 14 to 37) or not (29 ± 7·2 spikes ±SEM; range 14 to 46).

3.7 Postsynaptic conditioning in cells bathed in 4 mM Ca^{2+} ACSF.

I have already described LTD induction in the presence of ACSF containing 1 mM Ca^{2+}. I then tested the effect of IC in ACSF containing 4 mM Ca^{2+} to see whether LTD induction is facilitated by a restriction of Ca^{2+} entry through VDCCs, or conversely, by an enhanced Ca^{2+} entry, as previously suggested by Wickens & Abraham (1991; see Section 1.12). In six out of six cells postsynaptic conditioning produced no significant change in the EPSP slope at 10 min post-conditioning (98·8 ± 5·11% ±SEM; n = 6) or at 30 min post-conditioning (95·3 ± 5·10% ±SEM; n = 5). There were no significant change in any cell characteristics post-conditioning compared to control (see Table 3.7i). An individual experiment is shown in Figure 3.7i, the pooled data from all six cells is presented in Figure 3.7ii. The failure to produce LTD by intracellular conditioning in ACSF containing 4 mM Ca^{2+} suggests that a postsynaptic rise in dendritic $[Ca^{2+}]_i$ above that achieved following depolarization in ACSF containing 1 mM Ca^{2+} was not

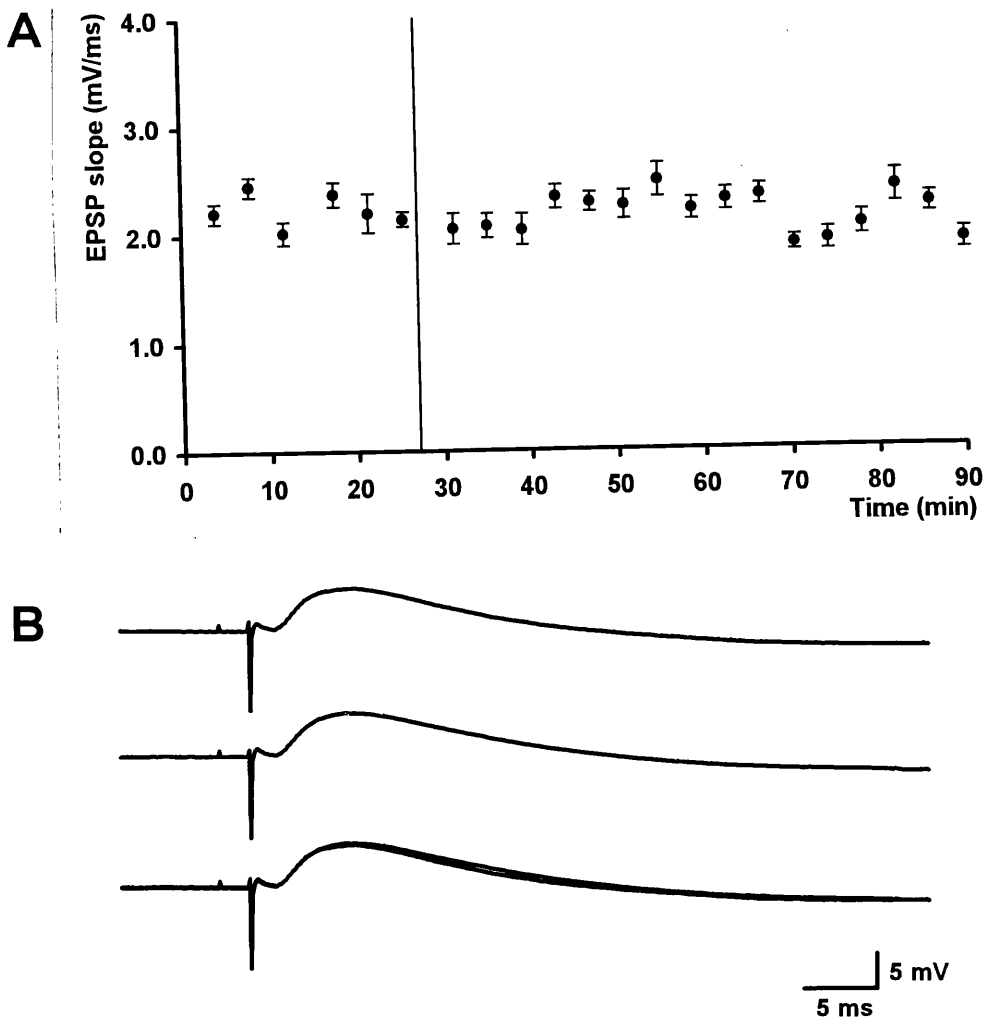

FIGURE 3.7i: Intracellular conditioning in ACSF containing 4 mM Ca^{2+} has no effect upon EPSP slope.

A Graph of mean EPSP slope against time in a single cell bathed in ACSF containing 4 mM Ca^{2+}. Test EPSPs were evoked by stimuli to stratum radiatum and recorded every 15 s. Intracellular conditioning consisted of eight 400 ms depolarizing pulses (1·0 to 1·5 nA) at 0·1 Hz, eliciting an average of 22 spikes/pulse (range 19 to 25; vertical line on graph). Each point is an average of 16 responses. The slice was bathed in ACSF containing 4 mM Ca^{2+} for 30 min before baseline recordings began.

B Representative averaged traces of EPSPs recorded from the CA1 neurone illustrated in A. Top: Average of 16 successive responses 4 min before the onset of conditioning. Middle: Average recorded 12 min following postsynaptic conditioning. Bottom: Pre- and postconditioning responses superimposed.

Control: Apparent R_{in} 30 MΩ; spike threshold 18 mV; spike amplitude 61 mV (threshold to peak). Forty minutes post conditioning: Apparent R_{in} 30 MΩ; spike threshold 17 mV; spike amplitude 63 mV. V_m on exit –73 mV.

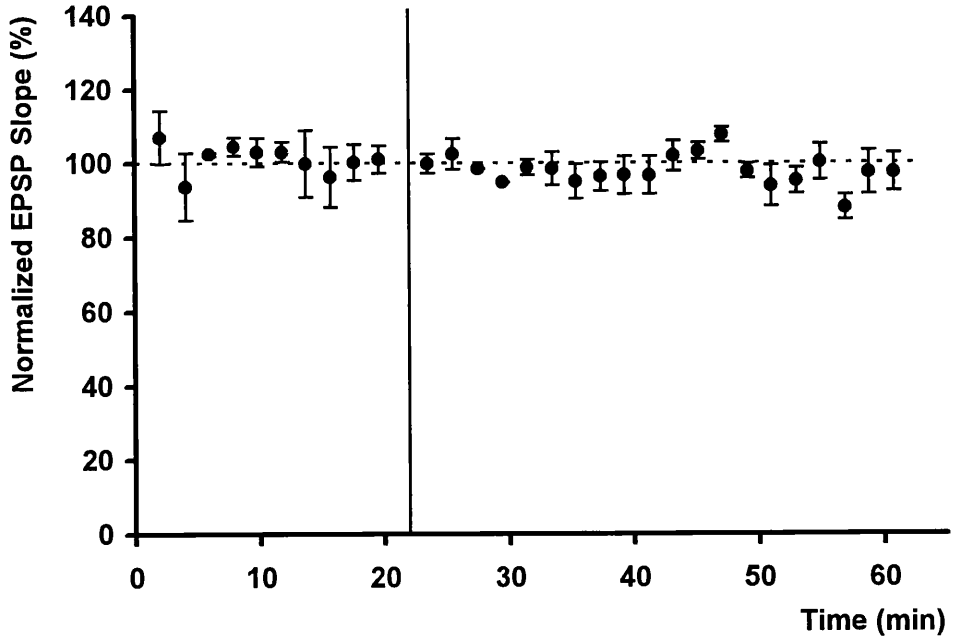

FIGURE 3.7ii: Intracellular conditioning in CA1 cells bathed in ACSF containing 4 mM Ca^{2+}.

Postsynaptic conditioning had no effect upon EPSP slope in CA1 cells bathed in ACSF containing 4 mM Ca^{2+}. Mean normalized EPSP slope from six cells is plotted against time (error bars are ±1 SEM). Conditioning pulses (vertical line on graph) elicited a median of 16 spikes/pulse (range 11 to 22). Slices were bathed in ACSF containing 4 mM Ca^{2+} for between 170 and 30 min before conditioning. Broken horizontal line gives the 100% value over the last 10 min of the control.

conducive for the induction of non-associative synaptic depression under our experimental conditions.

TABLE 3.7i: Electrophysiological properties of CA1 neurones bathed in ASCF containing 4 mM Ca^{2+} before and after postsynaptic conditioning.

	Control (n=6)		Post-conditioning (n=6)	
Cell Characteristic:	Mean	±1SEM	Mean	±1SEM
Apparent R_{in} (MΩ)	30·9	2·6	30·6	3·0
Firing threshold (mV)	15·2	0·9	14·4	0·8
Action potential (mV)	66·8	2·1	67·5	2·4
Total spike height (mV)	81·9	2·1	81·9	2·3
V_m on stepping out (mV)			−73·9	1·3

Control values were obtained over the last 10 min of the baseline period. Post-conditioning values were obtained 30 to 40 min post-conditioning, or over the last 10 min of the recording period.

3.8 Postsynaptic conditioning of neurones bathed in the $GABA_A$ receptor antagonist bicuculline methiodide.

The ability of synapses to undergo heterosynaptic LTD has been shown to be facilitated in the presence of $GABA_A$ receptor antagonists in the dentate gyrus (Zhang & Levy, 1993; Tomasulo et al., 1993), the CA3 (Bradler & Barrionuevo, 1989), and in the CA1 region of the hippocampus (Abraham & Wickens, 1991; Scanziani et al., 1996). It was suggested that this increased probability of LTD induction was due to an increased Ca^{2+} entry at the test synapses during conditioning, because of an increased space constant leading to greater depolarization at the test synapses. The reduction in recurrent inhibition seen in low Ca^{2+} ACSF could act in such a way, increasing Ca^{2+} entry above that in normal ACSF. Conversely raised $[Ca^{2+}]_o$ might increase inhibition and thereby block LTD. To test the role of inhibition in my experiments, conditioning was conducted in the presence of the $GABA_A$ receptor antagonist bicuculline.

Postsynaptic conditioning failed to induce LTD in 7 cells in the presence of bicuculline, and had no significant effect upon electrophysiological properties (see Table 3.8i). A representative result is illustrated in Figure 3.8i. Cells were bathed in 1 μM (n = 2), 10 μM (n = 5), and 20 μM (n = 1) bicuculline methiodide for 18 to 114 min before baseline recordings commenced. EPSP slope was not significantly different from control levels at 12 min (95·8 ± 4·51% ±SEM; n = 7), or 28 min (99·9 ± 10·17% ±SEM; n = 5) post-conditioning. The pooled data from all 7 cells is shown in Figure 3.8ii.

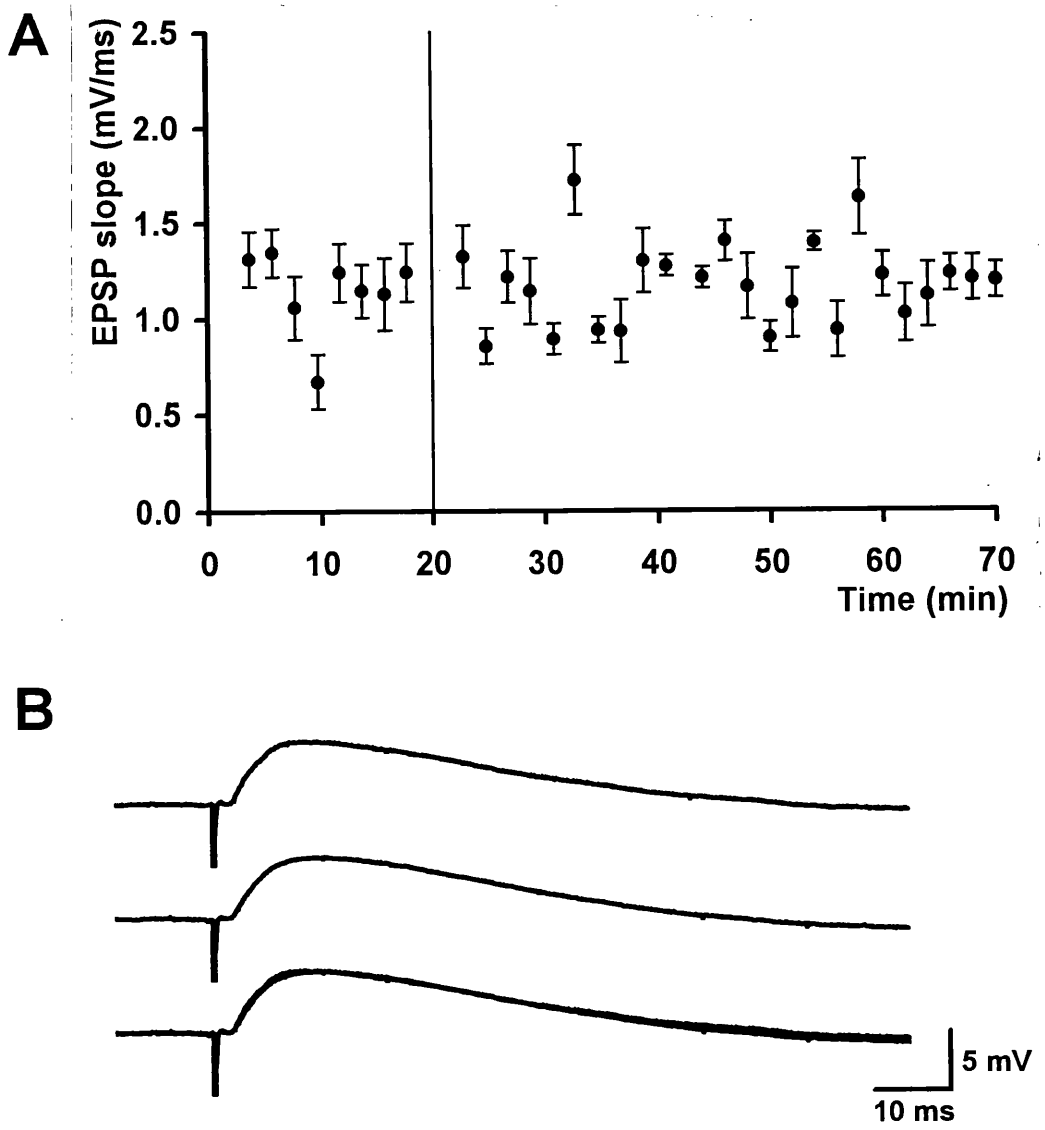

FIGURE 3.8i: Intracellular conditioning of a neurone bathed in the $GABA_A$ receptor antagonist bicuculline has no effect upon EPSP slope.

A Graph of mean EPSP slope against time in a single CA1 neurone bathed in the $GABA_A$ receptor antagonist bicuculline methiodide (10 μM). Intracellular depolarizing pulses (1× 1·0 nA; 4× 1·5 nA; 1× 1·7 nA and 2× 1·8 nA; vertical line on graph), evoking a mean of 19 spikes/pulse (range 16 to 22) failed to induce a depression of EPSP slope.

B Representative averaged traces of EPSPs from the CA1 neurone illustrated in A. Each is an average of 12 successive responses. Top: Recorded 10 to 6 min before the onset of postsynaptic conditioning. Middle: Recorded 30 to 34 min following conditioning. Bottom: Pre- and postconditioning responses superimposed.

Control: Apparent R_{in} 25 MΩ; spike threshold 11 mV; spike amplitude 80 mV (threshold to peak). Thirty minutes post conditioning: Apparent R_{in} 23 MΩ; spike threshold 12 mV; spike amplitude 79 mV. V_m on exit −74 mV.

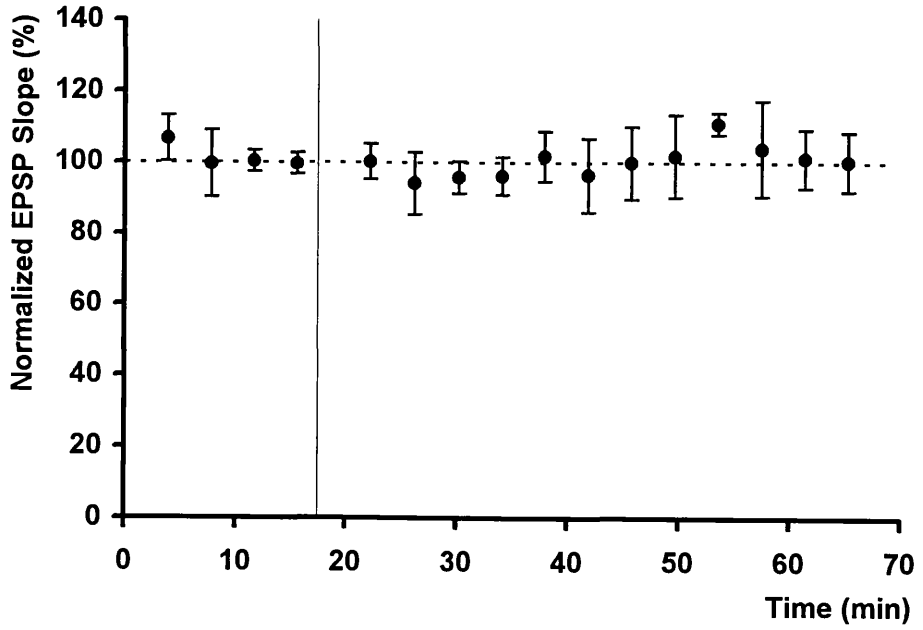

FIGURE 3.8ii: Failure to induce non-associative LTD in the presence of a $GABA_A$ receptor antagonist.

Postsynaptic conditioning had no effect upon EPSP slope in CA1 cells bathed in the $GABA_A$ receptor antagonist bicuculline methiodide (1, 10 or 20 μM). Mean normalized EPSP slope for seven cells is plotted against time (error bars are ±1 SEM). Conditioning pulses (vertical line on graph), +1·0 to 3·0 nA, elicited a median of 16 spikes/pulse (range 7 to 25). Slices were bathed in ACSF containing bicuculline for between 114 and 18 min before baseline recordings began. Broken horizontal line gives the 100% value over the last 8 min of the control.

TABLE 3.8i: Electrophysiological properties of CA1 neurones bathed in the $GABA_A$ receptor antagonist bicuculline before and after postsynaptic conditioning.

	Control (n=7)		Post-conditioning (n=7)	
Cell Characteristic:	Mean	±1SEM	Mean	±1SEM
Apparent R_{in} (MΩ)	28·8	4·1	26·6	4·1
Firing threshold (mV)	13·9	1·6	13·2	1·9
Action potential (mV)	71·8	4·6	72·7	4·4
Total spike height (mV)	85·7	3·9	85·9	3·6
V_m on stepping out (mV)			−73·0	2·4

Control values were obtained over the last 10 min of the baseline period. Post-conditioning values were obtained 30 to 40 min post-conditioning, or over the last 10 min of the recording period.

Comparing the number of spikes elicited during the conditioning period in bicuculline (16·3 ± 2·3 spikes ±SEM; n = 7), high $[Ca^{2+}]$ ACSF (16·9 ± 1·7 ±SEM; n = 6), and low $[Ca^{2+}]$ ASCF (27·6 ± 3·7 ±SEM; n = 9), a significant difference was found (single factor ANOVA; $P < 0·05$) between low Ca^{2+} ACSF and the other two media. Although significant, this finding may not be relevant since (as will be discussed in Section 3.13) intracellular conditioning in the presence of bicuculline resulted in non-associative depotentiation in 5 of 9 cells, with a mean of 17·0 ± 1·4 (±SEM) spikes per pulse. It may be that the difference in the number of spikes may not bear on LTD induction since it has been reported that action potential invasion of the dendrite fails with repeated spikes in a train (Spruston et al., 1995).

3.9 Postsynaptic conditioning and cæsium iontophoresis.

Kullmann et al., (1992) using unpaired postsynaptic depolarizing pulses (to 0 mV, 3 s duration 0·2 Hz, 20 pulses) reported synaptic enhancements which are NMDA receptor-independent and decremented back to baseline levels within 30 min. In these experiments intracellular electrodes or whole-cell patch pipettes contained cæsium ions, which would reduce K^+ conductances. This has been shown to allow a greater Ca^{2+} entry into the postsynaptic cell via VDCCs during the postsynaptic depolarization conditioning due to the increased space constant (Jaffe et al., 1992).

We repeated the technique of Kullmann et al., (1992), using our depolarizing pulse protocol. This protocol, in normal ACSF would provide another method of inducing large postsynaptic rises in $[Ca^{2+}]_i$ without interfering with inhibitory circuits. The recording pipettes were filled with 3 M CsAc, and recordings were made with a

steady negative current (−0·15 to −0·35 nA) to prevent leakage of Cs^+ into the postsynaptic cell. This steady "holding" current was removed during the conditioning procedure. Initially recordings were made from cells bathed in ACSF alone (n = 4), but in one cell, LTP of EPSP slope resulted from four pairings of afferent stimulation with depolarizing current pulses (resulting in only a single Na^+ spike) when testing for a reversed IPSP (Figure 3.9i). Subsequently all cells (n = 5) were bathed in the NMDA receptor antagonist D-APV (10 μM). The presence of D-APV was to prevent Ca^{2+} entry via the NMDA receptor-channel during pairing of presynaptic activity with postsynaptic depolarization or by NMDA receptor activation by ambient glutamate during postsynaptic depolarization (Sah et al., 1989).

Intracellular conditioning of cells under these conditions had variable effects. In two cells (both bathed in 10 μM D-APV) conditioning resulted in a short-term potentiation (STP) of EPSP slope similar to those reported by Kullmann et al., (1992). One of these cells is illustrated in Figure 3.9ii, showing also the typical appearance of the presumed Ca^{2+} spikes that were often seen during the conditioning protocol. A second conditioning in one of these cells after the potentiation had returned to baseline levels then resulted in a LTD of EPSP slope. A prolonged depression of synaptic transmission was also observed in another two cells in naive slices, one of which was bathed in D-APV. In two of these cells there was also an associated long-term increase in apparent R_{in} recorded following conditioning. Averaged normalized plots for EPSP slope and apparent R_{in} measurements for these three cells are illustrated in Figure 3.9iii. In an additional three cells (not shown) conditioning had no effect upon EPSP slope.

TABLE 3.9i: Electrophysiological properties of CA1 neurones before and after postsynaptic depolarization and Cs^+ iontophoresis, with or without the NMDA receptor antagonist D-APV.

	Control (n=7)		Post-conditioning (n=7)	
Cell Characteristic:	Mean	±1SEM	Mean	±1SEM
Apparent R_{in} (MΩ)	25·3	3·2	27·3	3·4
Firing threshold (mV)	13·0	1·4	12·5	1·9
Action potential (mV)	78·8	2·0	76·9	2·1
Total spike height (mV)	91·8	2·5	89·5	2·3
V_m on stepping out (mV)			−72·9	1·7

Control values were obtained over the last 4 min of the baseline period. Post-conditioning values 28 to 32 min after conditioning. All values measured when cell V_m held with −0·15 to −0·35 nA steady current.

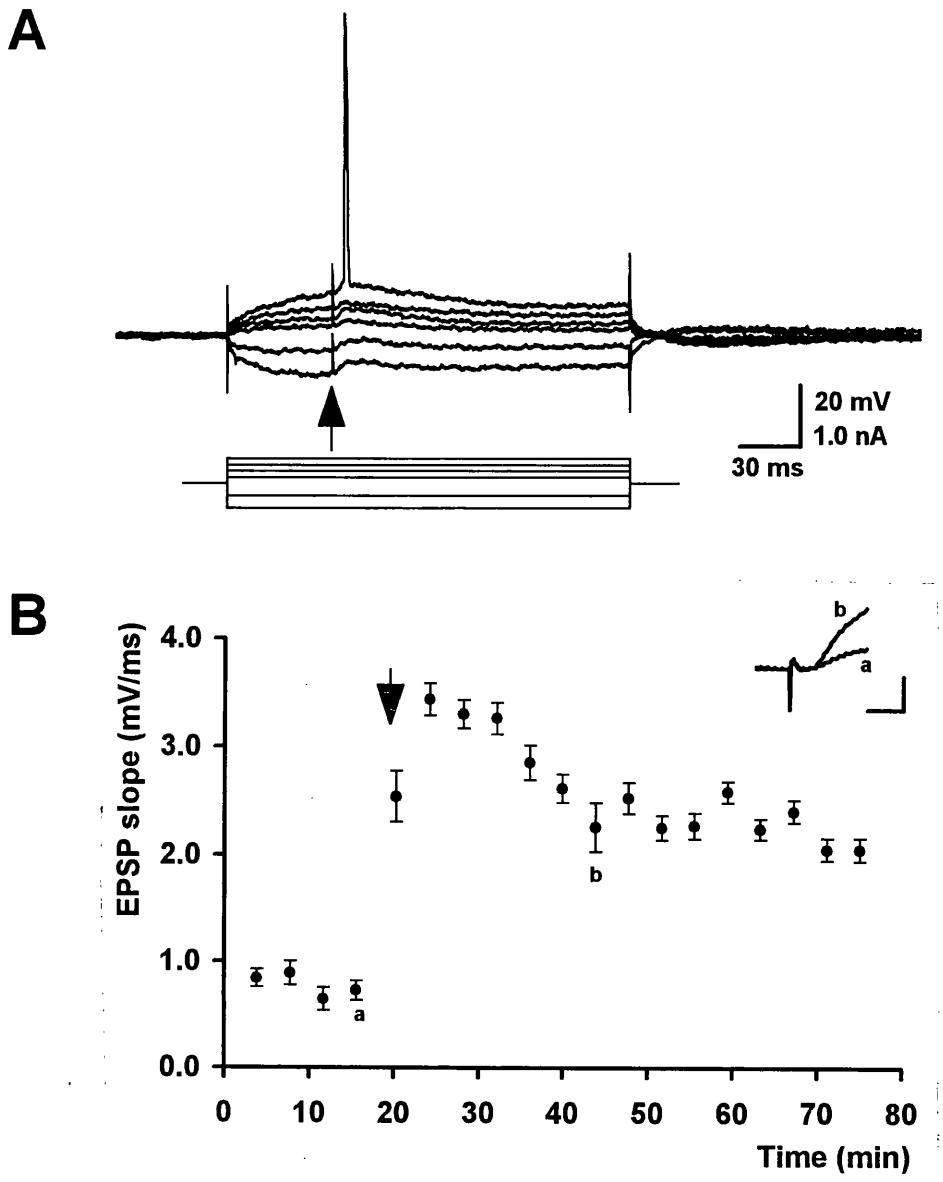

FIGURE 3.9i: LTP induced by pairing of orthodromic stimulation and depolarizing current pulses when Cs^+ is present in the electrode.

A Six superimposed responses to afferent stimulation occurring 50 ms (filled arrow) after the onset of varying levels on intracellularly injected steady current (–0·4 to +0·2 nA). Upper traces, voltage; lower traces current. Presumed ejection of Cs^+ into the cell at positive potentials paired with afferent stimulation has no major effect upon spike but caused long-term potentiation of the EPSP slope as shown in B.

B Graph of mean EPSP slope against time in a single cell before and after pairing of test stimulation with hyperpolarizing and depolarizing current pulses as shown in A (filled arrow on graph). Each point is an average of 16 responses. Inset: Representative averaged traces of EPSPs recorded a) 4 min before pairing and b) 28 min after pairing. Calibration bar: 5 mV, 10 ms.

Control: Apparent R_{in} 19 MΩ; spike threshold 15 mV; spike amplitude 75 mV (threshold to peak). Twenty eight minutes post conditioning: Apparent R_{in} 16 MΩ; spike threshold 15 mV; spike amplitude 89 mV. V_m on exit –62 mV.

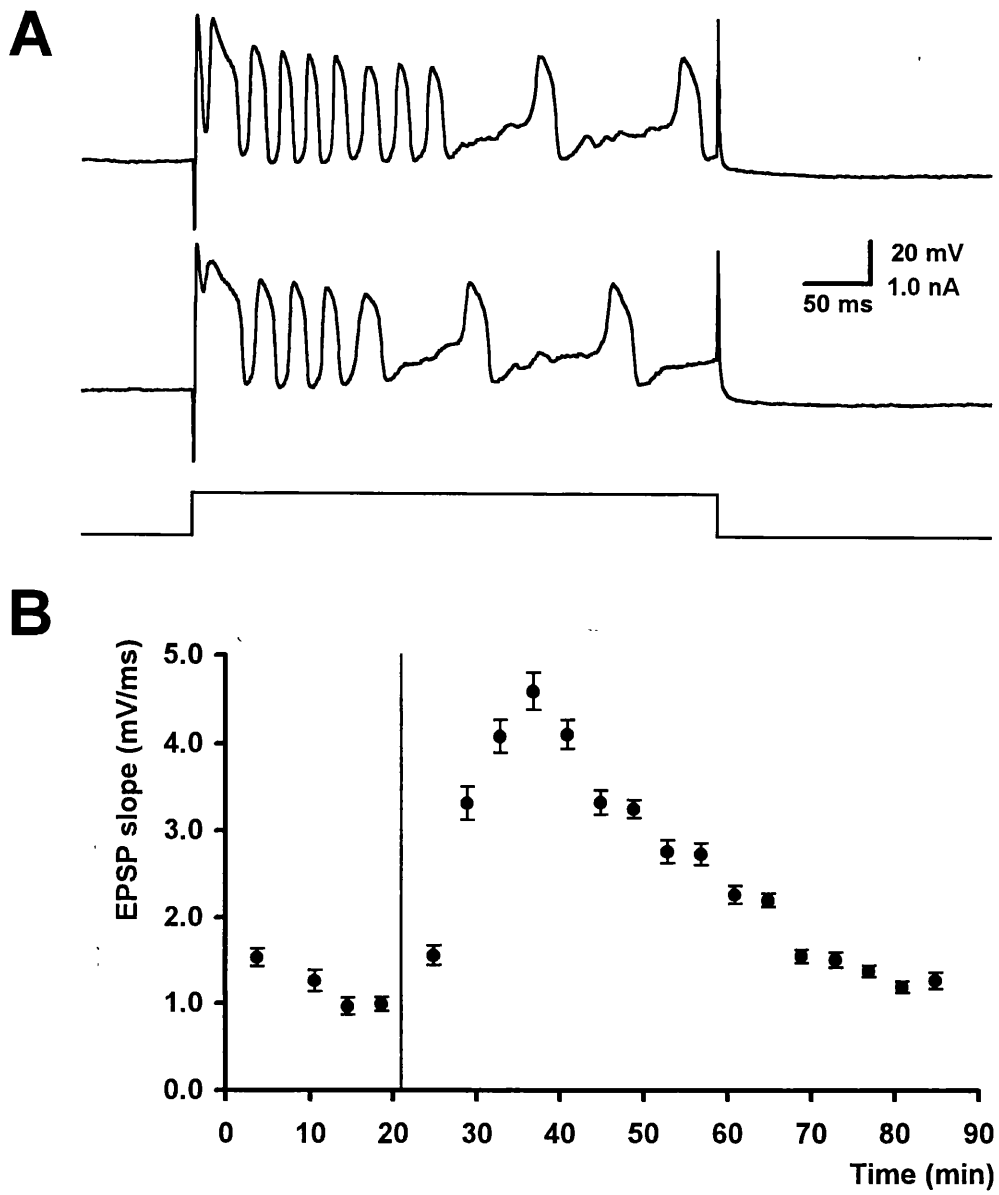

FIGURE 3.9ii: Intracellular injection of Cs^+ during conditioning can cause short term synaptic enhancements.

A Representative traces of spiking caused by iontophoretic injection of Cs^+ into a cell that caused a short term enhancement of EPSP slope (illustrated in B). Top and middle trace: voltage responses to the fourth and fifth (of eight) +1·0 nA depolarizing current pulses. Bottom: current.

B Graph of mean EPSP slope over time for a single cell showing a short-term potentiation of synaptic strength in response to Cs^+ entry during postsynaptic depolarization (vertical line). A constant negative current of –0·25 nA was applied to the cell for the duration of the experiment. The drug D-APV (10 μM) was present in the bathing solution throughout the experiment.

Control: Apparent R_{in} 38 MΩ; spike threshold 13 mV; spike amplitude 73 mV (threshold to peak). Thirty minutes post conditioning: Apparent R_{in} 29 MΩ; spike threshold 12 mV; spike amplitude 82 mV. V_m on exit –69 mV.

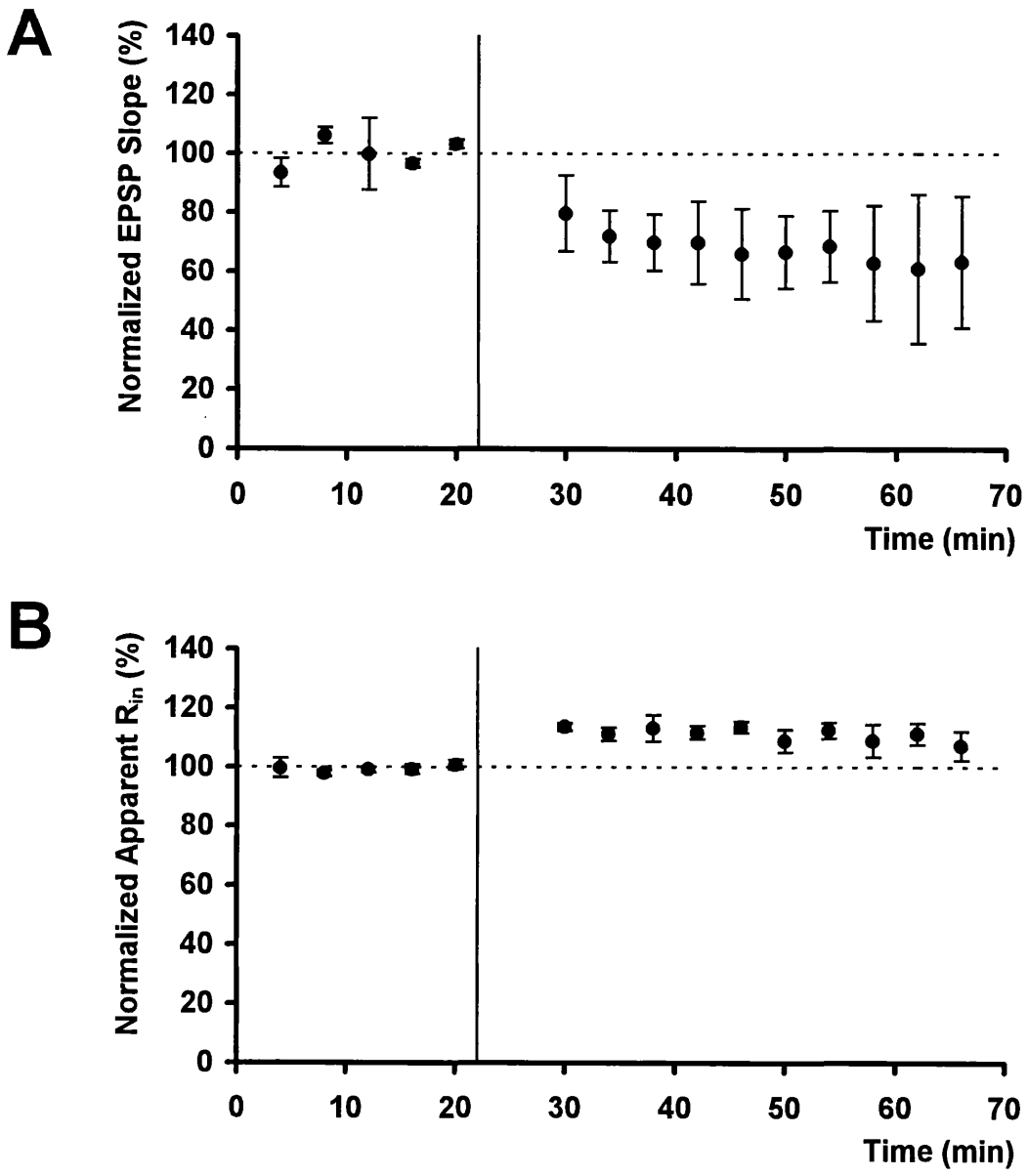

FIGURE 3.9iii: Intracellular injection of Cs^+ during conditioning can cause long-term depression of EPSP slope with an associated enhancement of apparent R_{in}.

A Mean normalized EPSP slope plotted against time for 3 cells that exhibited an LTD following postsynaptic depolarization and Cs^+ introduction into the cell. Error bars are ±1 SEM. Vertical line on graph indicates end of intracellular conditioning. Broken horizontal line gives the 100% value over the last 10 min of the control. The drug D-APV (10 μM) was present in the bathing solution of one of these cells.

B Mean normalized apparent R_{in} for the three cells illustrated in A, showing an increase following postsynaptic depolarization and Cs^+ introduction into the cell (Vertical line on graph). Error bars are ±1 SEM. Broken horizontal line gives the 100% value over the last 10 min of the control.

Generally there was a slight increase in mean apparent R_{in} following conditioning (n = 7; but it was not significant). In the cell illustrated in Figure 3.9ii there was a decrease. The possibility arises that following conditioning, cæsium ions introduced into the cell would have a greater effect upon the dendrites since some Cs^+ would have leaked into the soma between penetration and conditioning. Although there were no significant changes in cell characteristics comparing pre-and post-conditioning (see Table 3.9i), R_{in} and threshold measurements were carried out by postsynaptic injection of current which would mainly test somatic properties, while the effects of Cs^+ introduced into the dendrites during conditioning might not be detected. The blocking of dendritic K^+ channels could depolarize the dendrites resulting in a reduction in EPSP slope, without any corresponding changes in cell characteristics measured at the soma.

Assuming that all the effects seen following intracellular conditioning were physiological it may not be so surprising that LTD, no effect and STP were seen since it was difficult to ensure consistency of the conditioning protocol with Cs^+ in the recording electrode. It was in practice very hard to control the amount of Cs^+ that entered the cell and as a consequence the number of spikes elicited during conditioning varied in both width and number.

PART 3: The postsynaptic induction of non-associative depotentiation.

3.10 Introduction.

In the CA1 region of the hippocampus low frequency stimulation (LFS; ~900 pulses, 1 to 5 Hz) of the Schaffer collateral test pathway induced an input-specific homosynaptic LTD of the test synapses (Dudek & Bear, 1992; Mulkey & Malenka, 1992). Several groups however have failed to repeat the induction of LTD with LFS, but have seen a depotentiation of previously potentiated synaptic transmission using the same LFS protocol (Barrionuevo et al., 1980; Staubli & Lynch, 1990; Fujii et al., 1991; Bashir & Collingrigde,1994; O'Dell & Kandel, 1994).

A form of heterosynaptic depotentiation has also been reported to exist in the CA1 region of the hippocampus, when LFS stimulation applied to one afferent pathway reversed potentiation previously induced in a second afferent pathway to the same population of cells (Muller et al., 1995). The possibility that failure to postsynaptically induce non-associative LTD in many of my experiments was due to the test synapses

already being in a maximally depressed state was tested by inducing potentiation in the test pathway before intracellular conditioning was applied. Since the induction of LTP has been shown to be facilitated in the presence of a $GABA_A$ receptor antagonist (Wigström & Gustafsson, 1983), bicuculline was present in the bathing medium throughout these experiments.

3.11 Bath application of 25 mM TEA fails to induce LTP.

In order to study non-associative depotentiation, it was first necessary to induce a stable potentiation of EPSP slope. This was attempted first by the transient application of 25 mM tetraethylammonium (TEA) to the bathing medium (normal ACSF; 10 μM bicuculline) for a 7 min period. The addition of TEA to the bathing medium has been reported to result in a robust LTP, triggered by a large Ca^{2+} entry through VDCCs (Aniksztejn & Ben-Ari, 1991; Huang & Malenka 1993). TEA block of K^+ conductances causes a reversible increase in presynaptic activity and broadening of action potentials and Ca^{2+} entry through VDCCs. TEA-induced LTP has been shown to be partially (Huber et al., 1995) or totally NMDA receptor independent (Aniksztejn & Ben-Ari, 1991; Huang & Malenka 1993), but is presumed to share similar biochemical mechanisms since it partially occludes tetanus induced LTP.

In three cells tested, application of 25 mM TEA to the bathing medium failed to induce LTP, only producing a transient potentiation over a period of 50 to 60 min. The magnitude of potentiation in these cells at 16 to 18 min following TEA wash-out was maximal at 189·8 ± 14·2% (±SEM), but declined to 115·0 ± 23·0% (±SEM) at 58 to 60 min. A mean normalized plot of the three cells is illustrated in Figure 3.11iA. There was no significant change in cell characteristics at 16 to 20 or 56 to 60 min after TEA wash-out compared with control levels (see Table 3.11i).

During perfusion of TEA there was a large increase in the initial slope of the EPSP (resulting in cell spiking) which has been attributed to an increase in presynaptic release caused by a transient and reversible increase in the duration of the fibre volley (Huang & Malenka, 1993). In addition, TEA also broadens action potentials resulting in the initiation of Ca^{2+} spikes (Lancaster & Nicoll, 1987; Storm, 1987). Examples of representative EPSPs recorded before and during TEA perfusion from one of the three cells, is illustrated in Figure 3.11iB.

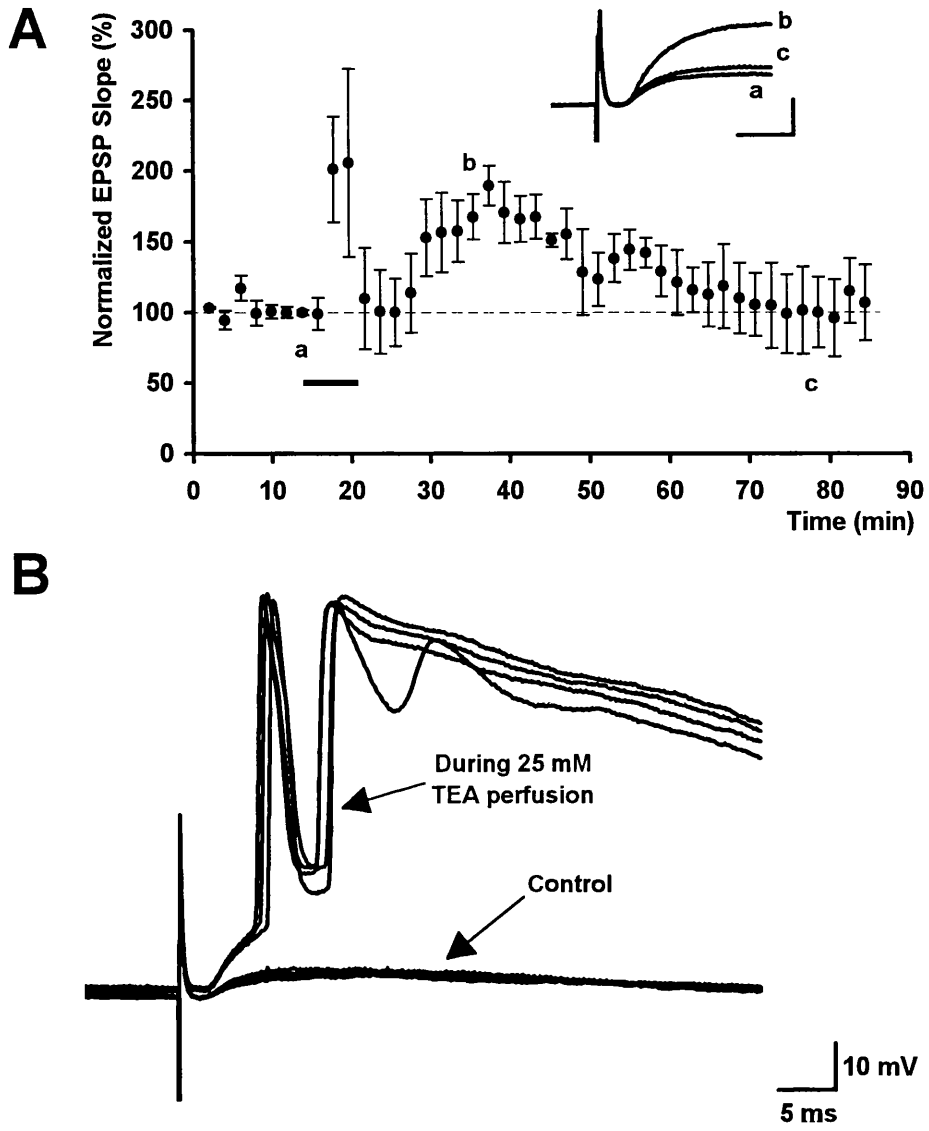

FIGURE 3.11i: Transient bath application of TEA does not produce LTP.

A Mean normalized EPSP slope (2 min averages) plotted against time for 3 cells that exhibited STP following a 7 min application of 25 mM TEA. Error bars are ±1 SEM. Thick horizontal line on graph indicates wash-in of TEA. Broken horizontal line gives the 100% value over the last 10 min of the control. 10 μM bicuculline was present throughout in all cells. Inset shows superimposed averages of six consecutive EPSPs from one of the cells recorded at times indicated on the main graph; a) the last 2 min before application of TEA; b) 14 to 16 min following wash-out of TEA; and c) 58 to 60 min following TEA washout. Calibration bar: 5 mV, 5 ms.

B Four successive responses recorded before and during application of 25 mM TEA. TEA block of K^+ mediated currents resulted in a transient large increase in EPSP slope (presumably increasing fibre volley duration and increased transmitter release) and prevented immediate repolarization following action potential generation. Control: Apparent R_{in} 32 MΩ; spike threshold 15 mV; spike amplitude 68 mV (threshold to peak). During TEA application: Apparent R_{in} 28 MΩ; spike threshold 15 mV; spike amplitude 71 mV; V_m on exit −70 mV.

TABLE 3.11i: Electrophysiological properties of CA1 neurones before and after bath application of 25 mM TEA.

	Control		16-20 min post TEA wash-out		56-60 min post TEA wash-out	
Cell Characteristic:	Mean	±1SEM	Mean	±1SEM	Mean	±1SEM
Apparent R_{in} (MΩ)	27·1	3·0	28·7	3·0	28·7	3·0
Firing threshold (mV)	13·7	1·3	14·6	0·6	14·8	1·5
Action potential (mV)	67·2	3·9	70·8	4·6	68·8	5·1
Total spike height (mV)	80·9	5·1	85·4	5·1	83·6	6·6
V_m on stepping out (mV)					−74·4	2·4

Control values were obtained over the last 4 min of the baseline period. n=3 throughout.

3.12 Induction of lasting potentiation with a theta burst stimulation protocol.

Since only transient short lasting increases in synaptic strength were achieved following the application of TEA to the bathing medium a different method was sought to produce non-decrementing synaptic potentiation. Theta burst stimulation (TBS) has been reported to induce stable LTP in both the *in vitro* (Larson & Lynch, 1986; Larson et al., 1986) and the *in vivo* preparation (Staubli & Lynch, 1987). TBS consists of short bursts (4 or 5 pulses at 100 Hz) repeated at a 'theta' rhythm (~5 Hz) which corresponds to the electroencephalogram (EEG) frequency found in exploring rats (Vanderwolf, 1969; Otto et al., 1991) and which modulates firing of CA1 pyramidal cells (Ranck, 1973). TBS induced LTP has been reported to occlude tetanus-induced LTP (Diamond et al., 1988) and is NMDA receptor dependent (Diamond et al., 1988; Larson & Lynch, 1988).

TBS resulted in a stable potentiation in 8 of 20 cells tested. In these 8 cells maximal potentiation was seen at 4 to 8 min after the end of TBS; stabilizing to 200·9 ± 33·3% (±SEM) of control levels at 16 to 20 min post-conditioning. In the other 12cells, TBS produced no effect, EPSP slope was 98·0 ± 6·5% (±SEM) of control levels at 16 to 20 min post-conditioning. Figure 3.12i illustrates pooled graphs of cells in which TBS had no effect and those in which TBS resulted in potentiation.

Table 3.12i illustrates cell characteristics measured before and after TBS for all 20 cells. There were no significant differences between the electrophysiological properties measured before and after TBS for the group as a whole (n=20) or within potentiation group (n=8) or the no effect group (n=12). In addition there were no significant differences in cell characteristics measured across the two groups.

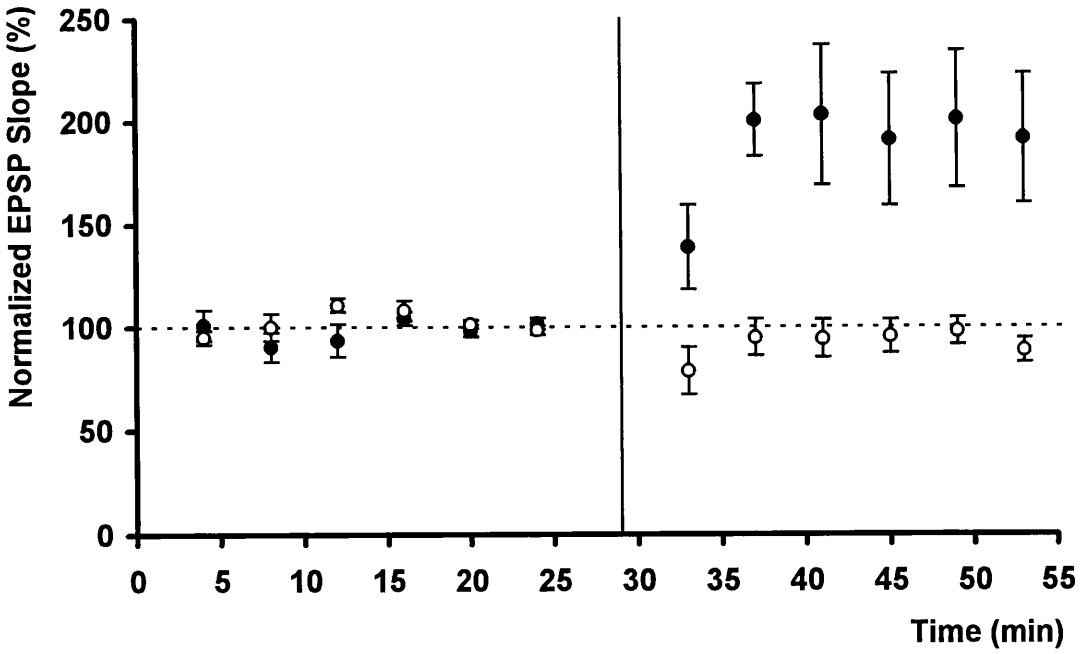

FIGURE 3.12i: TBS results in potentiation in only a population of cells.

Mean normalized slope (4 min averages) of cells in which TBS resulted in a potentiation of EPSP slope (closed circles; n=8) or had no effect (open circles; n=12). Error bars are ±1 SEM. Vertical line indicates end of TBS. Broken horizontal line gives the 100% value over the last 10 min of the control. 10 μM bicuculline was present throughout in all cells.

The reason why TBS induced potentiation of synaptic transmission in less than half the cells tested is unknown. It may be related to the increased width of the test stimulus during conditioning as Barr et al., (1995) have reported that under conditions in which TBS normally results in LTP, increasing the test shock strength tenfold led TBS to have no effect on synaptic transmission in naive synapses.

TABLE 3.12i: Electrophysiological properties of cells before and after TBS.

	Control (n=20)		Post-TBS (n=20)	
Cell Characteristic:	Mean	±1SEM	Mean	±1SEM
Apparent R_{in} (MΩ)	25·2	2·3	25·1	2·5
Firing threshold (mV)	13·3	0·5	12·9	0·6
Action potential (mV)	75·9	1·6	75·3	1·4
Total spike height (mV)	89·2	1·7	88·2	1·6
V_m on stepping out (mV)			−72·7	1·6

Control values were obtained over the last 4 min of the baseline period. Post-conditioning values 20 to 24 min after conditioning.

3.13 Induction of non-associative depotentiation by postsynaptic depolarization.

Twenty four minutes after the end of TBS in the eight cells that showed a clear potentiation of EPSP slope, intracellular conditioning was applied. Postsynaptic conditioning resulted in a depotentiation (> 15% depression of potentiated level) in three of these cells. Data from one of these cells is shown in Figure 3.13i. In all three cells the depotentiation was near maximal immediately following conditioning. The magnitude of depotentiation was different in all three cells. The cell illustrated in Figure 3.13i was depotentiated to above original pre-TBS baseline levels, of the other two cells one depotentiated to below baseline levels and one depotentiated to baseline levels. The extent of the depotentiation could be related to the magnitude of the TBS induced potentiation,where the greatest potentiation resulted in the least depression, but a larger sample would be needed to clarify this issue. Figure 3.13iiA illustrates a pooled graph of these three cells normalized to the eight minutes pre-TBS. Figure 3.13iiB is again a pooled graph of these three cells normalized to the eight minute period pre-intracellular conditioning showing a depotentiation of the mean normalized EPSP slope to 56·5 ± 5·01% (±SEM) at 40 to 44 min following postsynaptic conditioning. Several groups have reported that LFS was unable to induce a depotentiation once LTP had consolidated for around one hour (O'Dell & Kandel, 1994; Staubli & Chun, 1996).

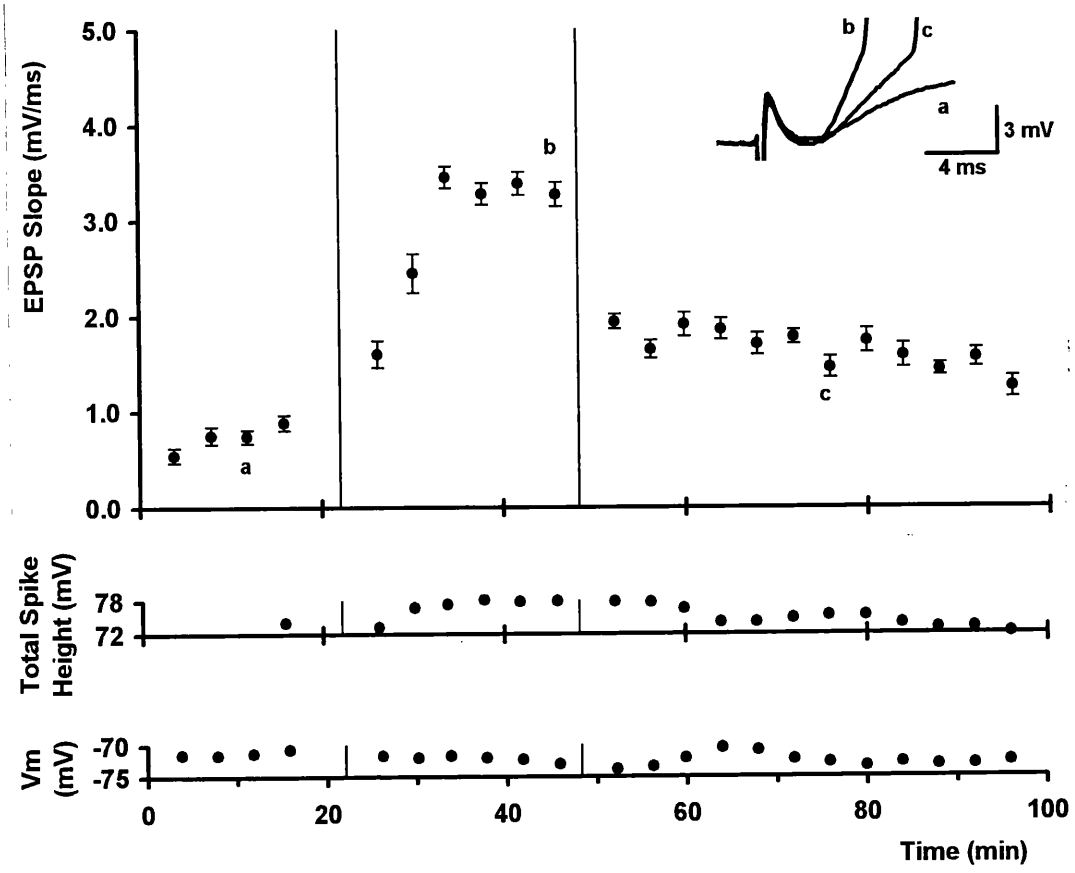

FIGURE 3.13i: Potentiation by TBS followed by depotentiation induced by postsynaptic conditioning.

Graphs from top down: EPSP slope against time, each point an average of 16 successive EPSPs; total spike height for action potentials on suprathreshold EPSPs, averages of $4 \leq n \leq 16$; resting membrane potential. First vertical line indicates end of theta burst stimulation. Second vertical line indicates the end of intracellular conditioning, eight 400 ms depolarizing pulses (+1·0 to 1·5 nA), eliciting an average of 15 spikes/pulse (range 11 to 20). Inset at top right illustrates the onset of three superimposed EPSPs (a, b and c), each an average of 16 traces taken from times indicated on the top graph; a) 4 to 8 min before afferent theta stimulation (all subthreshold); b) the last 4 min before intracellular conditioning (all suprathreshold); c) 28 to 32 min after the end of intracellular conditioning (all suprathreshold).

Control (4 min pre-theta stimulation): Apparent R_{in} 27 M ; spike threshold 10 mV; spike amplitude 64 mV (threshold to peak). Four minutes before intracellular conditioning: Apparent R_{in} 24 MΩ; spike threshold 8 mV; spike amplitude 68 mV. Thirty minutes post conditioning: Apparent R_{in} 28 MΩ; spike threshold 8 mV; spike amplitude 66 mV. V_m on exit −61 mV.

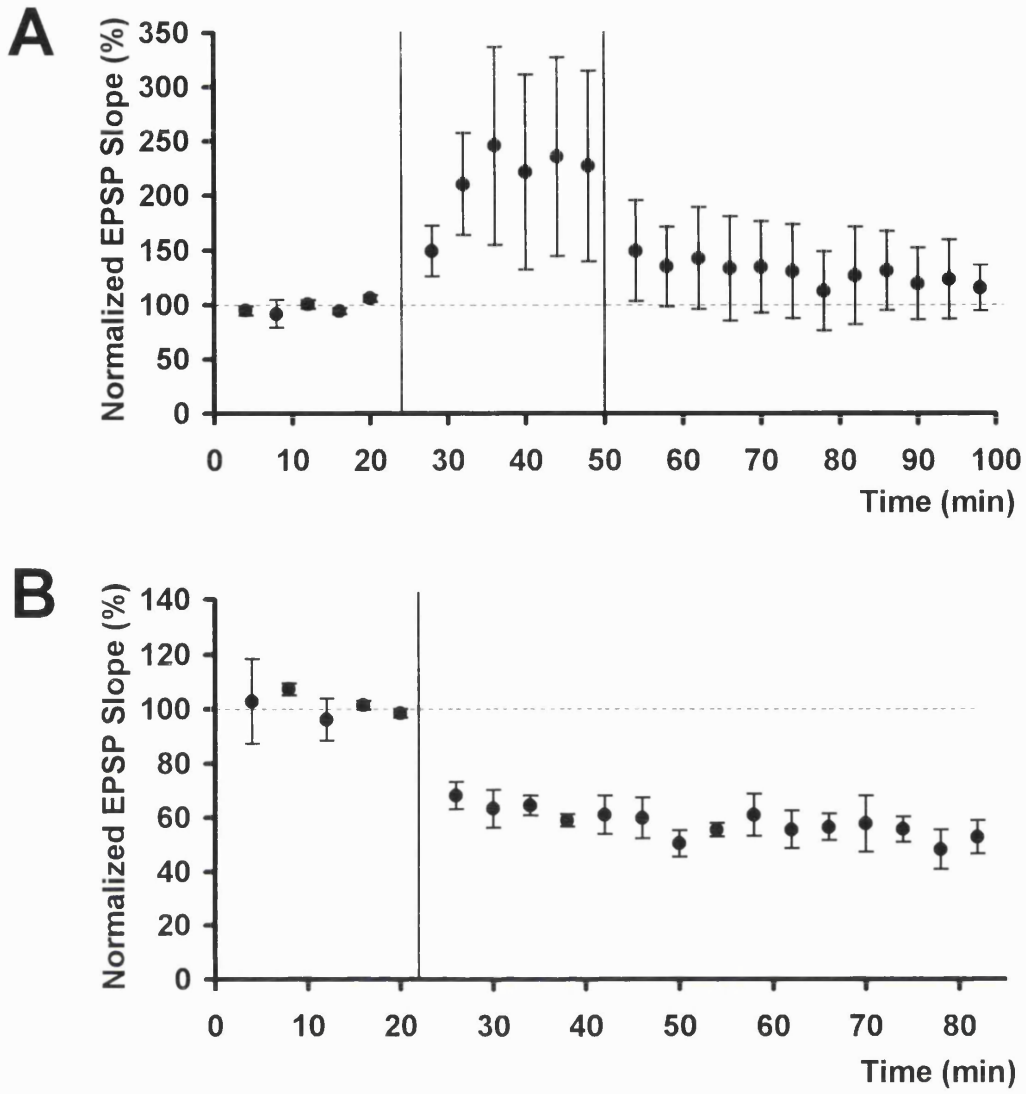

FIGURE 3.13ii: Postsynaptic induction of non-associative depotentiation following TBS induced potentiation.

A Mean normalized EPSP slope (4 min averages) plotted against time for 3 cells that exhibited a postsynaptically induced depotentiation following TBS induced potentiation of EPSP slope. Graph normalized to the last 8 min before TBS. Error bars are ±1 SEM. First vertical line represents the end of TBS, the second vertical line represents the end of intracellular conditioning. Broken horizontal line gives the 100% value over the last 8 min of the control. 10 μM bicuculline was present throughout in all cells.

B Mean normalized EPSP slope (4 min averages) plotted against time for 3 cells as shown in A, normalized to the last 8 min before intracellular conditioning. Error bars are ±1 SEM. Vertical line represents the end of intracellular conditioning. Broken horizontal line gives the 100% value over the last 8 min of the control. 10 μM bicuculline was present throughout in all cells.

Figure 3.13iii represents a single experiment where LFS (1 Hz; 900 pulses), in the presence of 1 μM bicuculline, induced a delayed LTP of greater than 50 min duration, after which intracellular conditioning induced a clear depotentiation of synaptic strength. These results indicates that non-associative depotentiation may be induced via different mechanisms than homosynaptic depotentiation.

Figure 3.13ivA is a pooled figure of the 9 cells in which intracellular conditioning was applied following the induction of potentiation in the test synapses divided into those cells in which no significant change was observed (n = 5; P = 0·65; comparing 36 to 40 min postconditioning levels to control) and those cells which a significant depotentiation was produced (n = 4; P = 0·0006; comparing 36 to 40 min postconditioning levels to control). Figure 3.13ivB is a pooled graph of all nine cells, in which a significant depotentiation was still evident (P = 0·01; compared with normalized potentiated control levels). Table 3.13i illustrates cell characteristics before and after intracellular conditioning for all 9 cells.

TABLE 3.13i: Electrophysiological properties of cells before and after intracellular conditioning compared with potentiated (control) levels.

	Control (n=9)		Post-conditioning (n=9)	
Cell Characteristic:	Mean	±1SEM	Mean	±1SEM
Apparent R_{in} (MΩ)	21·1	2·8	21·5	2·8
Firing threshold (mV)	13·2	0·8	13·5	0·9
Action potential (mV)	75·3	2·5	74·7	3·0
Total spike height (mV)	88·7	2·6	88·2	3·1
V_m on stepping out (mV)			−72·3	2·6

Control values were obtained over the last 4 min of the baseline period. Post-conditioning values 20 to 24 min after conditioning.

3.14 Postsynaptic conditioning of cells in which TBS had no effect.

Wexler & Stanton, (1993) reported that not only is the magnitude of LFS induced depression increased by prior LTP, but also by a subthreshold LTP-inducing tetanus. To test for the possibility that TBS itself might prime synapses for intracellular conditioning to induce a depression/depotentiation, conditioning was applied to six of the cells in which TBS had no effect.

Figure 3.14iA is a averaged graph of EPSP slope against time for a single cell where TBS failed to induce potentiation of synaptic strength followed by intracellular conditioning which again failed to change EPSP slope. Figure 3.14iB is a pooled graph of mean normalized EPSP slope against time for 6 cells where intracellular conditioning

FIGURE 3.13iii: Postsynaptic induction of non-associative depotentiation following a LFS induced LTP in a single cell.

A Graph of EPSP slope against time, each point an average of 16 successive EPSPs. Thick horizontal line indicates duration of afferent LFS (1 Hz; 900 pulses) which initially depressed EPSP slope, but then induced a long-term potentiation of synaptic strength. Second vertical line indicates the end of intracellular conditioning, eight 400 ms, 1·0 nA depolarizing pulses, eliciting an average of 19 spikes/pulse (range 16 to 22), which induced a non-associative depotentiation of EPSP slope. 1 μM bicuculline present throughout.

B Illustration of the onset of three averaged (16 consecutive sweeps) EPSPs taken: a) The last 4 min before LFS (all subthreshold); b) the last 6 to 2 min before intracellular conditioning, 56 to 50 min after the end of LFS (12 of 16 suprathreshold); c) 20 to 24 min after the end of intracellular conditioning (10 of 16 suprathreshold); d) all three superimposed. Calibration bar: 2 mV, 1 ms.

Control (4 min pre-LFS): Apparent R_{in} 19 MΩ; spike threshold 15 mV; spike amplitude 70 mV (threshold to peak). Four minutes before intracellular conditioning: Apparent R_{in} 25 MΩ; spike threshold 15 mV; spike amplitude 70 mV. Thirty minutes post conditioning: Apparent R_{in} 24 MΩ; spike threshold 14 mV; spike amplitude 68 mV. V_m on exit −67 mV.

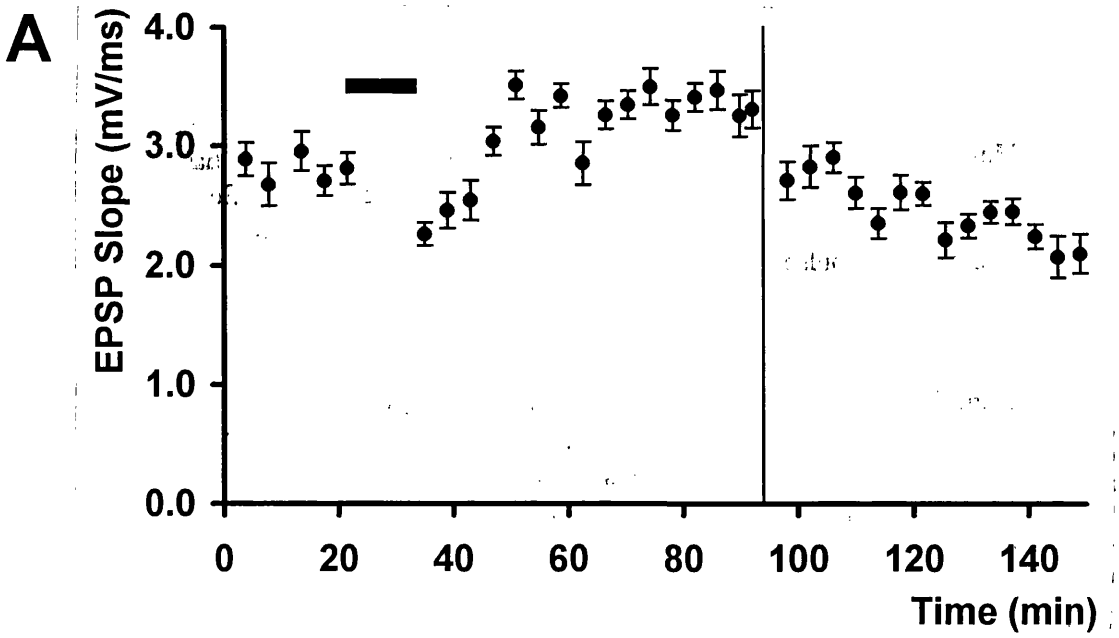
A
EPSP Slope (mV/ms)
4.0
3.0
2.0
1.0
0.0
0
20
40
60
80
100
120
140
Time (min)

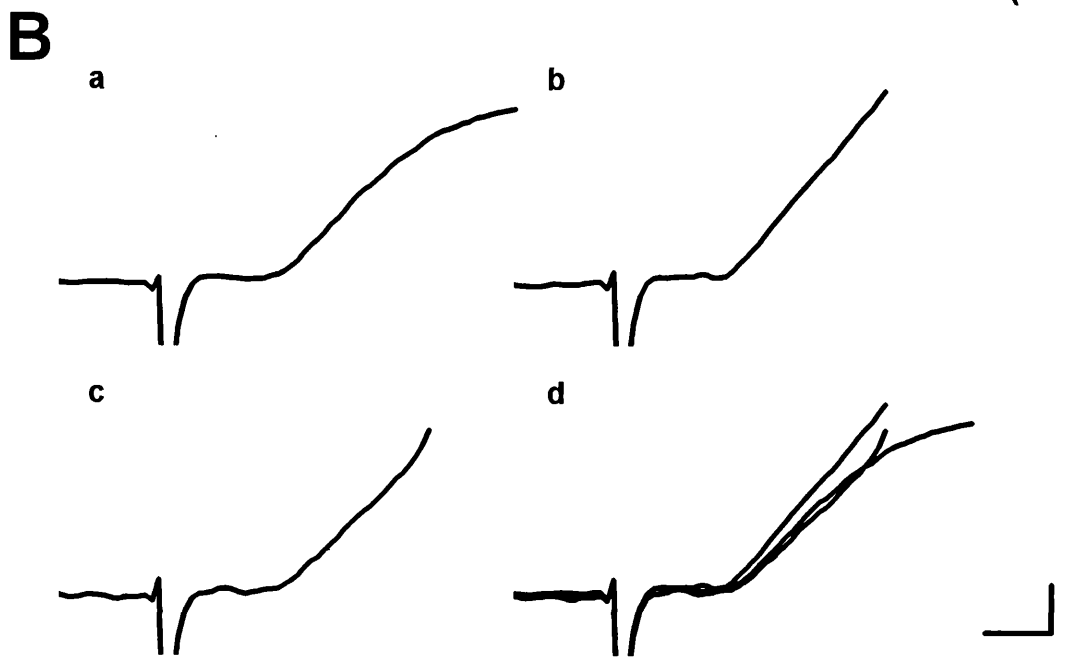
B
a
b
c
d

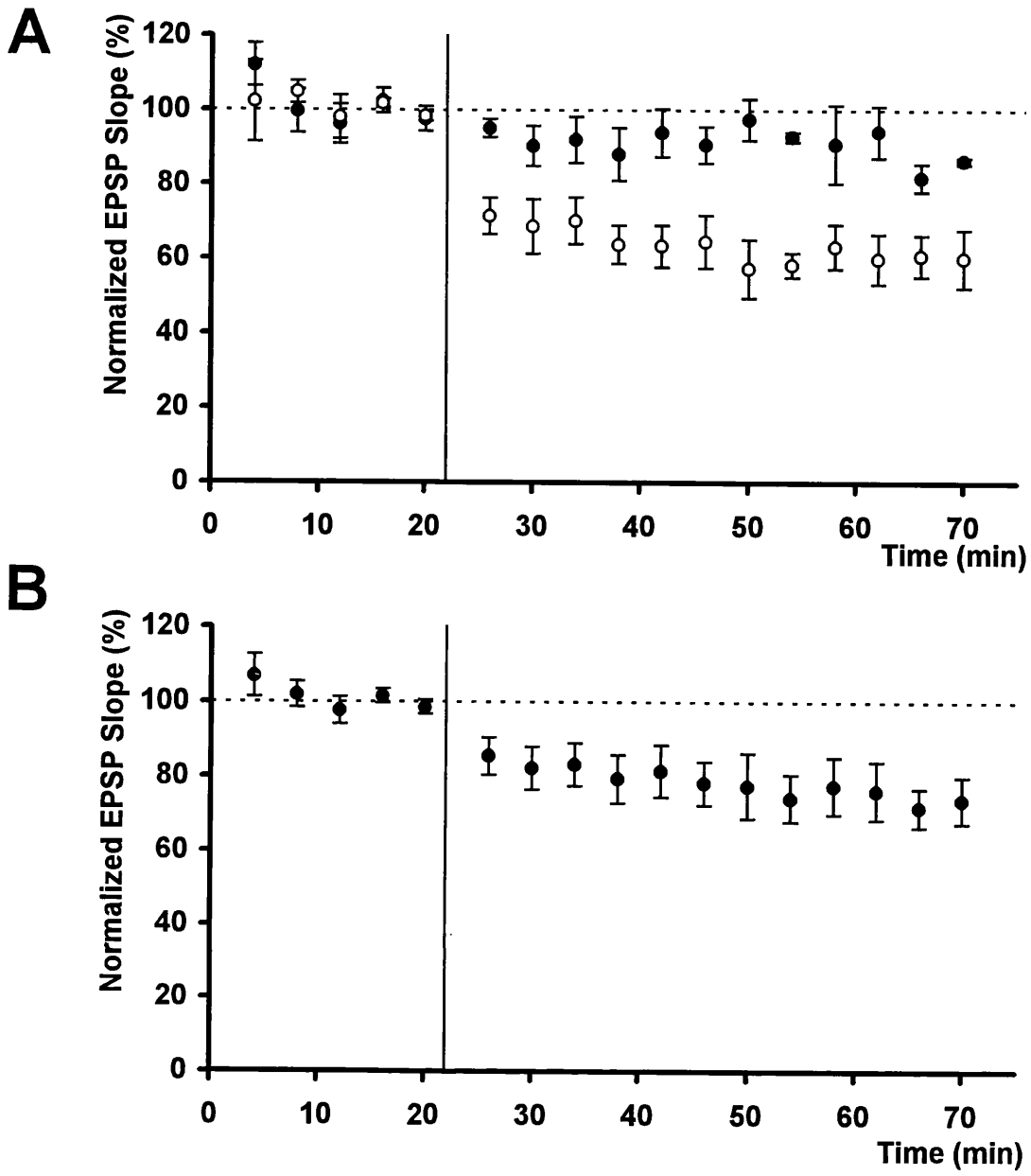

FIGURE 3.13iv: Postsynaptic induction of non-associative depotentiation.

A Mean normalized EPSP slope for 5 cells (closed circles) plotted against time for which postsynaptic conditioning had no effect on EPSP slope, and for the 4 cells (open circles) in which intracellular conditioning induced a non-associative depotentiation. Normalized to the last 8 min before intracellular conditioning. Error bars are ±1 SEM. Vertical line on graph indicates end of intracellular conditioning. Broken horizontal line gives the 100% value over the last 8 min of the control. 10 μM bicuculline present in all cells except one (1 μM).

B Mean normalized EPSP slope plotted against time for all 9 cells illustrated an A. A significant depotentiation of EPSP slope can be seen compared with control values, when all nine cells are pooled. Error bars are ±1 SEM. Vertical line on graph indicates end of intracellular conditioning.

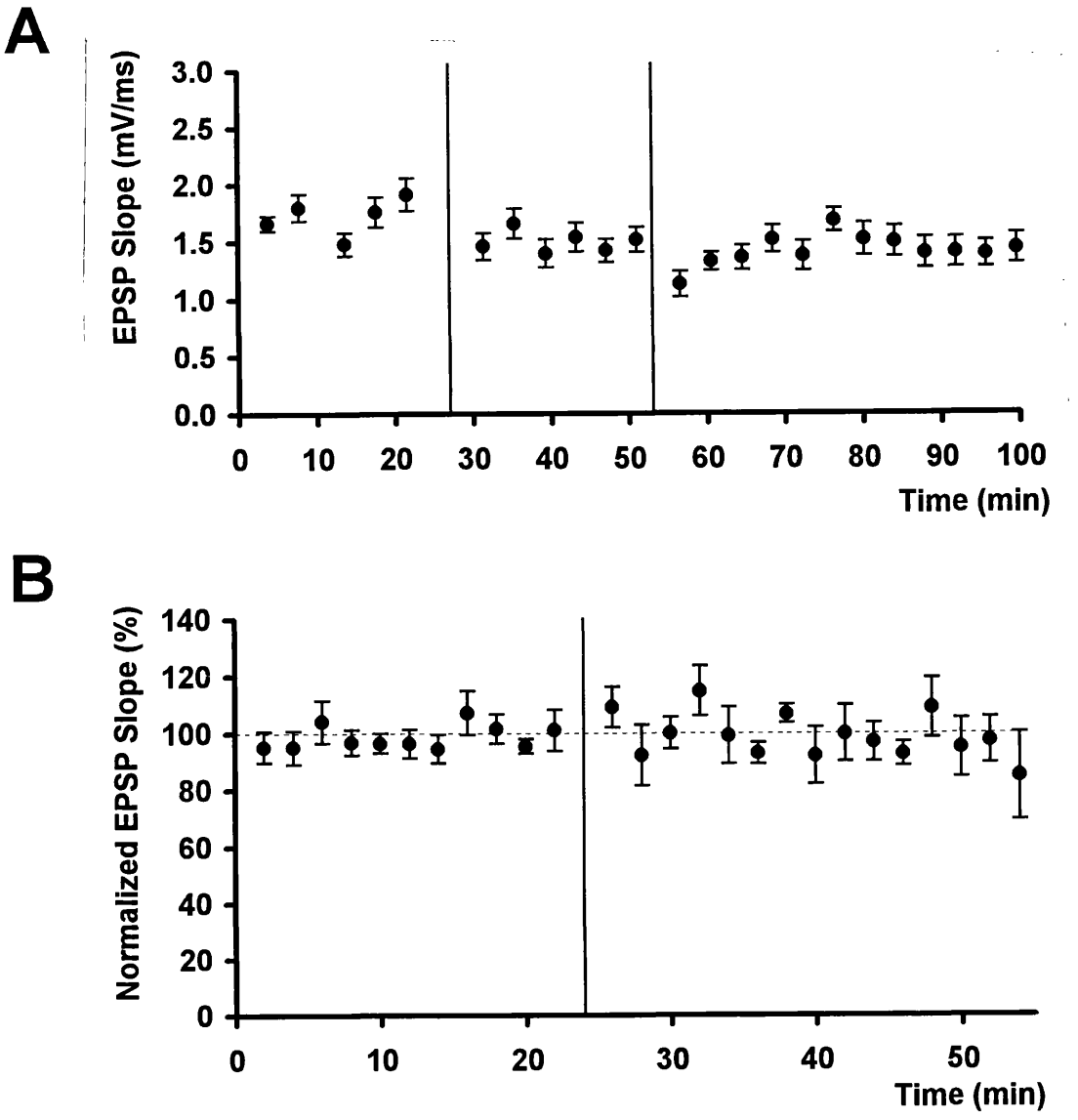

FIGURE 3.14i: Failure of intracellular conditioning to depress synaptic strength when TBS has no effect.

A Plot of EPSP slope against time for a single cell in which TBS failed to induce synaptic potentiation, followed by intracellular conditioning. Each point is an average of 16 consecutive EPSPs. First vertical line indicates the end of TBS. Intracellular conditioning (indicated by the second vertical line) consisted of eight, 400 ms, 1·0 nA depolarizing pulses eliciting an average of 17 spikes/pulse (range 16 to 19) failed to reduce the strength of synaptic transmission.

Control (4 min pre-TBS): Apparent R_{in} 40 MΩ; spike threshold 13 mV; spike amplitude 67 mV (threshold to peak). Four minutes before intracellular conditioning: Apparent R_{in} 38 MΩ; spike threshold 13 mV; spike amplitude 67 mV. Thirty minutes post conditioning: Apparent R_{in} 41 MΩ; spike threshold 12 mV; spike amplitude 67 mV. V_m on exit −69 mV.

B Mean normalized EPSP slope (2 min averages) plotted against time for 6 cells in which intracellular conditioning had no effect following TBS which failed to potentiate EPSP slope. Error bars are ±1 SEM. Vertical line indicates the end of intracellular conditioning. Broken horizontal line gives the 100% value over the last 10 min of the control. 10 μM bicuculline was present throughout in all cells.

followed a TBS no effect (not showing TBS). In all 6 cells intracellular conditioning failed to induce a significant decrease of synaptic transmission ($P = 0{\cdot}34$; at 28 to 30 min post conditioning compared with control levels), showing that 'priming' TBS had no effect on the outcome of subsequent IC in CA1 cells.

CHAPTER 4

RESULTS: Measurements of somatic and dendritic $[Ca^{2+}]_i$ during postsynaptic conditioning.

4.1 Introduction.

Experiments described in this section consist of measurements of intracellular calcium using the ratiometric calcium indicator Fura-2. Postsynaptic $[Ca^{2+}]_i$ measurements were obtained from 21 CA1 neurones from a total of 21 submerged hippocampal slices from 20 rats. Experiments are divided into two parts:

1) Those carried out in 1992; Ca^{2+} imaging experiments performed by Dr Alex Nowicky, Dr Lynn Bindman and Dr Stephen Bolsover, while concurrently recording post synaptic potentials. The initial fluorescence measurements were preformed by Dr Nowicky. Electophysiological analysis and all $[Ca^{2+}]_i$ calculations were performed by myself.

2) Those carried out in 1994; Ca^{2+} imaging experiments experiments performed by myself, Dr Richard Vickery, Dr Lynn Bindman and Dr Stephen Bolsover. In these experiments electrophysiological data was recorded but in the absence of test stimulation to evoke EPSPs.

All of the experiments described in this section were performed in the laboratory of Dr Stephen Bolsover.

4.2 Measurements of resting $[Ca^{2+}]_i$.

Throughout the experiment, at regular intervals, a ratio fluorescence measurement was obtained following excitation at 350 then 380 nm. Resting $[Ca^{2+}]_i$ could then be calculated. It was noted that the somatic resting $[Ca^{2+}]_i$ calculated for cells experimented on in 1992 were significantly higher than for the cells experimented on in 1994 (53 ± 5 nM; n = 11 and 24 ± 3 nM; n = 9 respectively; $P = 0{\cdot}0004$ unpaired t-test, 2 tailed). This inconsistency, perhaps accounted for by differences in calibration before each set of experiments was problematic when comparing experiments across these groups (see Section 4.7). The focus of the studies was on the effects of a particular protocol which raised $[Ca^{2+}]_i$ within a single cell. For such changes in $[Ca^{2+}]_i$, baseline differences are unlikely to matter particularly as most comparisons were made in one cell in successive measurements made in different bathing media.

Spatial and temporal distrubution on resting $[Ca^{2+}]_i$ were investigated by pooling resting $[Ca^{2+}]_i$ levels within three groups; soma (n =6), proximal apical dendrite (up to 100 μm from the soma; n = 6) and distal apical dendrite (100 to a maximum of 250 μm from the soma; n = 6), at different times during an experiment (see Figure 4.2i) from a total of nine cells. All data presented in this section are from experiments performed in 1992.

There were no significant differences observed between resting $[Ca^{2+}]_i$ measured in the soma (47 ± 8 nM; n=6), the proximal dendrite (59 ± 4; n=6) and the distal dendrite (85 ± 16; n=6; $P > 0{\cdot}05$ one way ANOVA) measured in ACSF at the start of each experiment. In addition no significant difference was found between resting $[Ca^{2+}]_i$ measured at the start of the experiment in the soma and the distal dendrite unsing the unpaired student *t*-test ($P > 0{\cdot}05$; two-tailed). Comparing each of these values with resting $[Ca^{2+}]_i$ measured 35 to 45 min later during the same experiments, again in ACSF following washout of a different medium or drug, again no significant differences in resting $[Ca^{2+}]_i$ were found: Soma, 47 ± 8 nM to 51 ± 5 nM ($P > 0{\cdot}5$); proximal dendrite, 59 ± 4 nM to 61 ± 7 nM ($P > 0{\cdot}5$); distal dendrite 85 ± 16 nM to 76 ± 9 nM ($P > 0{\cdot}3$; all paired *t* test, two tailed).

4.3 Measurements of $[Ca^{2+}]_i$ during postsynaptic depolarization when slices were bathed in ACSF containing 25 mM Mg^{2+} and 2 mM Ca^{2+} compared with normal ACSF.

The LTDs induced in an ACSF containing a $[Ca^{2+}]_o$ of only 1 mM (see Section 3.6), and the results of Pockett et al. (1990) and Chrostofi et al. (1993b) suggest that a restricted rise in $[Ca^{2+}]_i$ upon conditioning is necessary for non-associative LTD induction. However it is not clear how somatic depolarization during the induction of LTD affected dendritic Ca^{2+} levels at the test synapses. It is possible that reduced inhibition due to an increased $[Mg^{2+}]$ or decreased $[Ca^{2+}]$ in the ACSF could generate the conditions where the dendritic Ca^{2+} rise is enhanced. The reduction in inhibitory conductances would increase the cell's space constant, leading to a greater dendritic depolarization compared with control conditions.

We therefore set out to measure soma and dendritic $[Ca^{2+}]_i$ during conditioning in normal ACSF compared to conditioning during synaptic block with 25 mM Mg^{2+} while also recording test postsynaptic potentials. Calcium measurements were obtained from 7 cells. In 2 cells only dendritic $[Ca^{2+}]_i$ rises were monitored. In 3 cells, only somatic

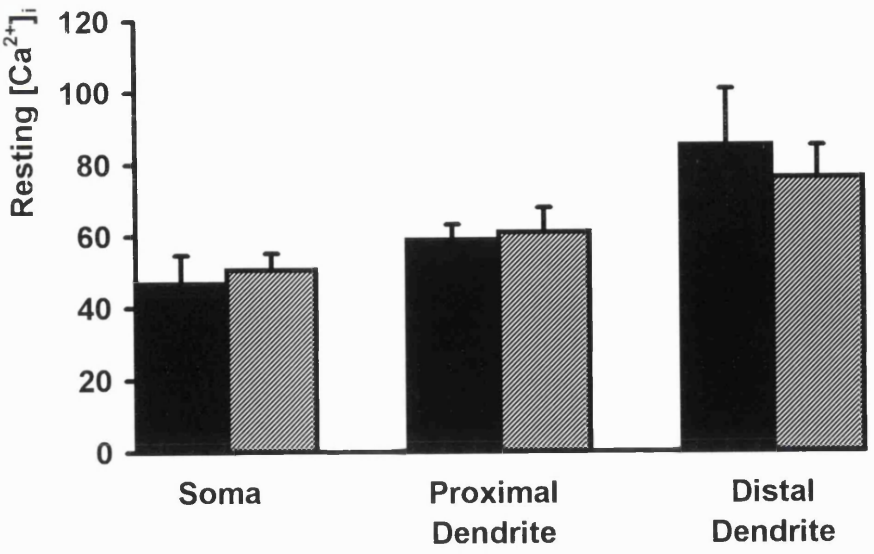

FIGURE 4.2i: Temporal and spatial effects on resting $[Ca^{2+}]_i$.

A histogram showing mean resting $[Ca^{2+}]_i$ measured in ACSF (filled columns) and 35 to 45 minutes later (hatched columns) following a transient wash (approximately 5 min) of a different medium or drug for both the proximal (up to 100 μm from soma) and distal apical dendrites (100 to 250 μm) of six cells and the soma of six cells (three cells from which dendritic measurements were also taken). All columns +1SEM.

$[Ca^{2+}]_i$ rises were monitored and in another 2 cells both somatic and dendritic $[Ca^{2+}]_i$ rises were recorded.

Electrophysiology.

In the 4 cells where dendritic $[Ca^{2+}]_i$ rises were recorded, electrophysiological data was also obtained. Of these four cells, intracellular conditioning in the presence of ACSF containing 25 mM Mg^{2+} resulted in 3 LTDs and 1 no effect. A typical LTD in one of these cells is illustrated in Figure 4.3i. The failure to induce LTD in the cell illustrated in Figure 4.3ii, demonstrates a full recovery of the EPSP to control levels within 20 min of the washout of ACSF containing 25 mM Mg^{2+}. This is comparable to the recovery period following a 5 min application of ACSF containing 25 mM Mg^{2+} in the absence of a conditioning procedure (Pockett et al., 1990). Figure 4.3iii presents a mean normalized plot of EPSP slope over time for all four cells showing a depression to 54·73 ± 19% (±SEM) of control at 30 min following washout of ACSF containing 25 mM Mg^{2+}. Comparing the raw data values (2 min averages) over last 8 min of the control period with that of the last eight min (22 to 30 min), using one way ANOVA the depression is highly significant (Control: 2·02 ± 0·26 mV/ms ±SEM; n_o=13; compared with 0·94 ± 0·05 mV/ms ±SEM; n_o=16; P = 0·0001; where n_o is the number of 2 min averages across the four cells).

$[Ca^{2+}]_i$ measurements.

Postsynaptic depolarization in ACSF containing 25 mM Mg^{2+} resulted in a lower rise in both somatic and dendritic $[Ca^{2+}]_i$ compared to conditioning in ACSF in the control and washout phases of the experiment in 6 of 7 cells. Examples of individual somatic and dendritic recordings are illustrated in Figure 4.3iv and Figure 4.3v respectively. Pooled normalized rises in somatic $[Ca^{2+}]_i$ during control, ACSF containing 25 mM Mg^{2+} and washout are illustrated, as are pooled normalized values in dendritic $[Ca^{2+}]_i$, in Figure 4.3vi.

Comparing raw somatic $[Ca^{2+}]_i$ rises (270 to 510 ms after the start of postsynaptic depolarization; see Table 4.3i), postsynaptic depolarization in ACSF containing 25 mM Mg^{2+} produced a highly significant reduction in the somatic rise in $[Ca^{2+}]_i$ compared to that in normal ACSF ($P < 0·0001$; one way ANOVA). There was however, no significant difference in the rise of somatic $[Ca^{2+}]_i$ following postsynaptic

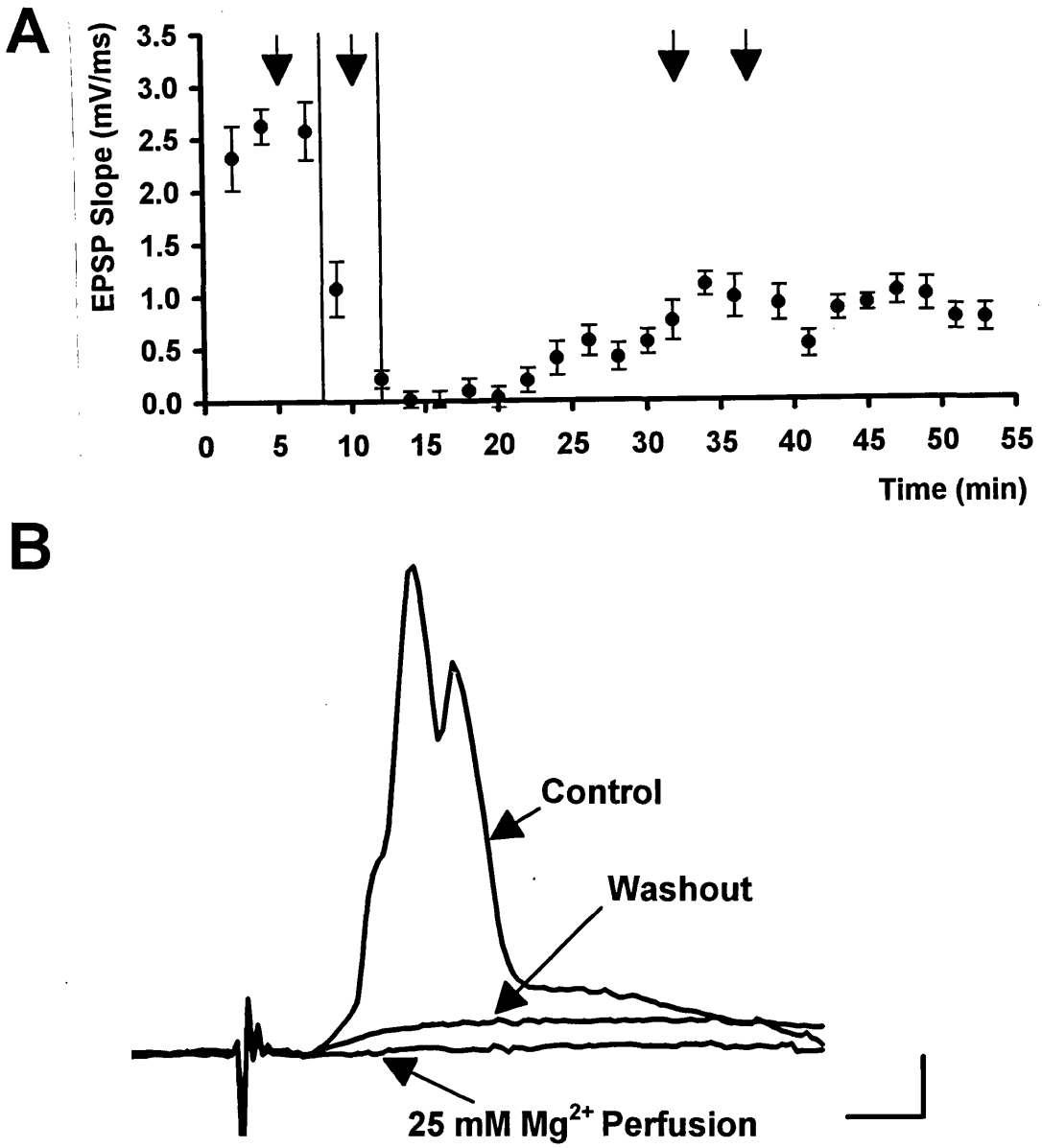

FIGURE 4.3i: Induction of LTD in a single cell by postsynaptic depolarization in ACSF containing 25 mM Mg^{2+} and 2 mM Ca^{2+}.

A A graph of EPSP slope plotted against time for a cell in which intracellular conditioning during a transient perfusion of ACSF containing 25 mM Mg^{2+}, 2 mM Ca^{2+} medium (between vertical bars) resulted in a lasting depression of synaptic strength. Arrows represent times at which intracellular conditioning was applied.

B Plotted are three superimposed traces of six consecutive averaged responses taken from different times in the experiment illustrated in A. Control responses were obtained 5 min before the onset of 25 mM Mg^{2+} perfusion (all suprathreshold); 25 mM Mg^{2+} perfusion responses were obtained 2 min before the start of washout; washout responses were obtained 20 min following the washout of 25 mM Mg^{2+}. Calibration bar: 5 mV, 3 ms.

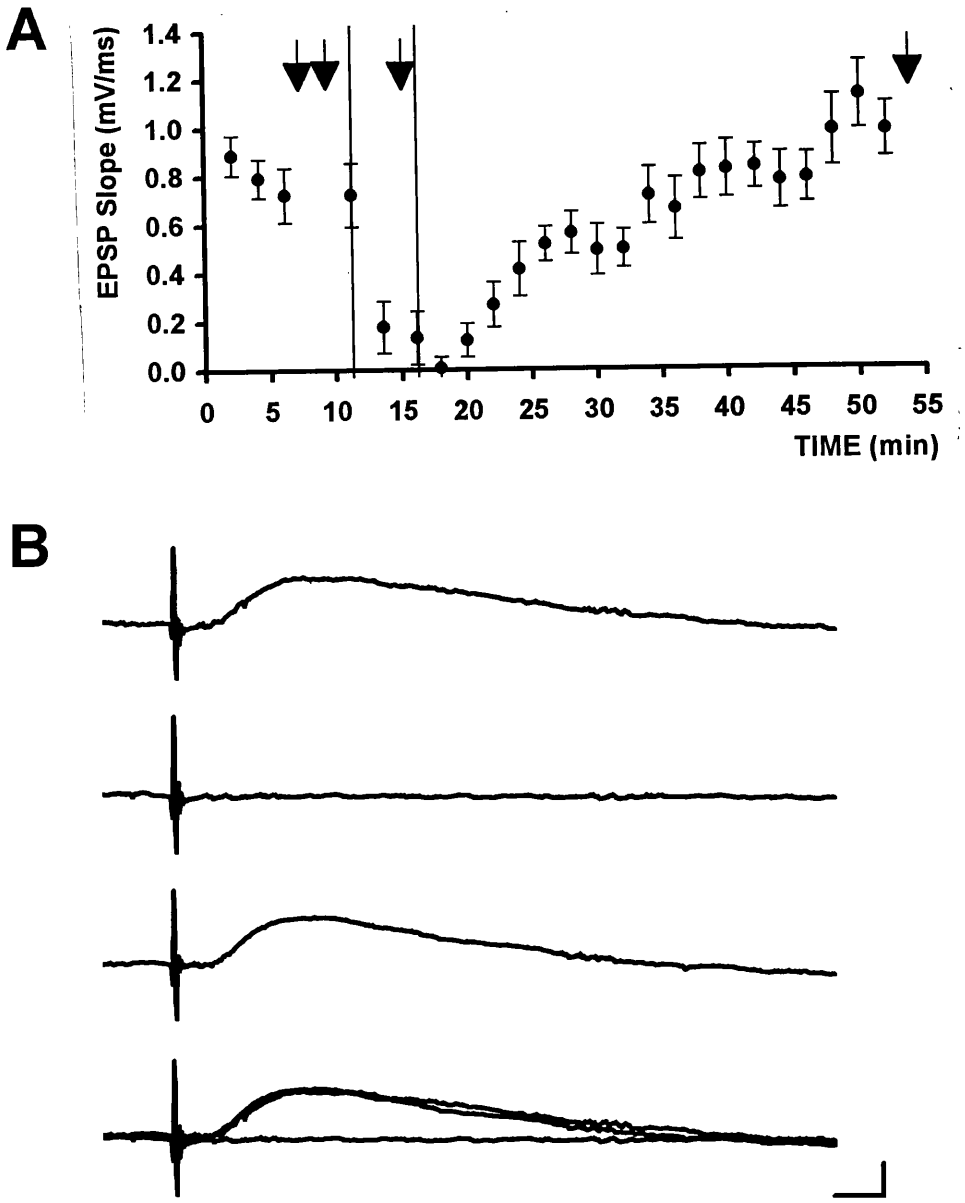

FIGURE 4.3ii: Failure to induce LTD in a single cell by postsynaptic depolarization in ACSF containing 25 mM Mg^{2+} and 2 mM Ca^{2+}.

A EPSP slope plotted against time for a cell in which intracellular conditioning during a transient perfusion of ACSF containing 25 mM Mg^{2+}, 2 mM Ca^{2+} medium (between vertical bars) did not result in a lasting depression of synaptic strength. Arrows represent times at which intracellular conditioning was applied.

B Traces of six consecutive averaged responses taken at different times in the experiment illustrated in A. From top to bottom: Control EPSP taken 5 min before the application of the 25 mM Mg^{2+} medium; EPSP obtained during the last minute of 25 mM Mg^{2+} application; EPSP obtained 30 min following washout of the 25 mM Mg^{2+} medium; All three responses superimposed. Calibration bar: 4 mV, 5 ms.

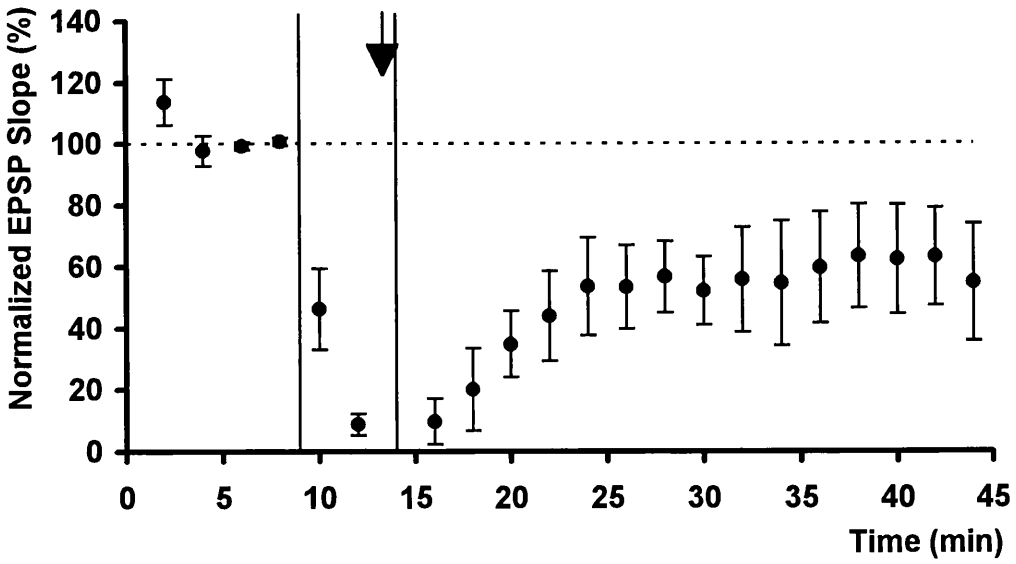

FIGURE 4.3iii: LTD obtained by intracellular conditioning in the presence of ACSF containing 25 mM Mg^{2+} and 2 mM Ca^{2+}.

Mean normalized EPSP slope (2 min averages) plotted against time for 4 cells, showing a significant depression of EPSP slope following intracellular conditioning during transient (5 min) perfusion of ACSF containing 25 mM Mg^{2+}, 2 mM Ca^{2+} medium. Error bars are ±1 SEM. Vertical lines illustrate the period of 25 mM Mg^{2+} perfusion. Arrow represents period of intracellular conditioning. Broken horizontal line gives the 100% value over the last 4 min of the control.

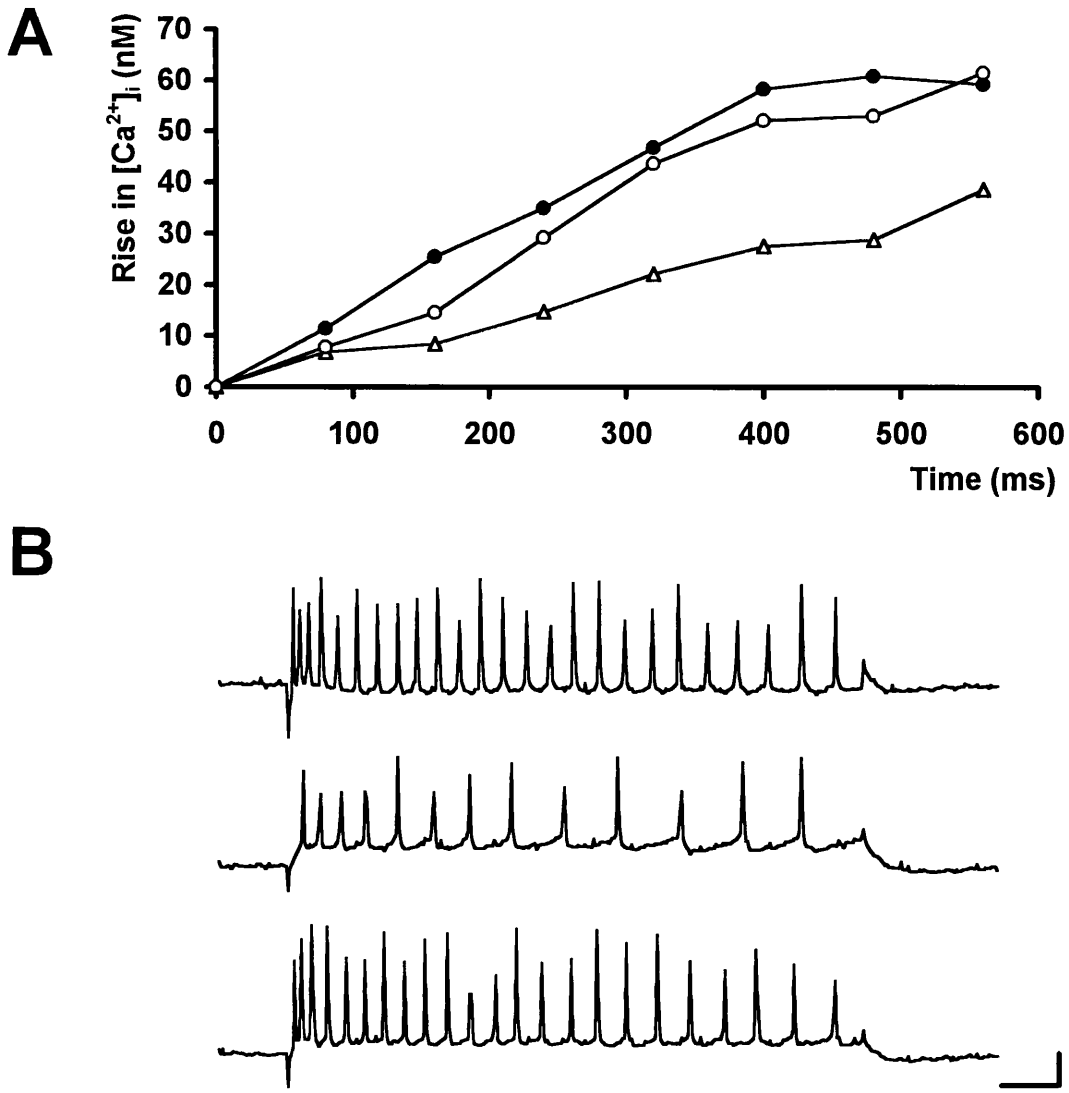

FIGURE 4.3iv: Measurements of somatic $[Ca^{2+}]_i$ during postsynaptic depolarization in ACSF containing 25 mM Mg^{2+} and 2 mM Ca^{2+} compared to control conditions in a single cell.

A Graph of the rise in somatic $[Ca^{2+}]_i$ against time in response to 500 ms depolarizing current pulses (delivered between 50 and 550 ms). Filled circles; control depolarization (+0·8 nA) in ACSF, each point an average of 8 consecutive responses, eliciting an average of 26·4 spikes per pulse. Open triangles; depolarization (+0·8 nA) during 25 mM Mg^{2+} perfusion, eliciting an average of 13·0 spikes per pulse. Open circles; depolarization (+0·6 nA) 30 min following washout of 25 mM Mg^{2+}, eliciting an average of 22·8 spikes per pulse.

B Postsynaptic response to current pulses (first pulse of 8) in each of the conditions described in A, from top to bottom; Control ACSF, during 25 mM Mg^{2+} perfusion and washout. Note that spikes are severely attenuated due to a low acquisition resolution. Calibration bar: 20 mV, 50 ms.

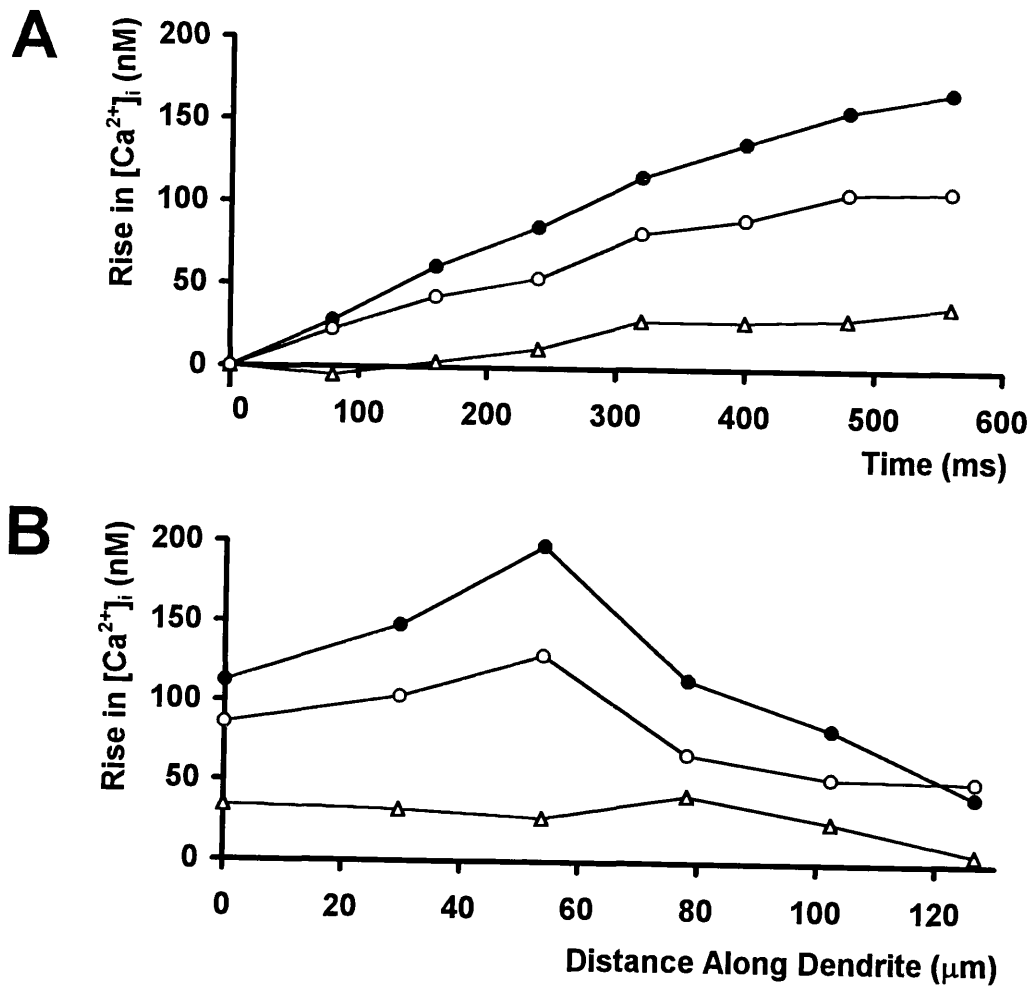

FIGURE 4.3v: Measurements of dendritic $[Ca^{2+}]_i$ during postsynaptic depolarization in ACSF containing 25 mM Mg^{2+} and 2 mM Ca^{2+} compared to control conditions in a single cell.

A Graph of dendritic $[Ca^{2+}]_i$ rise (0 to 100μm from soma) against time in response to 500 ms depolarizing current pulses (delivered between 50 and 550 ms). Filled circles; control depolarization (+0·5 nA) in ACSF, each point an average of 8 consecutive responses, eliciting an average of 21·6 spikes per pulse. Open triangles; depolarization (+1·3 nA) during 25 mM Mg^{2+} perfusion, eliciting an average of 19·4 spikes per pulse. Open circles; depolarization (+0·5 nA) 30 min following washout of 25 mM Mg^{2+}, eliciting an average of 23·0 spikes per pulse.

B Graph of dendritic $[Ca^{2+}]_i$ rise (average of 400 to 560 ms) against distance along dendrite (including soma at point zero) in response to 500 ms depolarizing current pulses for the same cell illustrated in A. Filled circles; control, ACSF. Open triangles; depolarization during 25 mM Mg^{2+} perfusion. Open circles; depolarization 30 min following washout of 25 mM Mg^{2+}.

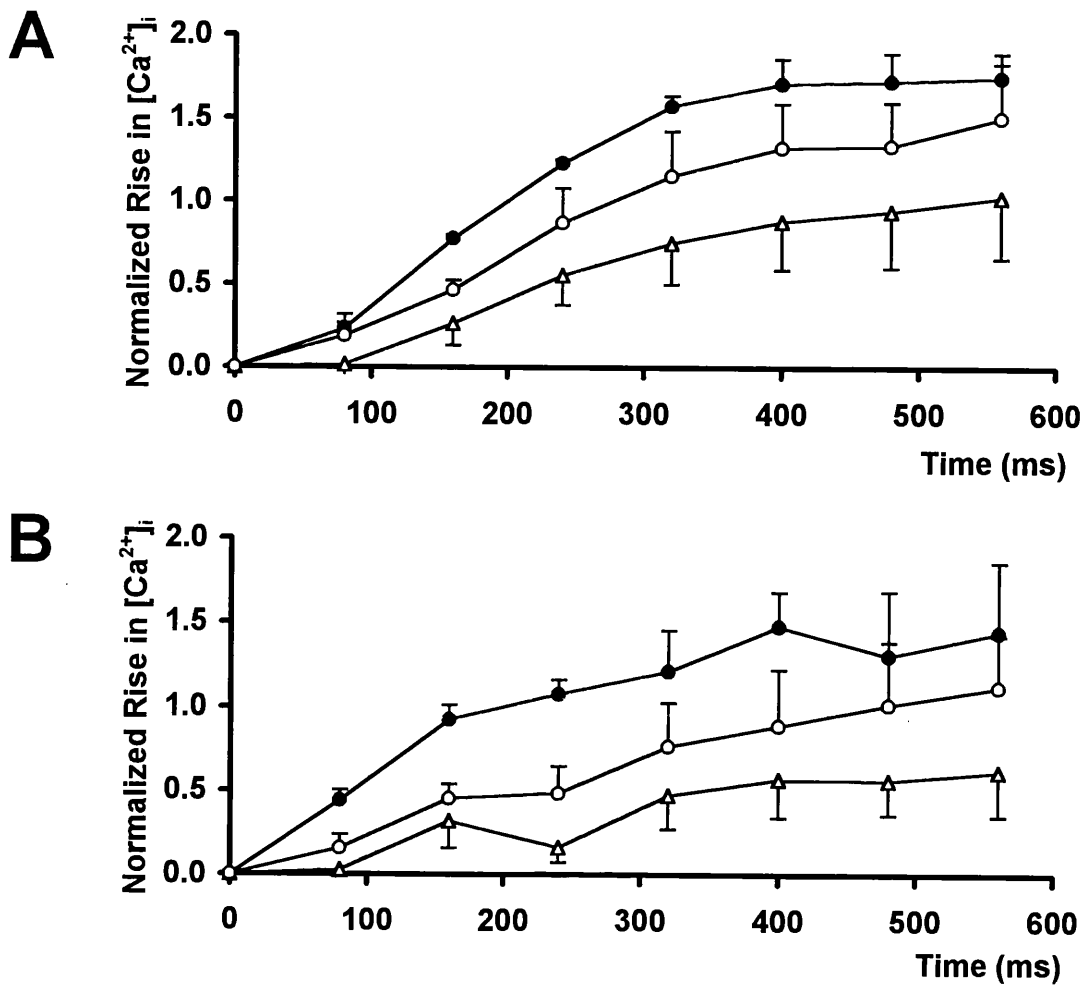

FIGURE 4.3vi: Postsynaptic depolarization in the presence of ACSF containing 25 mM Mg^{2+} and 2 mM Ca^{2+} results in a lower somatic $[Ca^{2+}]_i$ rise compared with control and washout conditions.

A Mean normalized plot of somatic $[Ca^{2+}]_i$ rise against time in response to 500 ms depolarizing current pulses (delivered between 50 and 550 ms) in ACSF (filled circles; +1 SEM; n=5), 25 mM Mg^{2+} (open triangles; −1 SEM; n=5), and washout (open circles; +1 SEM; n=4). Normalized to the $[Ca^{2+}]_i$ rise at 80 to 160 ms in ACSF.

B Mean normalized plot of dendritic $[Ca^{2+}]_i$ rise (pooling responses up to 100 μm distal to soma) against time in response to 500 ms depolarizing current pulses (delivered between 50 and 550 ms) in ACSF (filled circles; +1 SEM; n=4), 25 mM Mg^{2+} (open triangles; −1 SEM; n=4), and washout (open circles; +1 SEM; n=3). Normalized to the Ca^{2+} rise at 80 to 160 ms in ACSF.

depolarization between control and washout conditions (Bonferroni intercomparison, post ANOVA).

TABLE 4.3i: Somatic rises in $[Ca^{2+}]_i$ 270 to 510 ms after the start of postsynaptic depolarization in control, ACSF containing 25 mM Mg^{2+}/2 mM Ca^{2+} and washout.

	Control (n=5)	25 mM Mg^{2+} (n=5)	Washout (n=4)
Resting $[Ca^{2+}]_i$ (nM) ± SEM	41 ± 7 (n_o=5)	30 ± 4 (n_o=3)	48 ± 6 (n_o=4)
Mean rise in $[Ca^{2+}]_i$ (nM) ± SEM	79·4 ± 5·3 (n_o=20)	38·6 ± 5·6 (n_o=20)	61·1 ± 7·3 (n_o=16)
Mean current /pulse (nA) ± SEM	0·72 ± 0·21 (n_o=5)	1·06 ± 0·25 (n_o=5)	0·45 ± 0·06 (n_o=4)
Mean number of spikes/pulse ± SEM	20·3 ± 2·4 (n_o=5)	18·4 ± 4·5 (n_o=5)	19·2 ± 3·3 (n_o=4)

Where n is the number of cells and n_o is the number of data points taken from each cell.

Dendritic rises in $[Ca^{2+}]_i$ following depolarization (see Table 4.3ii) in 25 mM Mg^{2+} were found to be significantly lower than depolarization in control ACSF alone in the control ($P < 0·001$), but not following washout.

TABLE 4.3ii: Dendritic rises in $[Ca^{2+}]_i$ 270 to 510 ms after the start of postsynaptic depolarization in control, ACSF containing 25 mM Mg^{2+}/2 mM Ca^{2+} and washout.

	Control (n=4)	25 mM Mg^{2+} (n=4)	Washout (n=3)
Resting $[Ca^{2+}]_i$ (nM) ± SEM	59 ± 8 (n_o=4)	50 (n_o=2)	60 ± 10 (n_o=4)
Mean rise in $[Ca^{2+}]_i$ (nM) ± SEM	122·9 ± 16·9 (n_o=16)	35·6 ± 4·6 (n_o=16)	76·0 ± 14·9 (n_o=12)
Mean current /pulse (nA) ± SEM	0·53 ± 0·09 (n_o=4)	1·05 ± 0·10 (n_o=4)	0·47 ± 0·09 (n_o=3)
Mean number of spikes/pulse ± SEM	18·8 ± 3·9 (n_o=4)	21·1 ± 5·7 (n_o=4)	18·8 ± 4·7 (n_o=3)

Where n is the number of cells and n_o is the number of data points taken from each cell.

It was noted that in certain cells (for example see Figure 4.3iv) the average number of spikes per pulse was lower in the presence of ACSF containing 25 mM Mg^{2+} compared to control and washout conditions which might account for the lower rise in $[Ca^{2+}]_i$ following depolarization in 25 mM Mg^{2+}. Further examination across all cells showed that although a greater amount of current was required to elicit the spikes during perfusion of ACSF containing 25 mM Mg^{2+}, there was no significant difference observed

between the number of spikes produced in all three conditions. In addition an increased current should favour more Ca^{2+} influx.

These decreases in the rise of $[Ca^{2+}]_i$ upon postsynaptic depolarization in ACSF containing 25 mM Mg^{2+} compared with control ACSF, confirm and extend the observations made by Christofi et al., (1993b). The increased $[Mg^{2+}]$ in the ACSF presumably restricts Ca^{2+} entry by partially blocking VDCCs during postsynaptic depolarization (Almers & Palade, 1981). These results, together with the electrophysiological data on LTD, suggest a strong correlation between non-associative LTD induction and a decreased rise in $[Ca^{2+}]_i$ in the dendrites. However, it should be noted that one cell in which the dendritic $[Ca^{2+}]_i$ rise was not reduced by postsynaptic depolarization in 25 mM Mg^{2+}, did produce LTD. Conversely, the cell in which postsynaptic conditioning in 25 mM Mg^{2+} failed to induce LTD, a large decrease in the dendritic $[Ca^{2+}]_i$ rise was observed compared with control levels. These results may suggest that there is not a simple relationship between the rise in dendritic $[Ca^{2+}]_i$ and LTD induction. However the failure to induce LTD in the cell with a large decrease in dendritic $[Ca^{2+}]_i$ could be explained by the ABS rule of synaptic plasticity (Artola & Singer, 1993), since the ABS model proposes a threshold of LTD induction which requires a significant rise in postsynaptic $[Ca^{2+}]_i$, a threshold which may not have been reached in this case.

4.4 Measurements of $[Ca^{2+}]_i$ during postsynaptic depolarization when slices were bathed in ACSF containing 15 mM Mg^{2+} and 0 mM Ca^{2+}.

The theory proposed by Lisman (1989) argued that the magnitude of the rise in postsynaptic $[Ca^{2+}]_i$ determines the direction of synaptic change. In addition it is also suggested that a critical level of postsynaptic $[Ca^{2+}]_i$ must be reached to trigger LTD. Experimentally this has been confirmed for both homosynaptic (Mulkey & Malenka, 1992), and non-associative LTD (Cummings et al., 1996) where the Ca^{2+} chelator BAPTA when introduced into the cell blocked LTD induction. In a bid to test this hypothesis using intracellular conditioning, $[Ca^{2+}]_i$ measurements were acquired in conjunction with electrophysiolocal recordings before, during and after bath application of ACSF containing 15 mM Mg^{2+} and 0 mM Ca^{2+}.

Dual electrophysiological and $[Ca^{2+}]_i$ measurements were obtained from 2 cells. One cell showed an LTD following postsynaptic depolarization during a 7 min application of 15 mM Mg^{2+} and 0 mM Ca^{2+} (Figure 4.4i). The second cell showed full

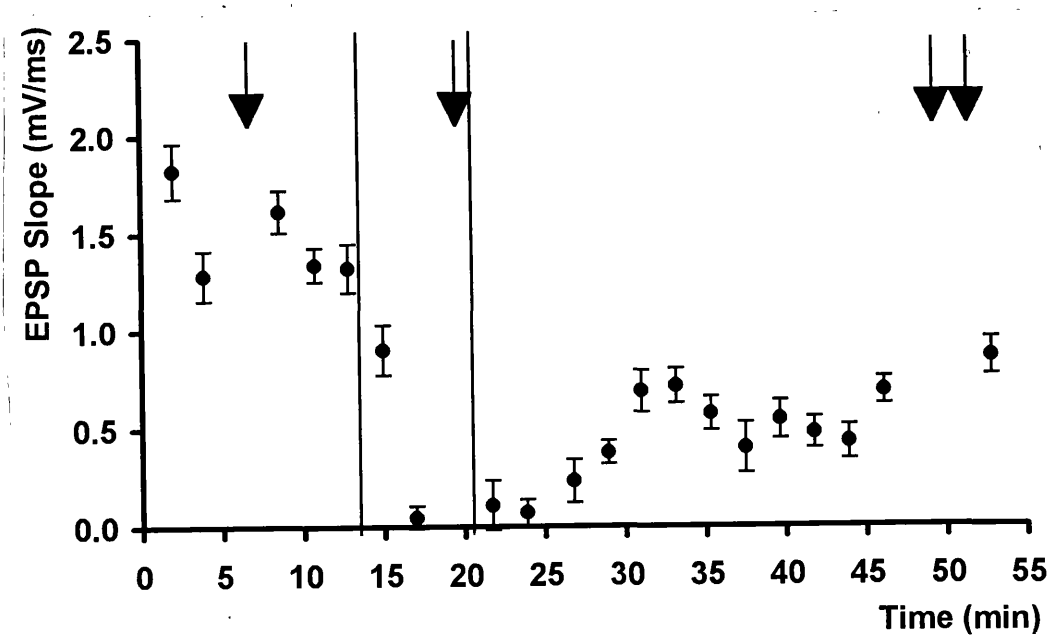

FIGURE 4.4i: Induction of LTD in a single cell by postsynaptic depolarization in ACSF containing 15 mM Mg^{2+} and 0 mM Ca^{2+}.

A graph of EPSP slope plotted against time for a cell in which intracellular conditioning during a transient perfusion of a 15 mM Mg^{2+}, 0 mM Ca^{2+} medium (between vertical bars) resulted in a lasting depression of synaptic strength. Arrows represent times at which intracellular conditioning was applied.

recovery of the EPSP to control levels 30 min after conditioning during a 5 min application of ACSF containing 15 mM Mg^{2+} (not illustrated). In addition $[Ca^{2+}]_i$ measurements alone were obtained from a further three cells.

Figure 4.4ii illustrates somatic rises in $[Ca^{2+}]_i$ recorded from a single cell (which resulted in LTD) and the pooled results across 5 cells. A clear reduction in the rise of somatic calcium following depolarization in 15 mM Mg^{2+} and 0 mM Ca^{2+} compared to control ACSF was observed in all 5 cells. These somatic calcium changes are quantified in Table 4.4i. The somatic rises in $[Ca^{2+}]_i$ upon depolarization in 15 mM Mg^{2+} (14·7 ± 2·2 nM; n_o=20) were found to be significantly smaller than those following depolarization in 25 mM Mg^{2+} (38·6 ± 4·4 nM; n_o=20; $P < 0·01$; Bonferroni P value following ANOVA) although there was no significant difference between the rise in somatic $[Ca^{2+}]_i$ in normal ACSF across the two groups.

TABLE 4.4i: Somatic rises in $[Ca^{2+}]_i$ 270 to 510 ms after the start of postsynaptic depolarization in control, ACSF containing 15 mM Mg^{2+}/0 mM Ca^{2+} and washout.

	Control (n=5)	15 mM Mg^{2+} (n=5)	Washout (n=2)
Resting $[Ca^{2+}]_i$ (nM) ± SEM	59 ± 6 (n_o=5)	61 ± 9 (n_o=5)	55 (n_o=2)
Mean rise in $[Ca^{2+}]_i$ (nM) ± SEM	63·9 ± 4·4 (n_o=20)	14·7 ± 2·2 (n_o=20)	44·4 ± 4·0 (n_o=8)
Mean current /pulse (nA) ± SEM	0·50 ± 0·06 (n_o=5)	0·51 ± 0·06 (n_o=5)	0·60 (n_o=2)
Mean number of spikes/pulse ± SEM	17·1 ± 2·5 (n_o=5)	14·0 ± 2·4 (n_o=5)	21·2 (n_o=2)

Where n is the number of cells and n_o is the number of data points taken from each cell.

A large reduction in the dendritic rise in $[Ca^{2+}]_i$ on postsynaptic conditioning in 15 mM Mg^{2+} was also observed in the one cell (which resulted in LTD) that revealed clear dendritic images (Figure 4.4iii).

Due to the difficulty in obtaining long-lasting dual electrophysiological and dendritic $[Ca^{2+}]_i$ measurements, a clear relationship between this lower calcium rise and the induction of non-associative LTD could not be made. Correlations between dendritic rises in $[Ca^{2+}]_i$ and changes in synaptic strength for all cells where dendritic $[Ca^{2+}]_i$ were obtained are presented in Section 4.8.

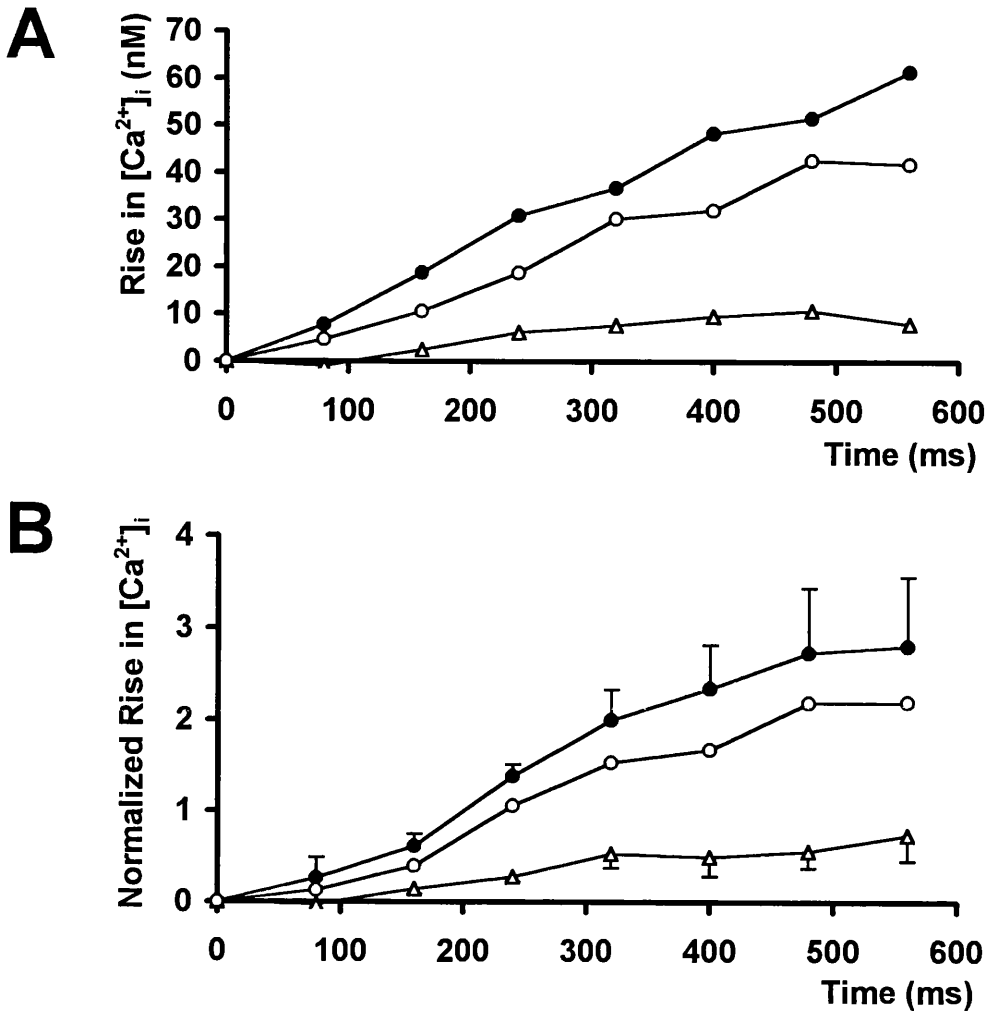

FIGURE 4.4ii: Postsynaptic depolarization in the presence of 15 mM Mg^{2+} and 0 mM Ca^{2+} results in a lower somatic $[Ca^{2+}]_i$ rise compared with control conditions.

A Graph of the rise in somatic $[Ca^{2+}]_i$ against time in response to 500 ms depolarizing current pulses (delivered between 50 and 550 ms) in a single cell. Filled circles; control depolarization (+0·4 nA) in ACSF, each point an average of 8 consecutive responses, eliciting an average of 22·0 spikes per pulse. Open triangles; depolarization (+0·9 nA) during 15 mM Mg^{2+}, 0 mM Ca^{2+} perfusion, eliciting an average of 12·3 spikes per pulse. Open circles; depolarization (+0·8 nA) 29 min following washout of the 15 mM Mg^{2+}, 0 mM Ca^{2+} medium, eliciting an average of 26·4 spikes per pulse.

B Mean normalized plot (pooled data) of the rise in somatic $[Ca^{2+}]_i$ against time in response to 500 ms depolarizing current pulses (delivered between 50 and 550 ms) in ACSF (filled circles; +1 SEM; n=5), 15 mM Mg^{2+}/0 mM Ca^{2+} (open triangles; 1 SEM; n=5), and washout (open circles; n=2). Normalized to the Ca^{2+} rise at 80 to 160 ms in ACSF.

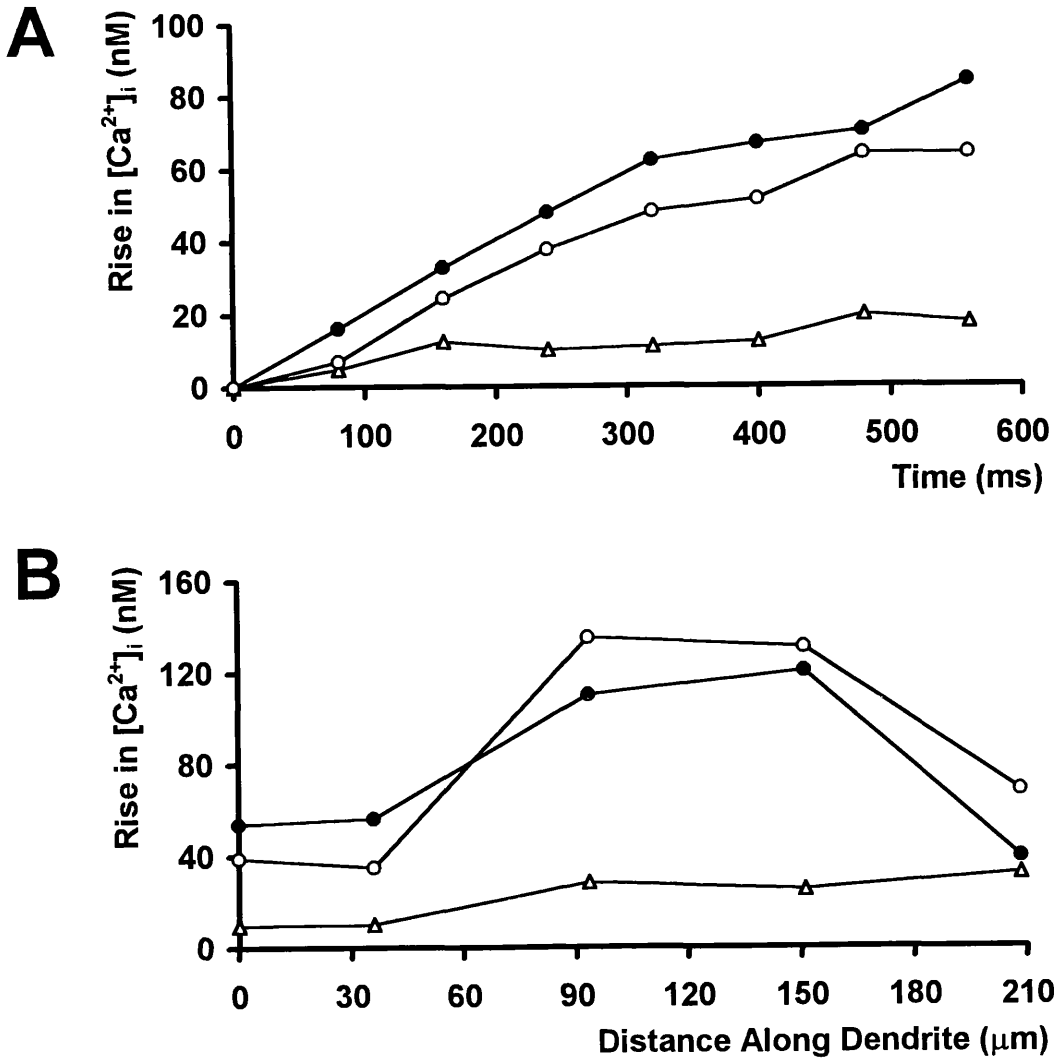

FIGURE 4.4iii: Measurements of dendritic $[Ca^{2+}]_i$ during postsynaptic depolarization in ACSF containing 15 mM Mg^{2+} and 0 mM Ca^{2+} in a single cell.

A Graph of the rise in dendritic $[Ca^{2+}]_i$ (up to 210 μm from soma) against time in response to 500 ms depolarizing current pulses (delivered between 50 and 550 ms). Filled circles; control depolarization (+0·4 nA) in ACSF, each point an average of 8 consecutive responses, eliciting an average of 22·0 spikes per pulse. Open triangles; depolarization (+0·9 nA) during 15 mM Mg^{2+}/0 mM Ca^{2+} perfusion, eliciting an average of 12·3 spikes per pulse. Open circles; depolarization (+0·8 nA) 30 min following washout of 25 mM Mg^{2+}, eliciting an average of 26·4 spikes per pulse.

B Graph of the rise in dendritic $[Ca^{2+}]_i$ (average of 400 to 560 ms) against distance along dendrite (including soma at point zero) in response to 500 ms depolarizing current pulses for the same cell illustrated in A. Filled circles; control, ACSF. Open triangles; depolarization during 15 mM Mg^{2+}/0 mM Ca^{2+} perfusion. Open circles; depolarization 30 min following washout of 25 mM Mg^{2+}.

4.5 Measurements of somatic $[Ca^{2+}]_i$ during postsynaptic depolarization applied during perfusion of ACSF containing 1 mM Ca^{2+} and 2 mM Mg^{2+}.

As described in Section 4.3 the effect of intracellular depolarization in the presence of ACSF containing 25 mM Mg^{2+}/2 mM Ca^{2+} was to limit the intracellular Ca^{2+} rise, hence facilitating LTD induction. The induction of non-associative LTD, as described in Section 3.6 and Barry et al., (1996c), by intracellular depolarization in the presence of 1 mM Ca^{2+}/2 mM Mg^{2+} was designed to mimic these effects. To test directly the effect of this process on intracellular $[Ca^{2+}]$, somatic Ca^{2+} measurements were made from 2 cells during postsynaptic depolarization before, during and after bathing the slice in ACSF containing 1 mM Ca^{2+}/2 mM Mg^{2+}. The first of these cells showed no change in the somatic $[Ca^{2+}]_i$ rise in 1 mM Ca^{2+} ACSF (33·9 nM; 11·4 spikes; 1·5 nA) compared to control conditions (27·1 nM; 11·0 spikes; 1·5 nA). The second cell, illustrated in Figure 4.5iA, exhibited a significant drop in the Ca^{2+} rise upon depolarization in 1 mM Ca^{2+} ACSF. The conditioning current in 1 mM Ca^{2+} ACSF evoked a few more action potentials per pulse (Figure 4.5iB) therefore a change in firing rate did not account for the reduced rise in cytosolic $[Ca^{2+}]_i$.

Although there was a reduction in somatic $[Ca^{2+}]_i$ rise in 1 mM Ca^{2+} compared with that in control ACSF in only 1 of the 2 cells tested, it was also true that postsynaptic depolarization in 1 mM Ca^{2+} ACSF gave rise to non-associative LTD in only a proportion of cells (5 of 9).

4.6 Measurements of somatic $[Ca^{2+}]_i$ during postsynaptic depolarization in the presence of 2 μM bicuculline.

As described in Section 3.8 postsynaptic conditioning in the presence of the $GABA_A$ receptor antagonist bicuculline can induce a non-assocative depotentiation of synaptic strength. The effect of the $GABA_A$ receptor antagonist, bicuculline, on Ca^{2+} rise following postsynaptic depolarization was examined in 5 cells. Comparing somatic $[Ca^{2+}]_i$ rises (140 to 860 ms after the start of postsynaptic depolarization; see Table 4.6i) there was found to be a significant reduction in the rise of $[Ca^{2+}]_i$ in bicuculline compared to control but not washout conditions ($P < 0·01$; Bonferroni P value following one way ANOVA). There was no significant difference between the mean number of spikes elicited per pulse, the mean depolarizing current in the pulses, the resting membrane potential (–85·4 ± 5·8 mV; –88·0 ± 5·3 mV; –88·7 ± 6·1mV) or in the mean resting $[Ca^{2+}]_i$ in all three conditions. In addition there was no significant difference between the

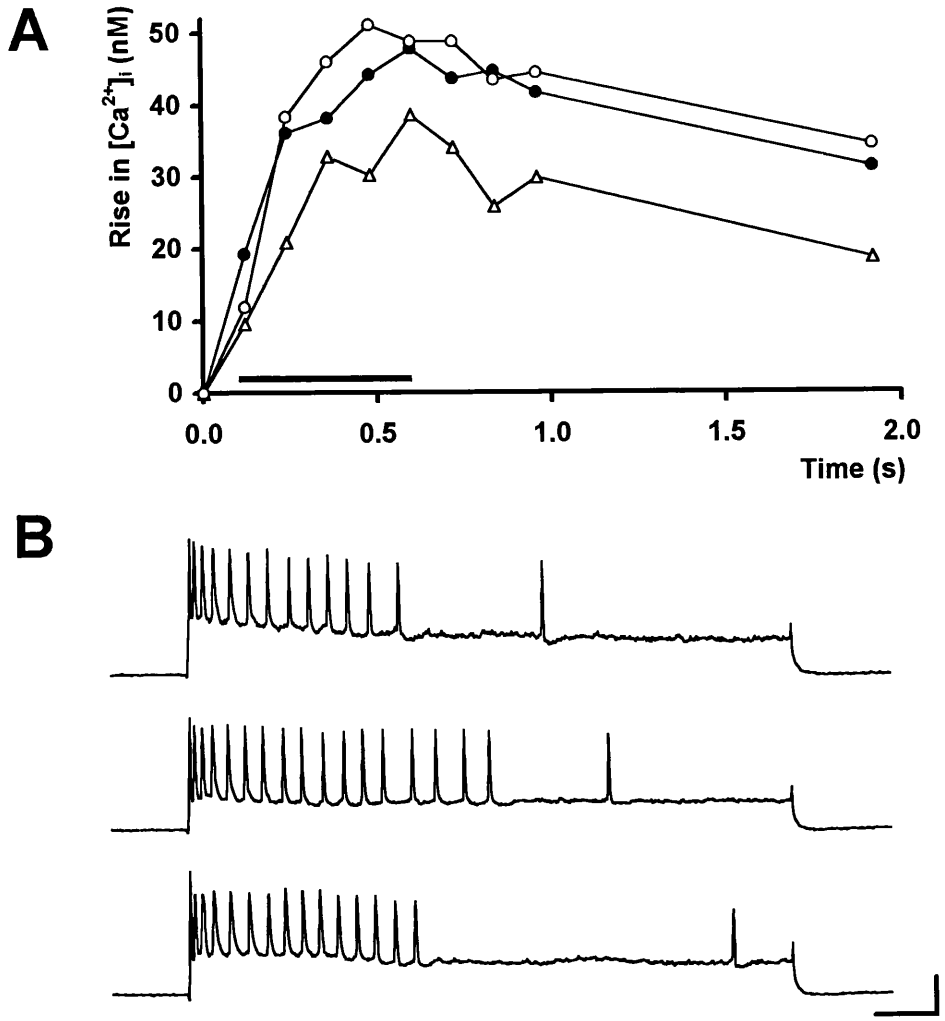

FIGURE 4.5i: Postsynaptic depolarization in the presence of 2 mM Mg^{2+} and 1 mM Ca^{2+} results in a lower somatic $[Ca^{2+}]_i$ rise compared with control conditions.

A Graph of somatic $[Ca^{2+}]_i$ rise against time in response to 500 ms depolarizing current pulses (delivered between 0·1 and 0·6 s; thick horizontal bar) in a single cell. Filled circles; control depolarization (+1·4 nA) in ACSF, each point an average of 8 consecutive responses, eliciting an average of 13·0 spikes per pulse. Open triangles; depolarization (+0·7 nA) during 2 mM Mg^{2+}/1 mM Ca^{2+} perfusion, eliciting an average of 17·6 spikes per pulse. Open circles; depolarization (+0·8 nA) 20 min following washout of 2 mM Mg^{2+}/1 mM Ca^{2+}, eliciting an average of 14·8 spikes per pulse.

B Postsynaptic response to current pulses (fourth pulse of 8) in each of the conditions described in A, from top to bottom; Control ACSF, during 2 mM Mg^{2+}/1 mM Ca^{2+} perfusion and washout. Calibration bar: 30 mV, 50 ms. Spike amplitude 76 mV threshold to peak in the control, 75 mV in 1 mM Ca^{2+} and 74 mV in the washout. V_m on exit, −84 mV.

mean spike amplitude (threshold to peak) 77·1 ± 2·4 mV in bicuculline, CSF and washout. A mean normalized plot of mean rise in $[Ca^{2+}]_i$ against time during postsynaptic conditioning in both ACSF and 2 μM bicuculline is shown in Figure 4.6i.

TABLE 4.6i: Somatic rises in $[Ca^{2+}]_i$ 140 to 860 ms after the start of postsynaptic depolarization in control, 2 μM bicuculline and washout.

	Control (n=6)	Bicuculline (n=6)	Washout (n=5)
Resting $[Ca^{2+}]_i$ (nM) ± SEM	26 ± 5 (n_o=6)	19 ± 4 (n_o=6)	21 ± 5 (n_o=5)
Mean rise in $[Ca^{2+}]_i$ (nM) ± SEM	44·7 ± 7·5 (n_o=36)	24·2 ± 2·8 (n_o=36)	31·4 ± 2·6 (n_o=28)
Mean current /pulse (nA) ± SEM	1·53 ± 0·44 (n_o=6)	1·38 ± 0·32 (n_o=6)	1·30 ± 0·38 (n_o=5)
Mean number of spikes/pulse ± SEM	11·7 ± 1·7 (n_o=6)	13·3 ± 2·0 (n_o=6)	15·2 ± 3·7 (n_o=5)

Where n is the number of cells and n_o is the number of data points taken from each cell.

Although the lowering of Ca^{2+} entry on depolarization is comparable with those obtained while investigating the other manoeuvres that induced non-associative LTD, the observation that bicuculline restricts the rise in somatic $[Ca^{2+}]_i$ is somewhat surprising and unexplainable. Measurements of dendritic $[Ca^{2+}]_i$ in the presence of bicuculline compared to control conditions for both naïve and potentiated synapses are required to construct a relationship between calcium rise and the induction of non-associative depotentiation in the hippocampus.

4.7 Measurements of $[Ca^{2+}]_i$ during postsynaptic depolarization in the presence of the AMPA receptor antagonist CNQX.

The bicuculline induced decrease in somatic calcium rise following depolarization might be due to an effect of the drug on VDCCs. To test for this possibility, recurrent inhibitory circuits were blocked by application of the AMPA receptor antagonist CNQX (Andreasen & Lambert, 1991). This manoeuvre would specifically block AMPA receptor activation and hence reduce synaptic transmission, and thereby recurrent inhibitory circuits.

Measurements of intracellular $[Ca^{2+}]_i$ were made using the ratiometric calcium indicator Fura-2 in an attempt to ascertain the magnitude of Ca^{2+} rise upon depolarization in the presence of CNQX. Somatic calcium measurements were taken

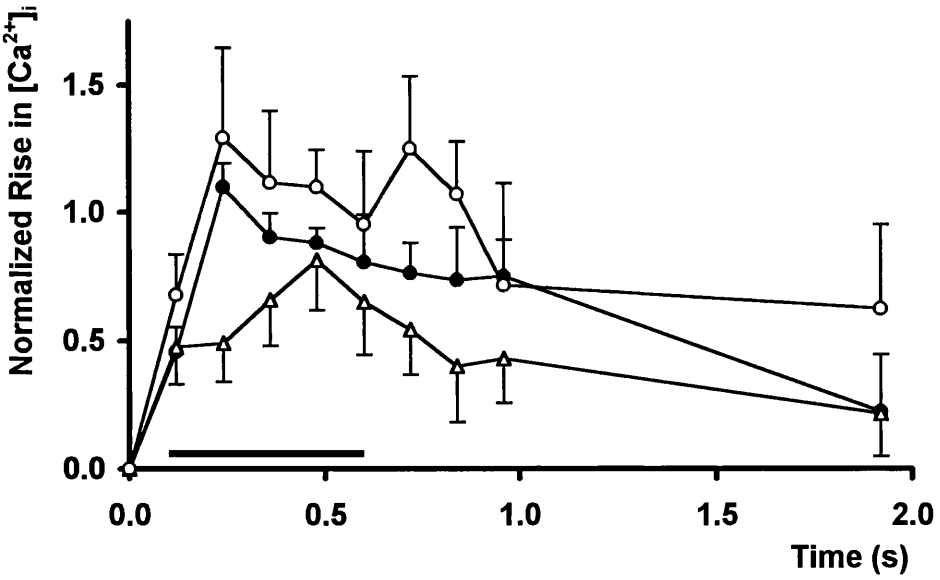

FIGURE 4.6i: Measurements of somatic $[Ca^{2+}]_i$ during postsynaptic depolarization in ACSF containing 2 μM bicuculline compared with control conditions.

A normalized plot of mean rise in $[Ca^{2+}]_i$ against time during postsynaptic conditioning in both ACSF (filled circles), 2 μM bicuculline (open triangles), and drug washout (open circles). The rise in $[Ca^{2+}]_i$ for six cells is normalized to $[Ca^{2+}]_i$ rise in control ACSF (mean values at 0·24 and 0·36 s). Horizontal bar between 100 ms and 600 ms represents conditioning pulse duration. The ACSF and bicuculline data from 0·14 s to 0·86 s after the onset of the depolarizing pulse are significantly different (P = 0·05, n = 6, one way ANOVA). There was no significant difference in the mean firing rate during depolarizing pulses in the first 200 ms or over the full 500 ms in the three conditions. There were also no significant differences between mean depolarizing current, mean resting $[Ca^{2+}]_i$, mean resting potential, mean spike threshold or mean spike amplitude between the three conditions.

from three cells. Dual calcium and electrophysiological recordings were made from one of these cells, which also provided dendritic calcium measurements. Figure 4.7i illustrates the electrophysiological data from this cell. Following the acquisition of control EPSPs, 10 μM CNQX was added to the perfusate for a period of 7 min. At the end of this period when the magnitude of the EPSP was significantly reduced, conditioning pulses (8 × 1·2 nA) were applied in the absence of test shocks, eliciting on average 22·3 spikes per pulse. At 40 min postconditioning a depression of 63% was seen in this cell compared to control levels.

The rise in somatic $[Ca^{2+}]_i$ following depolarization in ASCF, CNQX and washout for the above cell is illustrated in Figure 4.7iiA. Measurements of somatic rises in $[Ca^{2+}]_i$ from the other 2 cells were from the 1994 group of experiments and to minimize error due to the variation of resting $[Ca^{2+}]_i$ (Section 4.2), comparison between all three cells were expressed as normalized ΔF/F (Figure 4.7iiB and Table 4.7i). Comparison of somatic ΔF/F for depolarization in ACSF, CNQX and washout show no significant differences ($P > 0{\cdot}8$; ANOVA).

TABLE 4.7i: Somatic rises in $[Ca^{2+}]_i$ 240 to 480 ms after the start of postsynaptic depolarization in control, 10 μM CNQX and washout.

	Control (n=3)	10 μM CNQX (n=3)	Washout (n=3)
Resting $[Ca^{2+}]_i$ (nM) ± SEM	17 (n_o=2)	75 (n_o=1)	41 ± 24 (n_o=3)
Mean rise in $[Ca^{2+}]_i$ (nM)± SEM	79·4 ± 23·9 (n_o=9)	79·3 ± 20·5 (n_o=9)	79·4 ± 27·7 (n_o=9)
ΔF/F ± SEM	0·16 ± 0·02 (n_o=9)	0·19 ± 0·04 (n_o=9)	0·18 ± 0·05 (n_o=9)
Mean current /pulse (nA) ± SEM	2·07 ± 0·47 (n_o=3)	2·10 ± 0·49 (n_o=3)	2·00 ± 0·75 (n_o=3)
Mean number of spikes/pulse ±SEM	13·8 ± 4·1 (n_o=3)	14·7 ± 3·8 (n_o=3)	14·0 ± 3·4 (n_o=3)

Where n is the number of cells and n_o is the number of data points taken from each cell.

In contrast to the lack of effect of CNQX on somatic Ca^{2+} influx, dendritic $[Ca^{2+}]_i$ measurements from the cell in which LTD was induced revealed a lower depolarization induced $[Ca^{2+}]_i$ rise in CNQX, than in control or washout conditions (Figure 4.7iii). Comparing the averaged rise in $[Ca^{2+}]_i$ over the 200 to 600 ms period (pooling dendritic values up to 200 μm from the soma) there was a drop to 61% of control values when depolarization took place in the presence of CNQX, which recovered to 113% of control values in the washout.

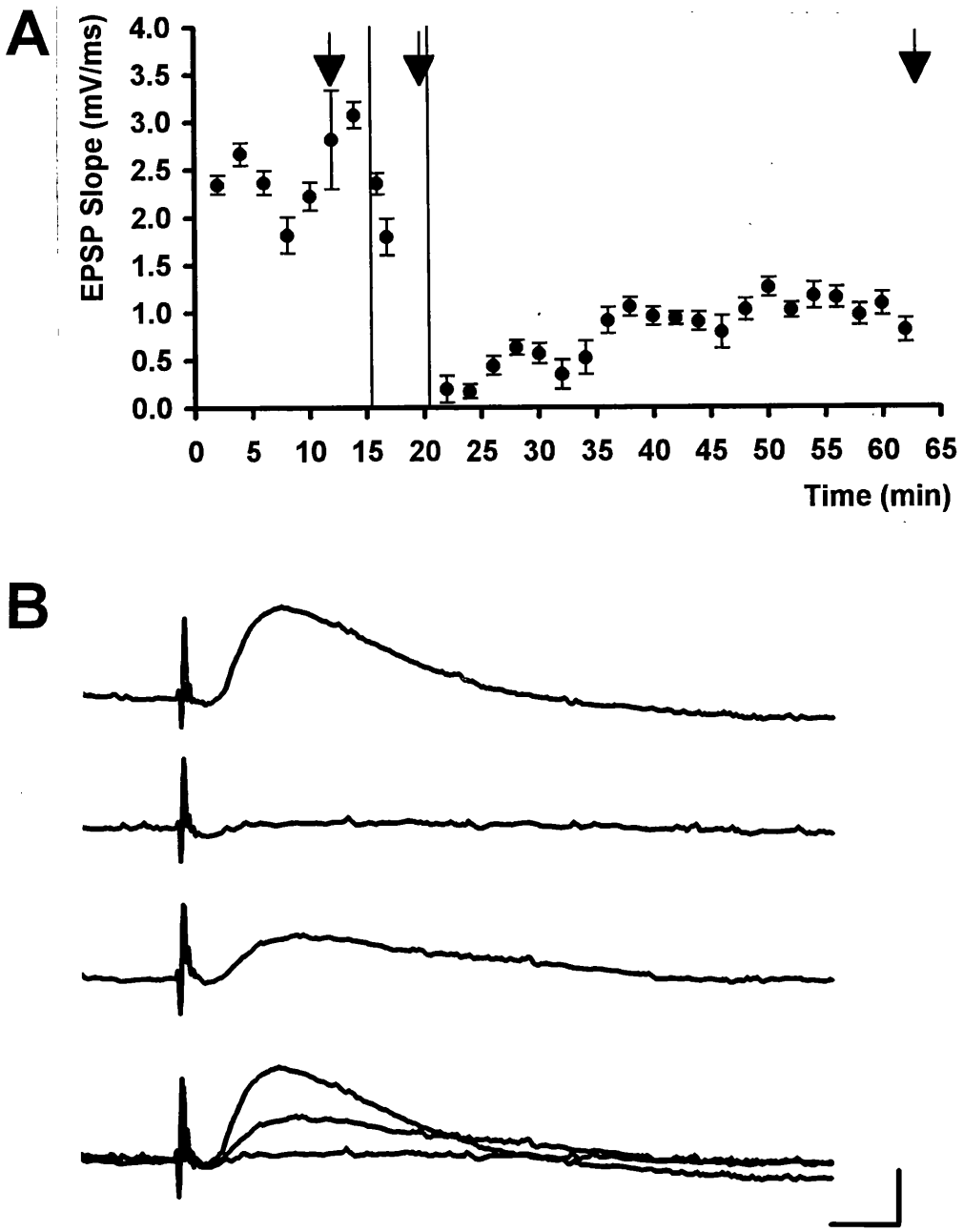

FIGURE 4.7i: LTD of synaptic strength following postsynaptic depolarization in the presence of 10 μM CNQX in a single neurone.

A A graph of mean EPSP slope plotted against time for a cell in which intracellular conditioning during a transient (7 min) perfusion of 10 μM CNQX (between vertical bars) resulted in a lasting depression of synaptic strength. Arrows represent times at which intracellular conditioning was applied.

B Plotted are traces of six consecutive averaged responses taken at different times in the experiment illustrated in A. From top to bottom: Control EPSP taken 5 min before the addition of 10 μM CNQX to the ACSF; EPSP obtained during the first minute of washout of CNQX; EPSP obtained 40 min following washout of CNQX; All three responses superimposed. Calibration bar: 5 mV, 5 ms.

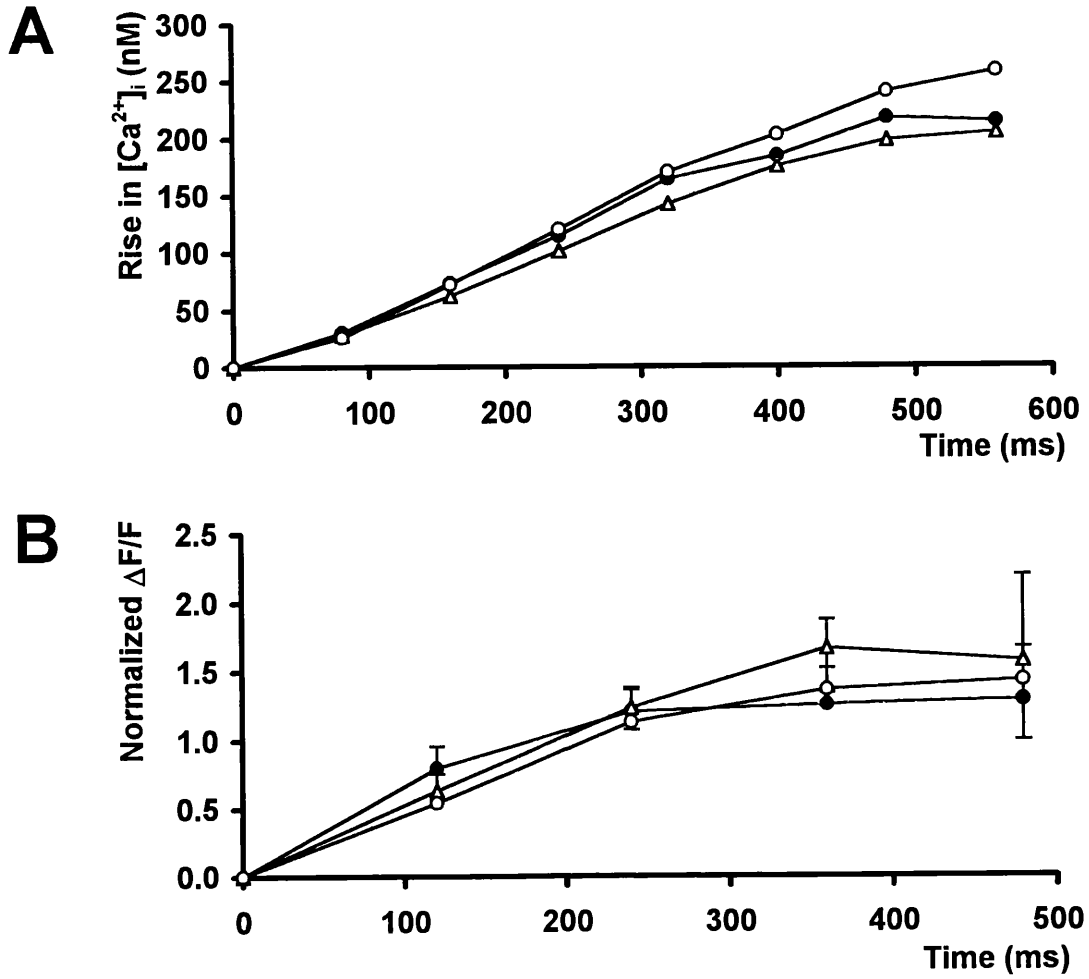

FIGURE 4.7ii: Postsynaptic depolarization in the presence of 10 μM CNQX fails to lower the rise in somatic $[Ca^{2+}]_i$ compared with control and washout conditions.

A Graph of the rise in somatic $[Ca^{2+}]_i$ against time in response to 500 ms depolarizing current pulses (delivered between 50 and 550 ms) in a single cell. Filled circles; control depolarization (+1·2 nA) in ACSF, each point an average of 8 consecutive responses, eliciting an average of 21·9 spikes per pulse. Open triangles; depolarization (+1·2 nA) in the presence of 10 μM CNQX, eliciting an average of 22·3 spikes per pulse. Open circles; depolarization (+0·5 nA) 42 min following washout of the CNQX, eliciting an average of 20·9 spikes per pulse.

B Mean normalized plot of ΔF/F against time in response to 500 ms depolarizing current pulses (delivered between 50 and 550 ms) in ACSF (filled circles; +1 SEM; n=3), 10 μM CNQX (open triangles; −1 SEM; n=3), and washout (open circles; +1 SEM; n=3). Normalized to ΔF/F at 120 ms in ACSF.

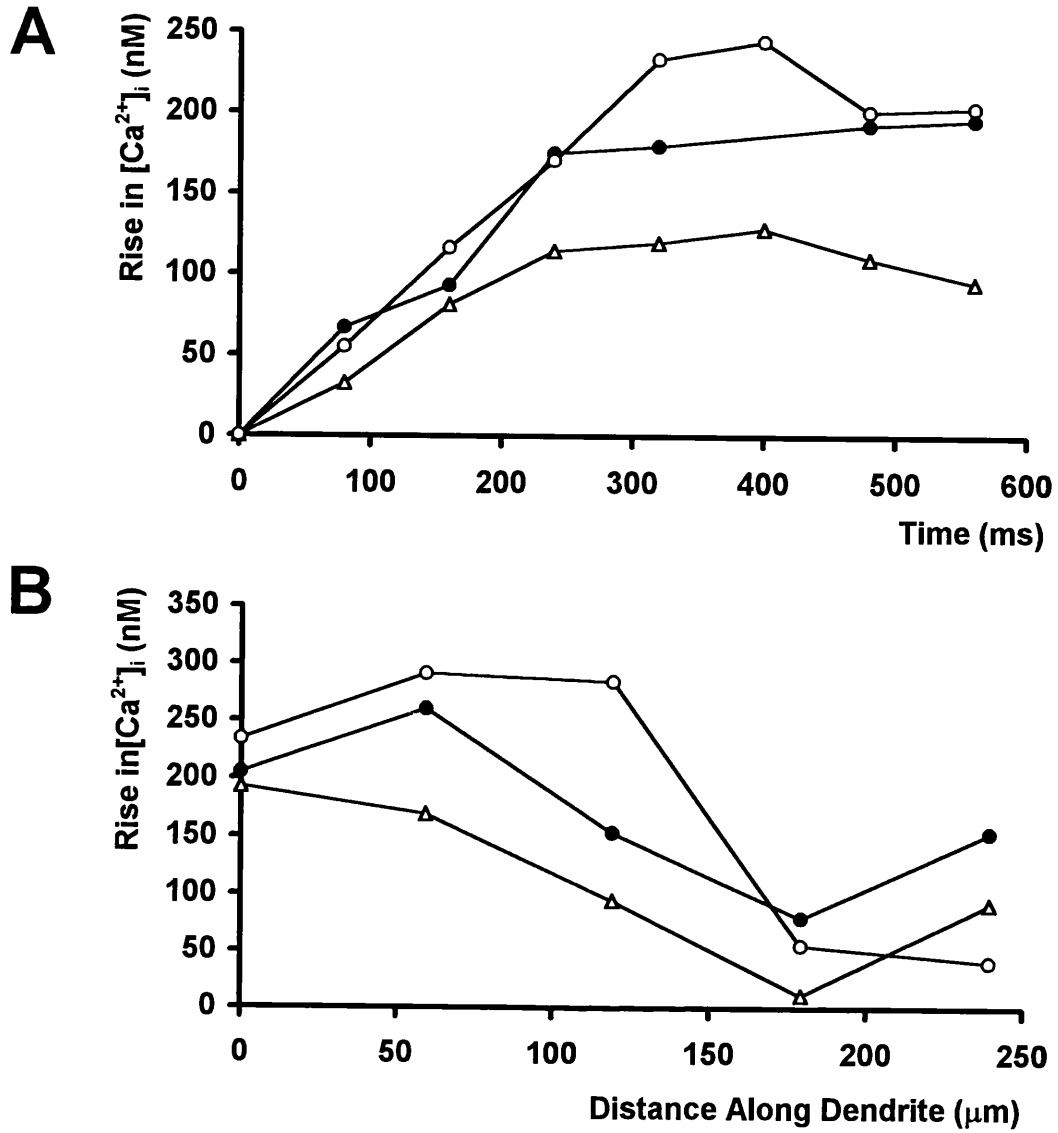

FIGURE 4.7iii: Postsynaptic depolarization in the presence of 10 μM CNQX results in a lower dendritic $[Ca^{2+}]_i$ rise compared with control conditions in a single cell.

A Graph of the dendritic rise in $[Ca^{2+}]_i$ (up to 200 μm from soma) against time in response to 500 ms depolarizing current pulses (delivered between 50 and 550 ms) in a single cell. Filled circles; control depolarization (+1·2 nA) in ACSF, each point an average of 8 consecutive responses, eliciting an average of 21·9 spikes per pulse. Open triangles; depolarization (+1·2 nA) during perfusion of 10 μM CNQX, eliciting an average of 22·3 spikes per pulse. Open circles; depolarization (+0·5 nA) 30 min following washout of CNQX, eliciting an average of 20·9 spikes per pulse.

B Graph of the rise in dendritic $[Ca^{2+}]_i$ (average of 400 to 560 ms) against distance along dendrite (including soma at point zero) in response to 500 ms depolarizing current pulses for the same cell illustrated in A. Filled circles; control, ACSF. Open triangles; depolarization during 10 μM CNQX perfusion. Open circles; depolarization 30 min following washout of CNQX.

The fact that somatic ΔF/F remained unchanged following depolarization in the presence of CNQX suggests that the $GABA_A$ receptor antagonist bicuculline may be acting in a non-specific manner in lowering the somatic rise in $[Ca^{2+}]_i$. The decrease in dendritic rise in $[Ca^{2+}]_i$ upon depolarization in the presence of CNQX could be due to a reduction in Ca^{2+} entry via the depolarized NMDA or AMPA receptor channel (Schneggenburger et al., 1993). In ACSF alone, Ca^{2+} entry through these receptor channels upon depolarization may be possible in the presence of ambient glutamate (Sah et al., 1989).

4.8 Correlations between the rise in postsynaptic $[Ca^{2+}]_i$ and synaptic change.

Measurements of EPSP slope following depolarization in ACSF were made between 2 and 16 min after conditioning. This time period was restricted because of the subsequent application of the test medium or drug.

Figure 4.8iA and B compares the effect of intracellular depolarization upon the resulting change in synaptic strength and rise in dendritic $[Ca^{2+}]_i$ and somatic $[Ca^{2+}]_i$ respectively linking control and test conditioning for each cell. These plots indicate that a reduction in the rise in postsynaptic $[Ca^{2+}]_i$ in the test medium compared to ACSF control upon depolarization did not always lead to induction of synaptic depression. Direct correlations of synaptic change against the rise in postsynaptic $[Ca^{2+}]_i$ for both dendrite and soma are presented in Figure 4.8iC and D respectively. Regression analysis of this data reveals that there was no correlation between either dendritic rises in $[Ca^{2+}]_i$ ($r^2 = 0{\cdot}1807$; n=12; $P > 0{\cdot}5$), or somatic rises in $[Ca^{2+}]_i$ ($r^2 = 0{\cdot}0177$; n=10; $P > 0{\cdot}7$) upon depolarization and the resulting change in EPSP slope.

These results suggest that there is no correlation between the rise in postsynaptic $[Ca^{2+}]_i$ and non-associative LTD induction, but it should be noted that EPSP depression did not follow conditioning in ACSF alone in any of the above experiments. It is possible that LTD induction requires some other factor acting in conjunction with the postsynaptic rise in $[Ca^{2+}]_i$ or alternatively that some priming mechanism is necessary.

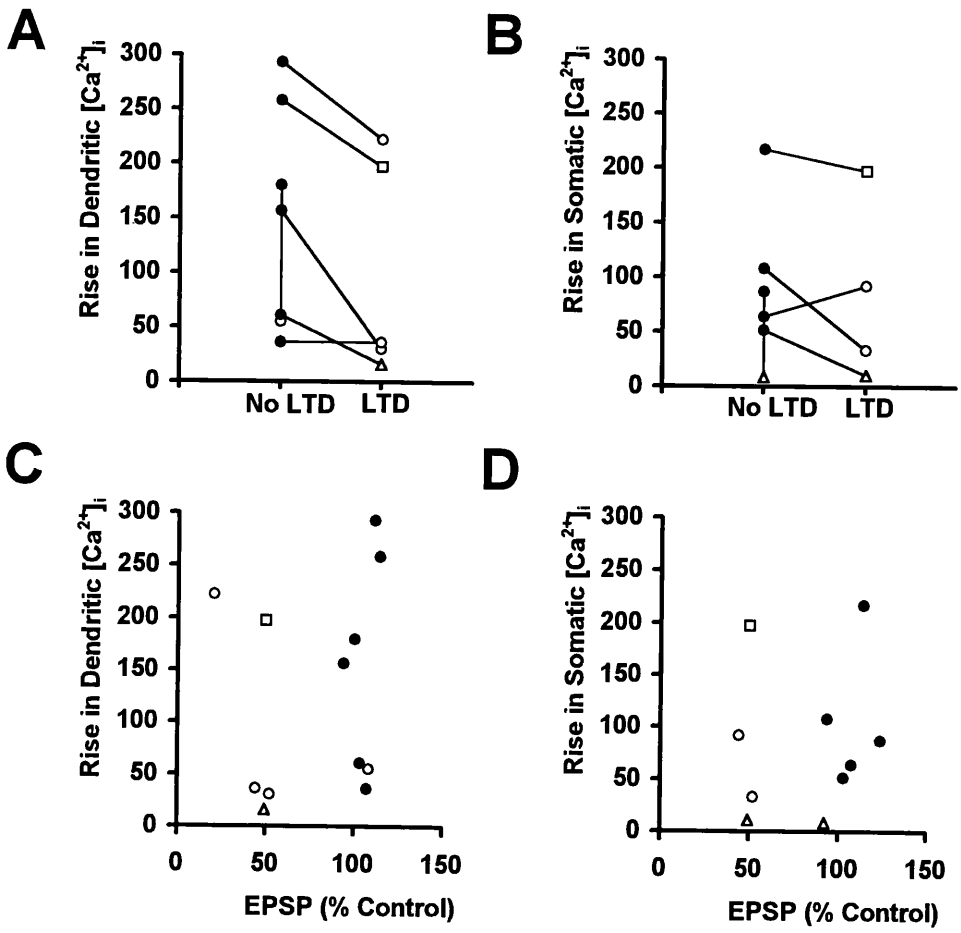

FIGURE 4.8i: Correlation between postsynaptic rises in $[Ca^{2+}]_i$ with changes in the strength of synaptic transmission.

A Plot of depolarization induced rises in dendritic $[Ca^{2+}]_i$ (maximum level during depolarization) that resulted in an LTD or no effect. Each experiment contained an internal control of depolarization in ACSF alone (filled circles), followed by depolarization in ACSF containing 25 mM Mg^{2+}/2 mM Ca^{2+} (open circles), 15 mM Mg^{2+}/0 mM Ca^{2+} (open triangles), or 10 μM CNQX (open square). Rises in $[Ca^{2+}]_i$ elicited by depolarization in ACSF and test solution from the same experiment are paired.

B As in A except pairing rises in somatic $[Ca^{2+}]_i$ in ACSF alone with the corresponding somatic $[Ca^{2+}]_i$ rises in the test solution.

C Scatter plot of rise in dendric $[Ca^{2+}]_i$ (maximum level during depolarization) against the resulting change in EPSP slope (% control), for depolarization in ACSF (filled circles), 25 mM Mg^{2+}/2 mM Ca^{2+} (open circles), 15 mM Mg^{2+}/0 mM Ca^{2+} (open triangles), or 10 μM CNQX (open square). Changes in EPSP slope were measured 30 min following washout of the test medium or CNQX; and 2 to 16 min following postsynaptic depolarization in ACSF alone and compared to the last 2 min before application of the test medium or before depolarization in ACSF.

D As in C but for somatic rises in $[Ca^{2+}]_i$.

CHAPTER 5

DISCUSSION

5.1 The Ca^{2+} hypothesis of synaptic plasticity.

Several synaptic modification rules have been proposed which expand the classical Hebb rule (Hebb, 1949; see Section 1.16). They include models proposed by Sejnowski (1977), and Bienenstock et al. (1982) which have a negative term to encompass LTD as well as LTP. These models suggest that the magnitude of postsynaptic depolarization (Bienenstock et al., 1982) or postsynaptic $[Ca^{2+}]_i$ increase (Lisman, 1989; Artola & Singer, 1993) determines the production and direction of synaptic change. Based on experimental evidence, these rules propose that a larger postsynaptic depolarization and hence a greater rise in postsynaptic $[Ca^{2+}]_i$ would result in LTP, whereas a smaller postsynaptic depolarization, and therefore a smaller rise in postsynaptic $[Ca^{2+}]_i$, would result in LTD.

The experimental evidence reported in support of this theory has focused on homosynaptic synaptic changes. Indirect methods of altering intracellular $[Ca^{2+}]$, were used such as lowering the amount of $GABA_A$ mediated inhibition (Artola et al., 1990), changing the stimulation frequency of the conditioning train (Dudek & Bear 1992) or increasing the extent of NMDA receptor antagonism (Cummings et al., 1996).

In this study non-associative, LTD induction was attempted by unpaired postsynaptic depolarization. Experiments were designed to indirectly reduce or enhance the rise of $[Ca^{2+}]_i$ during conditioning to test the Ca^{2+} hypothesis. In addition, $[Ca^{2+}]_i$ measurements during postsynaptic conditioning in conjunction with electrophysiological recordings were performed to directly explore the relationship between rises in $[Ca^{2+}]_i$ and changes in synaptic strength.

5.2 Postsynaptic conditioning of neurones bathed in ACSF containing variable concentrations of Ca^{2+} and Mg^{2+}.

Coussens & Teyler (1993), in the CA1 region of the hippocampus, reported LTP induction at synapses that had been tetanized by stimulating electrodes positioned in the centre of an array of recording electrodes which was surrounded by areas expressing heterosynaptic LTD. Teyler et al., (1994) proposed that the induction of LTD at the inactive synapses could be triggered by a lower rise in $[Ca^{2+}]_i$ at the synapses and might

be due to Ca^{2+} entry via VDCC or the diffusion of Ca^{2+} within the cell. Since Ca^{2+} is avidly buffered by many cytosolic binding proteins, such diffusion may not occur. It is more likely that cellular depolarization activating VDCCs facilitated Ca^{2+} entry. VDCC activation by strong tetanic stimulation has been reported to induce LTP in an NMDA receptor-independent manner (Grover & Teyler 1990, 1992), but it is also known that following tetanic stimulation there is a drop in the $[Ca^{2+}]_o$ when measured by a Ca^{2+} sensitive extracellular electrode (Melchers et al., 1988). Depolarizarion of synapses adjacent to those tetanized would therefore lead to VDCC activation and less Ca^{2+} entry than at the tetanized synapses, thus facilitating heterosynaptic LTD induction.

We have investigated in our laboratory mechanisms of non-associative LTD induction, testing the Ca^{2+} hypothesis by different means. By varying the $[Ca^{2+}]$ and $[Mg^{2+}]$ in ACSF, we have attempted to limit Ca^{2+} entry on postsynaptic depolarization and facilitate LTD induction. A large non-associative LTD was induced in 5 of 9 cells by intracellular conditioning when bathed in ACSF containing 1 mM Ca^{2+}. No LTD was seen following conditioning in cells bathed in ACSF containing 4 mM Ca^{2+}. In addition LTD was also seen in 3 out of 4 cells following conditioning during a transient wash with ACSF containing 25 mM Mg^{2+} and 2 mM Ca^{2+}. It is well to note that in the 1 mM Ca^{2+}/2 mM Mg^{2+} ACSF, with 19 mM $NaHCO_3$ in the bathing medium, the ionised $[Ca^{2+}]$ would be between 0·8 and 0·85 mM (Schaer, 1974). These values are closer to the ion concentrations measured by ion-sensitive electrodes in the brain *in vivo* (about 1·2 mM Ca^{2+} and 2·0 mM Mg^{2+}, see Leschinger et al., 1993) than the ACSF values for $[Ca^{2+}]$ of $\geq$2 mM used by most laboratories working on slices *in vitro*. Physiological induction of LTP in the brain would most probably not occur at the large numbers of synapses that are affected by tetanization via a stimulating electrode in the slice preparation and therefore the reduction in $[Ca^{2+}]_o$ following LTP induction would not be as great. It is possible that this lower physiological $[Ca^{2+}]_o$ would facilitate induction of heterosynaptic LTD on depolarization of inactive synapses adjacent to the LTP region.

The most straightforward conclusion from our experiments with cellular depolarization in ACSF containing different $[Ca^{2+}]$ and $[Mg^{2+}]$, is that the amount of Ca^{2+} entry during postsynaptic depolarization is a critical factor in the induction of non-associative LTD. Specifically, there is a level of activity-dependent increase of dendritic $[Ca^{2+}]_i$ that if exceeded precludes LTD induction. These results can in some respect be fitted to the ABS rule of synaptic plasticity (Artola & Singer 1993; see Figure 5.2iA) which accounts for synaptic change at the inactive test synapses. To do this a slight

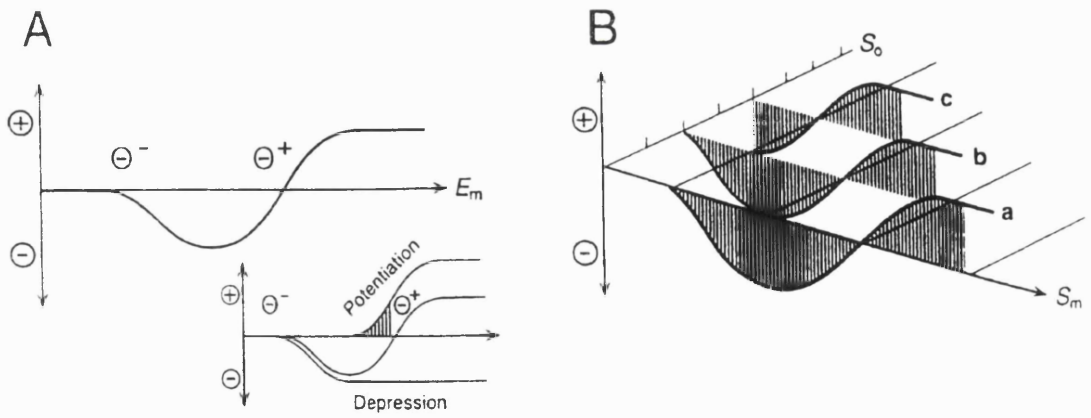

FIGURE 5.2i: The Artola, Bröcher and Singer (ABS) rule for synaptic modification.

A The original ABS rule, where the direction of synaptic change, LTP (⊕), or LTD (⊖) depends on the membrane potential (E_m) of the postsynaptic cell or in mechanistic terms, on the amplitude of the surge of $[Ca^{2+}]_i$. If the first threshold Θ^- is reached, a mechanism is reached that leads to LTD. If the second threshold Θ^+ is reached, another process is triggered that leads to LTP (see inset).

B The 'extended' ABS rule which accounts for changes in synaptic strength of a test input (S_m) as a function of the activation of other inputs (S_o). Increasing the activity of input S_o leads to a gradual leftward shift of the function describing the relationship between activation of input S_m, and the resulting modification of S_m.

Figure taken from Artola & Singer (1993).

reinterpretation of the model would have to be made. The ABS rule suggests that the direction of change of synaptic strength is dependent upon postsynaptic activity (or surge in $[Ca^{2+}]_i$ at the test synapses). Heterosynaptic changes in synaptic strength can be fitted to the rule, using the 'extended' ABS model (Artola & Singer 1993; Figure 5.2iB). The extended ABS rule suggests that activity at (homosynaptic) synapses *lowers* the *threshold* for LTD (and LTP) induction at independent test synapses such that synaptic depression (or potentiation) can occur when the test synapses are **inactive**. However it seems implausible that LTD at the inactive synapses is due to a lowering of the threshold such that the Ca^{2+} surge at these synapses is zero as suggested by the extended ABS rule. Ignoring the extended ABS model, the original ABS rule may used to incorporate both homo- and heterosynaptic events. Increasing activity at adjacent synapses would lead to a greater depolarization of the inactive (test) synapses. This depolarization at the test synapses would lead to activation of VDCCs and an increase in postsynaptic $[Ca^{2+}]$ that may trigger LTD, the threshold of which remains unchanged. This interpretation of the ABS model would assume that presynaptic activity at the test synapses is not necessary for LTD induction. Whether LTP induction would occur at higher levels of postsynaptic depolarization in the absence of presynaptic activity remains debatable.

Taking into account that our experiments attempted to limit Ca^{2+} entry by indirect means, our initial conclusion of the results from the high and low $[Ca^{2+}]_o$ ACSF experiments could be questioned. An alternative explanation for our results might concern the effect of altered $[Ca^{2+}]_o$ on inhibitory events. We noted that there was a reduction in inhibitory events following synaptic stimulation when the slice was bathed in ACSF containing 1 mM Ca^{2+}, most likely due to the reduction in release probability which in turn reduced the effect of recurrent inhibitory circuits (Lacaille et al., 1987). It has been shown that even the firing of a single neurone may result in recurrent inhibition because reciprocal connections exist between pyramidal neurons and basket cell inhibitory interneurones (Lacaille et al., 1987; Buhl et al., 1994). A decrease in inhibitory mechanisms would also be in effect during intracellular conditioning. ACSF containing 1 mM $[Ca^{2+}]_o$ may reduce inhibitory transmitter release (GABA) from interneurones during conditioning, leading to a reduction in the Cl^- conductance across the membrane of the activated cell reducing inhibitory shunting. This reduction in inhibitory shunting could lead to a greater depolarization in the dendrites of the conditioned cell and in turn increase the rise in $[Ca^{2+}]_i$ distally in the cell during somatic depolarization.

Another factor to take into consideration is that there was a higher divalent cation concentration in ACSF containing 4 mM Ca^{2+}. The increased $[Ca^{2+}]_o$ should enhance Ca^{2+} entry due to the increase in the gradient of free Ca^{2+} across the cell membrane, but the increase in the divalent cation concentration outside of the cell should have had the effect of increasing the threshold of VDCC activation (Hille, 1992). This difference in the gating properties of the VDCCs may not have exerted a major effect since the conditioning depolarizing current pulses were superimposed upon steady depolarization that took the cells to firing threshold.

In our experiments, LTD induction was attempted in single cells. Following conditioning in ACSF containing 1 mM Ca^{2+} a large LTD was seen in a population of these cells. The smaller heterosynaptic changes detected in field EPSPs (for example see Abraham & Wickens, 1991) may therefore be the result of averaging across many cells. There could be a number of reasons why LTD induction failed in 4 of the 9 cells tested in ACSF containing 1 mM Ca^{2+}. It is possible that these cells contained synapses that were not modifiable. This is unlikely since several studies have reported that most pyramidal cells can support non-associative LTD. Pockett et al., (1990) reported LTD following antidromic conditioning in ACSF containing 25 mM Mg^{2+} in all 11 cells tested, and Cummings et al., (1996) using the whole cell patch clamp technique reported a robust and reliable LTD following unpaired voltage pulses. A more likely reason is that there is a window of dendritic $[Ca^{2+}]_i$ that must be achieved in order to elicit LTD. Spruston et al. (1995) reported that following a train of back-propagating action potentials elicited by somatic depolarization, there was a decrease in calcium entry with distance along the dendrite away from the soma. In addition there was a large variability in the dendritic $[Ca^{2+}]_i$ level following the train of action potentials such that at 100 µm from the soma the rise in $[Ca^{2+}]_i$ ranged from approximately 200 to 700 nM. This variability suggests that the level of dendritic $[Ca^{2+}]_i$ following intracellular conditioning in ACSF containing 1 mM Ca^{2+} sometimes did not reach, and maybe sometimes surpassed, the level necessary for LTD induction. Another possibility is that the dendritic $[Ca^{2+}]_i$ rise following intracellular conditioning in these cells was fairly constant but the calcium rise necessary for LTD induction varied depending on the previous history of the synapse (Bienenstock et al., 1982). Finally it may be the case that the synapses were maximally depressed before conditioning occurred.

An enhanced dendritic Ca^{2+} influx facilitating LTD induction would appear to agree with the results of Wickens & Abraham, (1991). Alternatively a reduced Ca^{2+}

influx facilitating LTD induction would appear to agree with the results of Pockett & Lippold, (1986) and Pockett et al. (1990). Surprisingly all of these experiments can be fitted to the ABS rule taking into account the quite different induction and recording techniques. In the ABS rule there is a level of $[Ca^{2+}]_i$ that sits between the thresholds for LTD and LTP induction that if reached does not change synaptic strength. In addition there is also a level of $[Ca^{2+}]_i$ that is below the threshold for LTD induction that if reached has no effect. Therefore it may be the case that the failure to induce LTD reported by Wickens & Abraham (1991) was when the Ca^{2+} entry was below the threshold for LTD and hence enhancing the Ca^{2+} entry produced LTD. Conversely failure to induce LTD in our own experiments could have been due to the Ca^{2+} level being too high.

5.3 Postsynaptic conditioning with Cs^+ in the recording electrode.

Cummings et al., (1996) induced non-associative LTD by unpaired depolarizing voltage steps in individual cells using the whole cell patch clamp technique. In this study the LTD was blocked by presence of the calcium chelator BAPTA in the cell and by the L-type VDCC antagonist nifedipine. In addition, raising the $[Ca^{2+}]_o$ in the ACSF to 5 mM resulted in STP following conditioning. In a separate report Kullmann et al. (1992) reported STPs following depolarizing voltage pulses to 0 mV when Cs^+ was introduced into the cell. In our own experiments conditioning in ACSF containing 4 mM Ca^{2+} had no effect on synaptic strength. According to the ABS rule increasing the Ca^{2+} entry further again should result in synaptic potentiation. In an attempt to repeat the results of Kullmann et al. (1992), intracellular conditioning was applied to cells with recording electrodes containing Cs^+.

The effect of intracellular conditioning when Cs^+ was present in the recording electrode was varied. STP, no effect and LTD were all seen. The failure to repeat the findings of Kullmann et al. (1992) and Cummings et al. (1996), may have been due to the differences in induction protocol. The protocol used by Kullmann et al. (1992) used longer depolarizing pulses at higher frequencies. These presumably enabled a greater rise in $[Ca^{2+}]_i$ at the test synapses. Intracellular conditioning used in my study evoked broad, presumed Ca^{2+} spikes which varied in both number and width. Since it was difficult to control the magnitude of the dendritic rise of $[Ca^{2+}]_i$ using this technique it is not surprising that both STP, no effect and LTD were seen following conditioning. It is also true that the majority of experiments reported by Kullmann et al. (1992) were

performed using the whole cell patch clamp technique which would allow large amounts of Cs^+ to enter the cell at the start of each recording whereas using sharp electrodes the majority of Cs^+ presumably entered the cell during the conditioning procedure when positive current was applied. In two of the cells in which an LTD was seen there was also an associated rise in R_{in} following conditioning, probably due to an increase in the amount of Cs^+ present in the cell. An increase in the space constant following a reduction of the delayed rectifier K^+ current by intracellular Cs^+ (Dreyer, 1990) should not measurably affect EPSP slope (Spruston et al., 1994). It is possible that an unnoticed dendritic depolarization due to cell deterioration, exacerbated by poor space clamp may produce a reduction in EPSP slope. The inclusion of the NMDA receptor antagonist D-APV was not thought to affect the probability of STP induction since all of the experiments performed by Kullmann et al. (1992) was in the presence of this drug. Jaffe et al., (1992) using Ca^{2+} imaging techniques reported no difference in Ca^{2+} entry following postsynaptic depolarization in the presence of the K^+ channel blocker TEA with or without D-APV.

It is interesting that the only LTP I evoked was produced by the pairing of an EPSP with postsynaptic depolarization in the absence of the NMDA receptor antagonist D-APV. Kullmann et al. (1992) reported the induction of LTP only following depolarization paired with afferent stimulation. Conventional belief is that homosynaptic LTP in the CA1 usually requires NMDA receptor activation (Collingridge et al., 1983) through which Ca^{2+} enters the cell (Alford et al., 1993). The NMDA receptor-channel, acting as a molecular coincidence detector, opens in response to presynaptic release of glutamate together with postsynaptic depolarization, which relieves a voltage-dependent Mg^{2+} block (Ascher & Nowak, 1988). It has now been disputed that Ca^{2+} entry via the NMDA receptor-channel is necessary for LTP induction since using a high frequency tetanus Grover & Teyler, (1992) found that LTP was induced in an NMDA receptor-independent manner. It is now thought that Ca^{2+} entry during LTP induction may come from a number of sources depending on the induction protocol, and that glutamate release presynaptically is needed to activate postsynaptic NMDA and metabotropic glutamate receptors (mGluRs). Some groups have shown mGluR activation to be necessary in order to produce LTP in CA1 (Bashir et al., 1993; but see Selig et al., 1995b).

There have also been reports of LTP induction following postsynaptic depolarization without presynaptic activity. Volgushev et al. (1994) and Kuhnt et al.

(1994) reported and mixture of LTD, no effect and LTP following intracellular tetanization in the visual cortex and CA1 respectively. In addition Pockett et al. (1990) reported LTP or LTD, or no effect following conditioning in ACSF alone. In the studies using intracellular tetanization or conditioning it is possible that there was activation of mGluRs by the presence of ambient glutamate (Sah et al., 1989) released by activation of the target cell. Indeed mGluR activation has been implicated in LFS induced LTD (Bolshakov & Siegelbaum, 1994). Alternatively, the level of free $[Ca^{2+}]_i$ may not predict the direction or induction of synaptic change. Neveu & Zucker, (1996), reported that the photolytic release of intracellular calcium from a caged-Ca^{2+} compound (nitr-5) resulted in a mixture of LTP, LTD and no effect.

5.4 LTP induction.

In order to investigate whether non-associative depotentiation could be produced, it was first necessary to induce stable synaptic potentiation. It has already be seen that a large and stable LTP was induced by the pairing of a single EPSP with depolarizing current pulses when Cs^+ was present in the recording electrode. It is well established that the repeated pairing of large depolarizing current pulses with single EPSPs can result in LTP (Gustafsson et al., 1987) but the presence of Cs^+ and the resulting block of dendritic K^+ channels was probably a contributing factor in the LTP described in Section 3.9. An NMDA receptor-independent LTP induced by synaptic activation during K^+ channel block by TEA been reported by several groups (Aniksztejn & Ben-Ari, 1991; Huang & Malenka, 1993) which, like tetanus-induced LTP requires PKC activation (Petrozzino & Connor, 1994; Huber et al., 1995). In my experiments, a 7 min application of 25 mM TEA during synaptic activation failed to induce persistent increases in synaptic strength. Why TEA application resulted in only short term potentiation is unknown. Since I found this method of LTP induction to be unreliable, other means were sought.

Attempts to induce stable potentiation using theta burst stimulation (TBS; Larson & Lynch, 1986; Larson et al., 1986) were successful in 8 of 20 slices. It is unlikely that failure to induce LTP in some cells was due to insufficient depolarization since the $GABA_A$ receptor antagonist bicuculline (10 μM) was present throughout, and during the induction procedure the width of the test shock was doubled. Even though failure to induce LTP of extracellularly recorded EPSPs following TBS has been reported when

using an unusually high stimulation strength (Barr et al., 1995), it is entirely possible that there was a population of synapses that are unmodifiable in the slices.

5.5 Induction of depotentiation.

A higher probability of LTD induction following potentiation of the test synapses (depotentiation) compared with the probability of LTD induction in the naïve slice would suggest that there was maximal depression of some synapses in the naïve slice prior to intracellular conditioning. This hypothesis was tested by applying intracellular conditioning to cells bathed in the presence of the $GABA_A$ receptor antagonist bicuculline (normal ACSF; 2 mM Ca^{2+}) in the naïve and potentiated slice. This induction protocol has been reported to induce LTD in 40% of cases in the naïve slice (Christofi et al., 1993a). I was unable to repeat the results of Christofi et al. (1993a) in the naïve slice (Barry et al., 1996b). However, synaptic depotentiation was observed in 5 of 9 cells tested. Thus the previous history of the synapses in the slice may be relevant to whether or not LTD can be elicited.

A failure to produce homosynaptic LTD in naïve synapses, but successful depotentiation following LTP induction has been reported by many groups using LFS in field potential studies (Barrionuevo et al., 1980; Staubli & Lynch, 1990; Fujii et al., 1991; Bortolotto et al., 1994; O'Dell & Kandel, 1994; Wagner & Alger, 1995). It may be explained by the age of the animals used, since the magnitude of the LTD caused by LFS has been shown to decrease with the age of the animal (Dudek & Bear, 1993; Wagner & Alger, 1995; Errington et al., 1995). Since the rats used in my study were young adults this could be the case. Indeed heterosynaptic LTD has been reported to share common mechanisms with homosynaptic LTD following occlusion experiments (Scanziani et al., 1996). It should kept in mind, that although failure to induce LTD in the naïve slice could have been because of the mature animals used in this study, non-associative LTD can be induced in ACSF containing 1 mM Ca^{2+} in the naïve slice. In addition Vickery & Bindman (1997) using the same technique in younger rats (~3 weeks) also failed to induce LTD in bicuculline.

Several studies have suggested that synaptic activity which did not change synaptic strength in itself, could prime the synapse for synaptic change by a subsequent stimulus that would normally have had no effect (Huang et al., 1992; Wexler & Stanton, 1993). The results of priming experiments lend experimental evidence to the sliding threshold function in the synaptic modification rule proposed by Bienenstock et al.

(1982; see also Stanton 1996). We have no evidence for priming by TBS since subsequent intracellular conditioning did not induce LTD when no LTP was seen. It seems more likely that in the naïve slice some synapses were already maximally depressed and that depotentiation is in fact LTD (see Wagner & Alger, 1996).

Several laboratories have noted that the magnitude of LFS-induced depotentiation depends on the delay between the LTP-inducing stimulus and LFS. Depotentiation is smaller when there is a longer delay so, that after a period of 1 hour LTP has consolidated and the synapses are not so modifiable (Staubli & Chun, 1996; O'Dell & Kandel, 1994). In all but one of the cells tested in this study depotentiation was attempted 26 min following the LTP inducing stimulus and when depotentiation was seen its magnitude was variable. In one individual cell a large depotentiation was obtained following a lasting potentiation (> 40 min) of EPSP slope induced by LFS in the presence of bicuculline (as has been reported by Wagner & Alger, 1995). Although depotentiation following a 40 min delay was induced in only one cell, it was larger in magnitude than in all but one of the depotentiations induced following a 26 min delay. This result may indicate that depotentiation induced by LFS and by postsynaptic depolarization are acting via different mechanisms.

If it is the case that depotentiation, like LTD, is induced when the activity-dependent rise in postsynaptic [Ca^{2+}] is limited, how might bicuculline lower Ca^{2+} entry? It is known that a depolarizing action of GABA can be elicited on apical dendrites, mediated by $GABA_A$ receptors (Langmoen et al., 1978; Andersen et al., 1980; Alger & Nicoll, 1982a, b). Repetitive firing of inhibitory interneurones during conditioning could increase dendritic [Cl^-] and progressively depolarize the pyramidal cell dendrite (Grover et al., 1993), perhaps by activation of reciprocal inhibitory circuits between pyramidal neurons and basket cell inhibitory interneurones (Lacaille et al., 1987; Buhl et al., 1994) or by the spill over of GABA onto synapses after strong stimulation. Indeed Buhl et al. (1994) showed that biphasic hyperpolarizing/depolarizing responses, vulnerable to bicuculline, were elicited in pyramidal cells by basket cells, where the post-inhibitory facilitation was sufficient to cause firing. Hence bicuculline would reduce the amount of Ca^{2+} entering via VDCCs during conditioning by hyperpolarizing the dendrites.

5.6 Measurement of $[Ca^{2+}]_i$ during intracellular conditioning.

In order to investigate directly the role of Ca^{2+} in non-associative synaptic change, we have measured $[Ca^{2+}]_i$ during intracellular conditioning with the calcium indicator Fura-2 under conditions in which LTD could be produced.

Following the initial analysis of $[Ca^{2+}]_i$ measurements during intracellular conditioning, it was evident that manoeuvres designed to limit Ca^{2+} entry into the postsynaptic cell and induce LTD induction did indeed lower the rise in $[Ca^{2+}]_i$ following intracellular depolarization compared to depolarization in ACSF alone. Pockett et al. (1990) reported a robust and reliable LTD produced by an antidromic tetanus during a transient wash with ACSF containing 25 mM Mg^{2+} and 2 mM Ca^{2+} that blocked synaptic transmission. Replacing the antidromic tetanus with discrete intracellular depolarizing pulses we found, confirming the results of Christofi et al. (1993b), that the mean rise in somatic $[Ca^{2+}]_i$ was reduced on postsynaptic depolarization in ACSF containing 25 mM Mg^{2+} compared to depolarization in normal ACSF containing 1 mM Mg^{2+}. This reduced rise in mean $[Ca^{2+}]_i$ on depolarization in ACSF containing 25 mM Mg^{2+} was also seen in the four cells from which dendritic measurements were possible. This result suggests that the high $[Mg^{2+}]_o$ was acting as a competitive antagonist at VDCCs, thus lowering Ca^{2+} influx on cellular depolarization and hence facilitating non-associative LTD induction.

Christofi et al., (1991) reported that LTD induced by antidromic conditioning requires extracellular calcium. To test for intracellular rises in $[Ca^{2+}]$ following depolarization in the absence of extracellular calcium, intracellular conditioning was applied to cells bathed in ACSF with 15 mM Mg^{2+} and 0 mM Ca^{2+}. Using this procedure, rises in $[Ca^{2+}]_i$ were found to present, but at much lower levels than when applying intracellular conditioning to cells bathed in the ACSF containing 25 mM Mg^{2+} and 2 mM Ca^{2+}. The small rise in $[Ca^{2+}]_i$ when calcium was removed from the bathing medium may be due to residual calcium that remained in the slice following the wash in of ACSF containing 0 mM Ca^{2+}. Although this result may explain the observations of Christofi et al. (1991), since this very low rise in $[Ca^{2+}]_i$ is below the threshold for LTD induction, during my experiments LTD was seen in one cell but not in a second (see Section 5.7).

Measurement of somatic $[Ca^{2+}]_i$ was also made from two cells bathed in ACSF containing 1 mM Ca^{2+} and 2 mM Mg^{2+}. A reduction in the rise of $[Ca^{2+}]_i$ on postsynaptic depolarization in ACSF containing 1 mM Ca^{2+} compared to depolarization in normal

ACSF was seen in one of these cells. Under these conditions, LTD was induced in 5 of 9 cells (see Section 3.6). Failure to produce LTD in just under half of these cells tested could therefore be attributed to the failure of 1 mM Ca^{2+} ACSF to reduce Ca^{2+} entry on depolarization in this population of cells. This reason behind the failure of ACSF containing 1 mM Ca^{2+} to reduce Ca^{2+} entry on depolarization compared to control conditions in one of the cells tested was not known. There were no differences in cell characteristics or in the number of spikes produced per depolarizing pulse in the two conditions. It should be noted that in these two cells dendritic $[Ca^{2+}]_i$ measurements were not obtained due to the extremely poor fluorescence signals. It was not possible therefore to identify the effect (if any) the 1 mM Ca^{2+} ACSF had on dendritic Ca^{2+} transients. Further investigation into the precise effect depolarization in 1 mM Ca^{2+} ACSF has on dendritic $[Ca^{2+}]_i$, in conjunction with electrophysiological recording is necessary before any firm correlation between a reduced Ca^{2+} entry and non-associative LTD can be made.

Similar experiments performed on cells bathed in the $GABA_A$ receptor antagonist bicuculline revealed a reduction in the mean rise in somatic rise in $[Ca^{2+}]_i$ on depolarization compared to depolarization in ACSF alone. If depotentiation is simply LTD of synapses that were previously maximally depressed in the naïve slice, as the results suggest, the level of $[Ca^{2+}]_i$ achieved on depolarization in bicuculline is at the level necessary to trigger LTD expression. As with the experiments in ACSF containing 1 mM Ca^{2+}, the dendritic fluorescence signals were too weak to measure. The result obtained from somatic fluorescence measurements, that bicuculline reduced Ca^{2+} entry on depolarization was somewhat surprising. It had been thought that bicuculline could cause a decrease in dendritic Ca^{2+} as previously explained, but it is unknown how it might limit Ca^{2+} entry at the soma. It is a possibility that bicuculline may be acting non-specifically at VDCCs. This was tested in a indirect manner by the application of the AMPA receptor antagonist CNQX to the slice. On postsynaptic depolarization cellular activity would cause activation of recurrent inhibitory interneurones via glutamatergic synaptic connections. Addition of CNQX to the bathing medium at a concentration that blocks synaptic transmission would prevent activity of these interneurones a hence reduce activation of these recurrent inhibitory circuits. Fluorescence measurements from cells bathed in CNQX showed no difference in somatic Ca^{2+} transients on postsynaptic depolarization compared with ACSF alone. This result indicates that bicuculline may have been acting in a non-specific manner in lowering Ca^{2+} entry on depolarization. This

conclusion is complicated by the fact that in the one cell which yielded dendritic $[Ca^{2+}]_i$ measurements in CNQX, a large reduction in the rise of dendritic $[Ca^{2+}]_i$ was seen in the presence of the AMPA receptor antagonist. It is quite possible that ambient glutamate in the synaptic cleft is activating postsynaptic AMPA and NMDA receptors during depolarization in normal ACSF and that Ca^{2+} entry via the AMPA receptor-channel is reduced in the presence of CNQX. Alternatively it may be possible that the CNQX block on AMPA channels may reduce the amount of depolarization on conditioning, this would reduce Ca^{2+} entry via the NMDA receptor-channel which would also be activated in these circumstances.

5.7 Correlation of $[Ca^{2+}]_i$ measurements and electrophysiological data.

In a number of the cells from which $[Ca^{2+}]_i$ measurements were made, postsynaptic potentials induced by afferent stimulation were also recorded. As there was no change in synaptic strength following conditioning in ACSF alone in the 11 cells where dual electrophysiological and $[Ca^{2+}]_i$ measurements were made, it could be inferred that LTD is induced when there was a limited rise in postsynaptic $[Ca^{2+}]_i$. In fact, this correlation between a reduced Ca^{2+} influx and LTD induction was not so straightforward. In one of the 3 cells in which LTD was induced, a reduction in the rise in dendritic $[Ca^{2+}]_i$ in ACSF containing 25 mM Mg^{2+} was not seen. Additionally, there was a reduced rise in $[Ca^{2+}]_i$ following conditioning in ACSF containing 25 mM Mg^{2+} compared to ACSF alone in the cell that failed to produce LTD.

Further examination of a limited Ca^{2+} rise following postsynaptic depolarization on synaptic strength was performed by bathing the slice in a ACSF containing no added Ca^{2+} and 15 mM Mg^{2+}. Cummings et al. (1996) reported that heterosynaptic LTD induced by unpaired voltage pulses was prevented by the intracellular application of the Ca^{2+}-chelator BAPTA. This would fit our interpretation of the ABS synaptic modification rule in which there was a level of Ca^{2+} entry which is too low to trigger LTD induction. Intracellular conditioning applied to the two cells bathed in ACSF containing 15 mM Mg^{2+} and 0 mM Ca^{2+} resulted in one LTD and one no effect. Compiling the Ca^{2+} measurement data from these and three other cells, the rise in somatic $[Ca^{2+}]_i$ following depolarization in ACSF containing 15 mM Mg^{2+} and 0 mM Ca^{2+} was reduced compared to that in ACSF alone, and was proportionately less than conditioning in ACSF containing 25 mM Mg^{2+}. This data further complicates the simple Ca^{2+} level story. It is possible that there was some residual Ca^{2+} in the this ACSF

medium, but we have predicted that Ca^{2+} entry at this lower level would prevent LTD induction.

Comparison between rises in somatic $[Ca^{2+}]_i$ and changes in synaptic strength across the various experiments show poor correlation. Although this analysis suggests that the level of Ca^{2+} rise after cellular depolarization is not related to the induction of LTD, it must be remembered that these synaptic changes are occurring somewhere along the dendritic tree and not at the soma. It is possible that in the experiments where dendritic fluorescence images were not seen, Fura-2 was present in the dendrites, but the thickness of the slice caused sufficient scatter that no image was seen. If this were the case, the level of calcium buffering by Fura-2 in the dendrites may vary across the cells and influence whether LTD is triggered or not. Indeed, in previous calcium imaging studies using Fura-2 or Fluo-3 loaded cells, LTP or LTD induction has ~~not~~ been observed (Regehr & Tank, 1990; Regehr & Tank, 1992; Müller & Connor, 1991; Miyakawa et al., 1992; Alford et al., 1993; Perkel et al., 1993; Manilow et al., 1994), which was probably due to the strong Ca^{2+}-chelating action of Fura-2 and Fluo-3. Only when using the intracellular Ca^{2+}-indicator rhod-2 which has a much weaker Ca^{2+}-chelating action, has both LTP and LTD been induced by a strong and weak tetani respectively in the rat visual cortex (Yasuda & Tsumoto, 1996).

Comparison between the rise in dendritic $[Ca^{2+}]_i$ rather than somatic $[Ca^{2+}]_i$ to the induction of non-associative LTD would be preferable since it is in the dendrites where the synaptic change occurs. As in the soma there was no correlation found between the rise in dendritic $[Ca^{2+}]_i$ and LTD induction. The finding that there was no relationship between the rise in dendritic $[Ca^{2+}]_i$ and LTD induction differs from published models of synaptic change (Lisman, 1989; Artola & Singer, 1993) and much experimental data (Bröcher et al., 1992; Mulkey & Malenka, 1992; Cummings et al., 1996; Yasuda & Tsumoto, 1996) including our own initial conclusions but agrees with the work of Neveu & Zucker (1996). One major problem in interpreting these results is that the exact spatial position of the test synapses on dendrites is not known. It is known that the stimulating electrodes are placed within 100 μm of the CA1 pyramidal cell bodies in the stratum radiatum, therefore an average rise in $[Ca^{2+}]_i$ was calculated over this region. It is quite possible that across the cells tested, the position and the number of synapses tested differed. Differences in Ca^{2+} compartmentalization along the dendritic tree could mean that there are variable rises in $[Ca^{2+}]_i$ at individual sites. Using our method of data acquisition, fluorescence signals along the dendrite were split into boxes. Within a box

of approximately 20 μm in length, localized changes in the fluorescence (if any) would be averaged out. It is therefore possible that our measurements, although on a dendritic level, are not focused enough to adequately correlate $[Ca^{2+}]_i$ rise with LTD induction. This is not to say that it is incorrect.

It has been noted in at least one report (Scanziani et al., 1996) that heterosynaptic LTD can be induced in a calcium independent manner following tetanic activation of neighbouring cells. In another study Bolshakov & Siegelbaum (1994) reported LTD induction by depolarizing pulses but only when in conjunction with mGluR activation. The activation of mGluRs may have been necessary in order to increase the postsynaptic $[Ca^{2+}]_i$ via the release of calcium from intracellular stores to a level necessary for LTD induction. Alternatively, mGluR activation may have been necessary in order to produce a co-factor necessary to the induction of LTD. It is possible therefore that in my experiments, the absence or presence of an unknown co-factor may have distorted the relationship between dendritic $[Ca^{2+}]_i$ and LTD induction.

It is possible that the temporal features of the rise in dendritic $[Ca^{2+}]_i$ may also play a pivotal role in the induction of LTD. Debanne et al., (1994) reported an associative LTD in area CA1 by asynchronous pairing of pre- and postsynaptic activity. The time delay between the two was critical. Unfortunately in my study a correlation between LTD induction and duration of the calcium signal could not be made due to the temporal limitations on fluorescence data acquisition.

5.8 Summary.

Many laboratories have studied the characteristics of homosynatic LTD in the CA1 region of the hippocampus since the initial reports of Dudek & Bear (1992) and Mulkey & Malenka (1992). My study is one of the few to investigate the induction of non-associative LTD. In the first section of this study, electrophysiological experiments provided some evidence that the level of postsynaptic calcium influx is important in the induction of non-associative LTD. Specifically, experiments designed to lower calcium entry on postsynaptic depolarization increased the probability of LTD induction. It was also shown that the previous history of the synapse (i.e. prior LTP) is important in whether LTD can be induced. In the second part of this study, measurements of somatic and dendritic $[Ca^{2+}]_i$ on postsynaptic depolarization show that the indirect methods of restricting postsynaptic calcium used by our and other laboratories to induce LTD, do in general lower the rise in postsynaptic $[Ca^{2+}]_i$ compared to control conditions.

Although these experiments strongly suggest that LTD induction is facilitated by a restricted calcium entry on postsynaptic depolarization, measurements relating conditioning-induced intracellular calcium levels and EPSP depression show no correlation. Spatial limitations of our measurements were discussed and might account for the lack of correlation. Alternatively, the Ca^{2+} level hypothesis for changes in synaptic strength may be inadequate.

5.9 Further Experiments.

Further investigations into the Ca^{2+}-dependence of non-associative LTD could be approached using VDCC antagonists and compounds that enhance the action of VDCCs upon cellular depolarization (see Wickens & Abraham, 1991). Addition of the L-type VDCC antagonist nimodipine to normal ACSF would not significantly affect presynaptic transmitter release, and therefore not affect recurrent inhibitory circuits but would limit the entry of Ca^{2+} into the cell upon depolarization. Changing the concentration of nimodipine such that Ca^{2+} entry via VDCCs is possible but limited, may reproduce the results obtained in ACSF containing 1 mM Ca^{2+}, without the problems associated with lowering the $[Ca^{2+}]_o$.

Once a reliable method of non-associative LTD induction is found many other experiments could be performed. It is known that postsynaptic glutamate receptors can be activated by the action of ambient glutamate surrounding the cells (Sah et al., 1989). Although intracellular depolarization is performed in the absence of test stimulation, ambient glutamate may have a role in activating postsynaptic glutamate receptors. Therefore the dependence of non-associative LTD on NMDA, and metabotropic glutamate receptor activation should be investigated.

REFERENCES

Abraham, W.C. & Bear, M.F. (1996). Metaplasticity: The plasticity of synaptic plasticity. *Trends. Neurosci.* **19**, 126-130.

Abraham, W.C. & Goddard, G.V. (1983). Assymetric relationships between homosynaptic long-term potential and heterosynaptic long-term depression. *Nature* **305**, 717-719.

Abraham, W.C. & Wickens, J.R. (1991). Heterosynaptic long-term depression is facilitated by blockade of inhibition in area CA1 of the hippocampus. *Brain Res.* **546**, 336-340.

Aiba, A., Chen, C., Herrup, K., Rosenmund, C., Stevens, C.F. & Tonegawa, S. (1994). Reduced hippocampal long-term potentiation and context-specific deficit in associative learning in mGluR1 mutant mice. *Cell* **79**, 365-375.

Alford, S., Frenguelli, B.G., Schofield, J.G. & Collingridge, G.L. (1993). Characterization of Ca^{2+} signals induced in hippocampal CA1 neurons by the synaptic activation of NMDA receptors. *J. Physiol.* **469**, 693-716.

Alger, B.E., Dhanjal, S.S., Dingledine, R., Garthwaite, J., Henderson, G., King, G.L., Lipton, P., North, A., Schwartzkroin, T.A., Sears, T.A., Segal, M., Whittingham, T.S. & Williams, J. (1984). *Brain slices*. Dingledine & Raymond Editors. New York. Plenum Press.

Alger, B.E., Megela, A.L. & Teyler, T.J. (1978). Transient heterosynaptic depression in the hippocampal slice. *Brain Res. Bull.* **3**, 181-184.

Alger, B.E. & Nicoll, R.A. (1980). Epileptiform burst afterhyperpolarization: Calcium-dependent potassium potential in hippocampal CA1 pyramidal cells. *Science* **210**, 1122-1124.

Alger, B.E. & Nicoll, R.A. (1982a). Feed-forward dendritic inhibition in rat hippocampalpyramidal cells studied *in vitro*. *J. Physiol.* **328**, 105-123.

Alger, B.E. & Nicoll, R.A. (1982b). Pharmacological evidence for two kinds of GABA receptor on rat hippocampal pyramidal cells studied *in vitro*. *J. Physiol.* **328**, 125-141.

Alger, B.E. & Teyler, T.J. (1976). Long-term and short-term plasticity in the CA1, CA3 and dentate regions of the rat hippocampal slice. *Brain Res.* **110**, 463-480.

Almers, W. & Palade, P.T. (1981). Slow calcium and potassium currents across frog muscle membrane: Measurements with a vaseline-gap technique. *J. Physiol.* **312**, 159-176.

Andersen, P., Dingledine, R., Gjerstad, L., Langmoen, I.A. & Laursen, A.M. (1980). Two different responses of hippocampal pyramidal cells to application of γ-amino-butyric acid. *J. Physiol.* **305**, 279-296.

Andersen, P., Sundberg, S.H., Sveen, O. & Wigström, H. (1977). Specific long-lasting potentiation of synaptic transmission in hippocampal slices. *Nature* **266**, 736-737.
Andreasen, M. & Lambert, J.D. (1991). Noradrenaline receptors participate in the regulation of GABAergic inhibition in area CA1 of the rat hippocampus. *J. Physiol.* **439**, 649-669.

Aniksztejn, L. & Ben-Ari, Y. (1991). Novel form of long-term potentiation produced by a K^+ channel blocker in the hippocampus. *Nature* **349**, 67-69.

Artola, A., Bröcher, S. & Singer, W. (1990). Different voltage-dependent thresholds for inducing long-term depression and long-term potentiation in slices of rat visual cortex. *Nature* **347**, 69-72.

Artola, A. & Singer, W. (1993). Long-term depression of excitatory synaptic transmission and its relationship to long-term potentiation. *Trends Neurosci.* **16**, 480-487.

Ascher, P. & Nowak, L. (1988). The role of divalent cations in the *N*-methyl-D-aspartate responses of mouse central neurones in culture. *J. Physiol.* **399**, 247-266.

Ayala, G.F., Ditcher, M., Gumnit, R.J., Matsumoto, H. & Spencer, W.A. (1973). Genesis of epileptic interical spikes. New knowledge of cortical feedback systems suggest a neurophysiological explaination of brief paroxysms. *Brain Res.* **52**, 1-17.

Barr, D.S., Lambert, N.A., Hoyt, K.L., Moore, S.D. & Wilson, W.A. (1995). Induction and reversal of long-term potentiation by low- and high-intensity theta pattern stimulation. *J. Neurosci.* **15**, 5402-5410.

Barrionuevo, G., Schottler, F. & Lynch, G. (1980). The effects of repetitive low frequency stimulation on control and "potentiated" synaptic responses in the hippocampus. *Life Sci.* **27**, 2385-2391.

Barry, M.F., Vickery, R.M. & Bindman, L.J. (1996a). Postsynaptic induction of non-associative LTD and depotentiation in isolated slices of rat hippocampus. *J. Physiol. Paris*. In press.

Barry, M.F., Vickery, R.M. & Bindman, L.J. (1996b). A non-associative depotentiation of synaptic transmission can be induced postsynaptically in isolated slices of rat hippocampus. *J. Physiol.* In Press.

Barry, M.F., Vickery, R.M., Bolsover, S.R. & Bindman, L.J. (1996c). Intracellular studies of heterosynaptic long-term depression (LTD) in CA1 of hippocampal slices. *Hippocampus* **6**, 1-6.

Bashir, Z.I., Alford, S., Davies, S.N., Randall, A.D. & Collingridge, G.L. (1991). Long-term potentiation of NMDA receptor-mediated synaptic transmission in the hippocampus. *Nature* **349**, 156-158.

Bashir, Z.I., Bortolotto, Z.A., Davies, C.H., Berretta, N., Irving, A.J., Seal, A.J., Henley, J.M., Jane, D.E., Watkins, J.C. & Collingridge, G.L. (1993). Induction of LTP in the hippocampus needs synaptic activation of glutamate metabotropic receptors. *Nature* **363**, 347-350.

Bashir, Z.I. & Collingridge, G.L. (1992). NMDA receptor-dependent transient homo- and heterosynaptic depression in picrotoxin-treated hippocampal slices. *Eur. J. Neurosci.* **4**, 485-490.

Bashir, Z.I. & Collingridge, G.L. (1994). An investigation of depotentiation of long-term potentiation in the CA1 region of the hippocampus. *Exp. Brain Res.* **100**, 437-443.
Bear, M.F. & Malenka, R.C. (1994). Synaptic plasticity: LTP and LTD. *Curr. Opin. Neurobiol.* **4**, 389-399.

Bekkers, J.M. & Stevens, C.F. (1990). Presynaptic mechanism for long-term potentiation in the hippocampus. *Nature* **346**, 724-729.

Ben-Ari, Y., Aniksztejn, L. & Bregestovski, P. (1992). Protein kinase C modulation of NMDA currents: An important link for LTP induction. *Trends Neurosci.* **15**, 333-339.

Bienenstock, E., Cooper, L.N. & Munro, P. (1982). Theory for the development of neuron selectivity: Orientation specificity and binocular interaction in visual cortex. *J. Neurosci.* **2**, 23-48.

Bindman, L.J., Murphy, K.P.S.J. & Pockett, S. (1988). Postsynaptic control of induction of long-term changes in efficacy of transmission at neocortical synapses in slices of rat brain. *J. Neurophysiol.* **60**, 1053-1065.

Bliss, T.V.P. & Collingridge, G.L. (1993). A synaptic model of memory: Long-term potentiation in the hippocampus. *Nature* **361**, 31-39.

Bliss, T.V.P., Douglas, R.M., Errington, M.L. & Lynch, M.A. (1986). Correlation between long-term potentiation and release of endogenous amino-acids from dentate gyrus of anaesthetized rats. *J. Physiol.* **377**, 391-408.

Bliss, T.V.P. & Gardner-Medwin, A.R. (1973). Long-lasting potentiation of synaptic transmission in the dentate area of the unanaesthetized rabbit following stimulation of the perforant path. *J. Physiol.* **232**, 357-374.

Bliss, T.V.P. & Lømo, T. (1973). Long-lasting potentiation of synaptic transmission in the dentate area of the anaesthetized rabbit following stimulation of the perforant path. *J. Physiol.* **232**, 331-356.

Bohme, G.A., Bon, C., Stutzman, J.-M. & Blanchard, J.-C. (1991). Possible involvement of nitric oxide in long-term potentiation. *Eur. J. Pharmacol.* **199**, 379-383.

Bolshakov, V.Y. & Siegelbaum, S.A. (1994). Postaynaptic induction and presynaptic expression of hippocampal long-term depression. *Science* **264**, 1148-1152.

Bortolotto, Z.A., Bashir, Z.I., Davies, C.H. & Collingridge, G.L. (1994). A molecular switch activated by metabotopic glutamate receptors regulates induction of long-term potentiation. *Nature* **368**, 740-743.

Bortolotto, Z.A. & Collingridge, G.L. (1993). Characterization of LTP induced by the activation of glutamate metabotropic receptors in area CA1 of the hippocampus. *Neuropharmacology* **32**, 1-9.

Bradler, J.E. & Barrionuevo, G. (1989). Long-term potentiation in hippocampal CA3 neurons: Tetanized input regulates heterosynaptic efficacy. *Synapse* **4**, 132-142.

Bradley, P.M., Burns, B.D. & Webb A.C. (1991) Potentiation of synaptic responses in slices from the chick forebrain. *Proc. Royal. Soc. (Lond).* **243**, 19-24.

Bröcher, S. Artola, A. & Singer, W. (1992). Intracellular injection of Ca^{2+} chelators blocks induction of long-term depression in rat visual cortex. *Proc. Natl. Acad. Sci.* **89**, 123-127.

Brown, D.A., Gähwiler, B.H., Griffith, W.H. & Halliwell, J.V. (1990). Membrane currents in hippocampal neurons. *Prog. Brain Res.* **83**, 141-160.

Brown, T.H. & McAfee, D.A. (1982). Long-term synaptic potentiation in the superior cervical ganglion. *Science* **215**, 1411-1413.

Brown, R.E., Rabe, H. & Reymann, K.G. (1994). (RS)-α-methyl-4-carboxyphenylglygene (MCPG) does not block theta burst-induced long-term potentiation in area CA1 of rat hippocampal slices. *Neurosci. Lett.* **170**, 17-21.

Brown, T.H. & Zador, A.M. (1990). *The Synaptic Organization of the Brain.* Third Edition. Shepherd, G.M. Editor. Oxford University Press. Oxford. 346-388.

Buhl, E.H., Halasy, K. & Somogyi, P. (1994). Diverse sources of hippocampal unitary inhibitory postsynaptic potentials and the number of synaptic release sites. *Nature* **368**, 823-828.

Cajal, S.R. y (1894). La fine structure des centrex nerveux. *Proc.Roy. Soc. [Biol.]* **55**, 444-468.

Cajal, S.R. y (1911). *Histologie du Système Nerveux.* Paris. Maloine.

del Castillo, J. & Katz, B. (1954). Quantal components of the end-plate potential. *J. Physiol.* **124**, 560-573.

Charlton, M.P., Smith, S.J. & Zucker, R.S. (1982). Role of presynaptic calcium ions and channels in synaptic in synaptic facilitation and depression at the squid giant synapse. *J. Physiol.* **323**, 173-193.

Chetkovich, D.M., Klann, E. & Sweat, D.J. (1993). Nitric oxide synthase-independent long-term potentiation in area CA1 of the hippocampus. *NeuroReport* **4**, 919-922.

Chinestra, P., Aniksztejn, L., Diabira, D., & Ben-Ari, Y. (1993). (RS)-α-methyl-4-carboxyphenylglycine (MCPG) neither prevents induction of LTP nor antagonizes metabotropic glutamate receptors in CA1 hippocampal neurons. *J. Neurophysiol.* **70**, 2684-2689.

Christie, B.R. & Abraham, W.C. (1992). NMDA-dependent heterosynaptic long-term depression in the dentate gyrus of anaesthetized rats. *Synapse* **10**, 1-6.

Christie, B.R. & Abraham, W.C. (1994). L-type voltage sensitive calcium channel antagonists block heterosynaptic long-term depression in the dentate gyrus of anaesthetized rats. *Neurosci. Lett.* **167**, 41-45.

Christie, B.R., Kerr, D.S. & Abraham, W.C. (1994). Flip side of synaptic plasticity: Long-term depression mechanisms in the hippocampus. *Hippocampus* **4**, 127-135.

Christofi, G., Barry, M.F. & Bindman, L.J. (1993a). Heterosynaptic long-term depression of synaptic transmission in isolated slices of rat hippocampus can be induced postsynaptically in the presence of a $GABA_A$ receptor antagonist. *J. Physiol.* **473**, 31P.

Christofi, G., Nowicky, A.V., Bolsover, S.R. & Bindman, L.J. (1993b). The postsynaptic induction of non-associative long-term depression of excitatory synaptic transmission in rat hippocampal slices. *J. Neurophysiol.* **69**, 219-229.

Christofi, G., Nowicky, A.V. & Bindman, L.J. (1991). The postsynaptic induction of long-term depression (LTD) of synaptic transmission in isolated rat hippocampal slices requires extracellular calcium. *J. Physiol.* **438**, 257P.

Collingridge, G.L., Kehl, S.J. & McLennan, H. (1983). Excitatory amino acids in synaptic transmission in the Schaffer collateral-commissural pathway of the rat hippocampus. *J. Physiol.* **334**, 33-46.

Cormier, R.J., Mauk, M.D. & Kelly, P.T. (1993). Glutamate iontophoresis induces long-term potentiation in the absence of evoked presynaptic activity. *Neuron* **10**, 907-919.

Coussens, C.M. & Teyler, T.J. (1993). Dendritic localization of LTP and LTD. *Soc. Neurosci. Abs.* **19**, A547.17.

Cummings, J.A., Mulkey, R.M., Nicoll, R.A. & Malenka, R.C. (1996). Ca^{2+} signaling requirements for long-term depression in the hippocampus. *Neuron* **16**, 825-833.

Davies, S.N., Lester, R.A.J., Reymann, K.G. & Collingridge, G.L. (1989). Temporally distinct pre-and postsynaptic mechanisms maintain long-term potentiation. *Nature* **388**, 500-503.

Davies, C.H., Starkey, S.J., Pozza, M.F. & Collingridge, G.L. (1991). $GABA_B$ autoreceptors regulate the induction of LTP. *Nature* **349**, 609-611.

Debanne, D., Gähwiler B.H. & Thompson, S.M. (1994). Asynchronous pre- and postsynaptic activity induces associative long-term depression in area CA1 of the rat hippocampus *in vitro*. *Proc. Natl. Acad. Sci.* **91**, 1148-1152.

Debanne, D., & Thompson, S.M. (1996). Associative long-term depression in the hippocampus *in vitro*. *Hippocampus* **6**, 9-16.

Denny, J.B., Polan-Curtain, J., Rodriguez S., Wayner, M.J. & Armstrong, D.L. (1990). Evidence that protein kinase M does not maintain long-term potentiation. *Brain Res.* **534**, 201-208.

Diamond, D.M., Dunwiddie, T.V. & Rose, G.M. (1988). Characteristics of hippocampal primed burst potentiation *in vitro* and in the awake rat. *J. Neurosci.* **8**, 4079-4088.

Dodge, F.A. & Rahamimoff, R. (1967). Co-operative action of calcium ions in transmitter release at the neuromuscular junction. *J. Physiol.* **193**, 419-432.

Dolphin, A.C., Errington, M.L. & Bliss, T.V.P. (1982). Long-term potentiation of the perforant path *in vivo* is associated with increased glutanate release. *Nature* **297**, 496-498.

Drapeau, C., Pellerin, L., Wolfe, L.S. & Avoli, M. (1990). Long-term changes in synaptic transmission induced by arachidonic acid in the CA1 subfield of the rat hippocampus. *Neurosci. Lett.* **115**, 286-292.

Dreyer, F. (1990). Peptide toxins and potassium channels.
Rev. Physiol. Biochem. Pharmacol. **115**, 93-136.

Dudai, Y. (1989). *The Neurobiology of Memory.* Oxford. Oxford University Press. 254-257.

Dudek, S.M. & Bear, M.F. (1992). Homosynaptic long-term depression in area CA1 of hippocampus and effects of *N*-methyl-D-aspartate receptor blockade.
Proc. Natl. Acad. Sci. **89**, 4363-4367.

Dudek, S.M. & Bear, M.F. (1993). Bidirectional long-term modifications of synaptic effectiveness in the adult and immature hippocampus. *J. Neurosci.* **13**, 2910-2918.

Dunwiddie, T.V. & Lynch, G. (1978). Long-term potentiation and depression of synaptic responses in the rat hippocampus: Localization and frequency dependency.
J. Physiol. **276**, 353-367.

Dutar, P. & Nicoll, R.A. (1988). A physiological role for $GABA_B$ receptors in the central nervous system. *Nature* **332**, 156-158.

Edwards, F.A. (1995). LTP - a structural model to explain the inconsistencies. *Trends Neurosci.* **18**, 250-255.

Edwards, F.A., Konnerth, A., Sakmann, B. & Takahashi, T. (1989). A thin slice preparation for patch clamp recordings from neurones of the mammalian central nervous system. *Pflügers Arch.* **414**, 600-612.

Errington, M.L., Bliss, T.V.P., Richter-Levin, G., Yenk, K., Doyère, V. & Laroche, S. (1995). Stimulation at 1-5 Hz does not produce long-term depression or depotentiation in the hippocampus of adult rat *in vivo*. *J. Neurophysiol.* **74**, 1793-1799.

Foster, T.C. & McNaughton, B.L. (1991). Long-term enhancement of CA1 synaptic transmission is due to increased quantal size, not quantal content. *Hippocampus* **1**,79-91.

Frégnac, Y. (1991). *Long-Term Potentiation: A Debate of Current Issues.* Baudry, M. & Davies, J.L. Editors. Cambridge, Mass. M.I.T. Press. 425-435.

Fujii, S., Saito, K., Miyakawa, H., Ito, K. & Kato, H. (1991). Reversal of long-term potentiation (depotentiation) induced by tetanus stimulation of the input to CA1 neurons of guinea pig hippocampal slices. *Brain Res.* **555**, 112-122.

Fukunaga, K., Stoppini, L., Miyamoto, E. & Muller, D. (1993). Long-term potentiation is associated with an increased activity of Ca^{2+}/calmodulin-dependent protein kinase II. *J. Biol. Chem.* **268**, 7863-7867.

Garthwaite, J., Charles, S.L. & Chess-Williams, R. (1988). Endothelium-derived relaxing factor release on activation of NMDA receptors suggests role as intercellular messenger in the brain. *Nature* **336**, 385-388.

Gribkoff, V.K. & Lum-Ragan, J.T. (1992). Evidence for nitric oxide synthase inhibitor-sensitive and insensitive hippocampal synaptic potentiation. *J. Neurophysiol.* **68**, 639-642.

Greengard, P., Jen, J., Nairn, A.C. & Stevens, C.F. (1991). Enhancement of the glutamate response by c-AMP-dependent protein kinase in hippocampal neurones. *Science* **253**, 1135-1138.

Grover, L.M., Lambert, N.A., Schwartzkroin, P.A. & Teyler, T.J. (1993). Role of HCO_3^- ions in depolarizing $GABA_A$ receptor-mediated responses in pyramidal cells of rat hippocampus. *J. Neurophysiol.* **69**, 1541-1555.

Grover, L.M. & Teyler, T.J. (1990). Two components of LTP induced by different patterns of afferent activation. *Nature* **347**, 477-479.

Grover, L.M. & Teyler, T.J. (1992). *N*-methyl-D-aspartate receptor-independent long-term potentiation in area CA1 of rat hippocampus: Input specific induction and preclusion in a non-tetanized pathway. *Neurosci.* **49**, 7-11.

Grynkiewicz, G., Poenie, M. & Tsien, R.Y. (1985). A new generation of Ca^{2+} indicators with greatly improved fluorescence properties. *J. Biol. Chem.* **260**, 3440-3450.

Gu, J.G., Albuquerque, C., Lee, C.J. & MacDermott, A.B. (1996). Synaptic strengthening through activation of Ca^{2+}-permeable AMPA receptors. *Nature* **381**, 793-796.

Gustafsson, B., Wigström, H., Abraham, W.C. & Huang, Y.-Y. (1987). Long-term potentiation in the hippocampus using depolarizing current pulses as the conditioning stimulus to single volley action potentials. *J. Neurosci.* **7**, 774-780.

Haley, J.E., Wilcox, G.L. & Chapman, P.F. (1992). The role of nitric oxide in hippocampal long-term potentiation. *Neuron* **8**, 211-216.

Halpain, S. & Greengard, P. (1990). Activation of NMDA receptors induces rapid dephosphorylation of the cytoskeletal protein MAP2. *Neuron* **5**, 237-246.

Hawkins, R.D., Zhuo, M. & Arancio, O. (1994). Nitric oxide and carbon monoxide as possible retrograde messengers in hippocampal long-term potentiation. *J. Neurobiol.* **25**, 652-665.

Hebb, D.O. (1949). *The Organization of Behaviour.* New York. Wiley

Hestrin, S., Nicoll, R.A., Perkel, D.J. & Sah, P. (1990). Analysis of excitatory synaptic action in pyramidal cells using whole-cell recording from rat hippocampal slices. *J. Physiol.* **422**, 203-225.

Hille, B. (1992). *Ionic Channels of Excitable Membranes*, Second Edition. Sunderland, Massachusetts. Sinauer Associates. 445-471.

Hirsch, J.C. & Crepel, F. (1991). Blockade of NMDA receptors unmasks a long-term depression in synaptic efficacy in rat prefrontal neurons *in vitro*. *Exp. Brain Res.* **85**, 621-624.

Hotson, J.R. & Prince, D.A. (1980). A calcium-activated hyperpolarization follows repetitive firing in hippocampal neurons. *J. Neurophysiol.* **43**, 409-419.

Hotson, J.R., Prince, D.A. & Schwartzkroin, P.A. (1979). Anomalous inward rectification in hippocampal neurons. *J. Neurophysiol.* **42**, 889-895.

Huang, Y.-Y., Colino, A., Selig, D.K. & Malenka, R.C. (1992). The influence of proir synaptic activation on the induction of long-term potentiation. *Science* **255**, 730-733.

Huang, Y.-Y. & Malenka, R.C. (1993). Examination of TEA-induced synaptic enhancement in area CA1 of the hippocampus: The role of voltage-dependent Ca^{2+} channels in the induction of LTP. *J. Neurosci.* **13**, 568-576.

Huber, K.M., Mauk, M.D. & Kelly, P.T. (1995). Distinct LTP induction mechanisms: Contribution of NMDA receptors and voltage-dependent calcium channels. *J. Neurophysiol.* **73**, 270-279.

Isaac, J.T.R., Nicoll, R.A. & Malenka, R.C. (1995). Evidence for silent synapses: Implications for the expression of LTP. *Neuron* **15**, 427-434.

Ito, M., Sakurai, M. & Tongroach, P. (1982). Climbing fibre induced depression of both mossy fibre responsiveness and glutamate sensitivity of cerebellar Purkinje cells. *J. Physiol.* **324**, 113-134.

Izumi, I. & Zorumski, C.F. (1993). Nitric oxide and long-term synaptic depression in the rat hippocampus. *NeuroReport* **4**, 1131-1134.

Jaffe, D.B., Johnston, D., Lasser-Ross, N., Lisman, J.E., Miyakawa, H. & Ross, W.N. (1992). The spread of Na^+ spikes determines the pattern of dendritic Ca^{2+} entry into hippocampal neurons. *Nature* **357**, 244-246.

Jahr, C.E. & Stevens, C.F. (1987). Glutamate activates multiple single channel conductances in hippompal neurones. *Nature* **325**, 522-525.

Johnston, D., Williams, D., Jaffe, R. & Gray, R. (1992). NMDA-receptor independent long-term potentiation. *Ann. Rev. Physiol.* **54**, 489-505.

Kato, N. (1993). Dependence of long-term depression on postsynaptic glutamate receptors in visual cortex. *Proc. Natl. Acad. Sci.* **90**, 3650-3654.

Kato, K., Clark, G.D., Bazan, N.G. & Zorumski, C.F. (1994). Platelet-activating factor as potential retrograde messenger in CA1 hippocampal long-term potentiation. *Nature* **367**, 175-179.

Kato, K. & Zorumski, C.F. (1993). Nitric oxide inhibitors facilitate the induction of hippocampal long-term potentiation by modulating NMDA responses. *J. Neurophysiol.* **70**, 1260-1263.

Kauer, J.A., Malenka, R.C. & Nicoll, R.A. (1988). A persistent postsynaptic modification mediates long-term potentiation in the hippocampus. *Neuron* **1**, 911-917.

Kelso, S.R., Ganong, A.H. & Brown, T.H. (1986). Hebbian synapses in the hippocampus. *Proc. Natl. Acad. Sci.* **83**, 5326-5331.

Kerr, D.S. & Abraham, W.C. (1993). Comparison of associative and non-associative conditioning procedures in the induction of LTD in the CA1 of the hippocampus. *Synapse* **14**, 305-313.

Konorski, J. (1948). *Conditioned Reflexes and Neuron Organization.* London: Cambridge University Press.

Koyano, K., Kuba, K. & Minota, S. (1985). Long-term potentiation of transmitter release induced by repetitive presynaptic activities in bull-frog sympathetic ganglia. *J. Physiol.* **359**, 219-233.

Krug, M., Müller-Welde, P., Wagner, M., Ott, T. & Matthies, H. (1995). Functional plasticity in two afferent systems of the granule cells in the rat dentate area: Frequency-related changes, long-term potentiation and heterosynaptic depression. *Brain Res.* **360**, 264-272.

Kuhnt, U., Kleschevnikov, A.M. & Voronin, L.L. (1994). Long-term enhancement of synaptic transmission in the hippocampus after tetanization of single neurones by short intracellular current pulses. *Neurosci. Res. Comm.* **14**, 115-123.

Kullmann, D.M., Erdemli, G. & Asztély, F. (1996). LTP of AMPA and NMDA receptor-mediated signals: Evidence for presynaptic expression and extrasynaptic glutamate spill-over. *Neuron* **17**, 461-474.

Kullmann, D.M. & Nicoll, R.A. (1992). Long-term potentiation is associated with increases in quantal content and quantal amplitude. *Nature* **357**, 240-244.

Kullmann, D.M., Perkel, D.J., Manabe, T. & Nicoll, R.A. (1992). Ca^{2+} entry via postsynaptic voltage-sensitive Ca^{2+} channels can transiently potentiate excitatory synaptic transmission in the hippocampus. *Neuron* **9**, 1175-1183.

Lacaille, J.-C., Mueller, A.L., Kunkel, D.D. & Schwartzkroin, P.A. (1987). Local circuit interactions between oriens/alveus interneurons and CA1 pyramidal cells in hippocampal slices: Electrophysiology and morphology. *J. Neurosci.* 7, 1979-1993.

Lancaster, B. & Nicoll, R.A. (1987). Properties of two calcium-activated hyperpolarizations in rat hippocampal neurons. *J. Physiol.* **389**, 187-203.

Langmoen, I.A., Andersen, P., Gjerstad, L., Laursen, A.M. & Ganes, T. (1978). Two separate effects of GABA on hippocampal pyramidal cells *in vitro*. *Acta. Physiol. Scand.* **102**, 28A-29A.

Larkman, A., Hannay, T., Stratford, K. & Jack, J. (1992). Presynaptic release probability influences the locus of long-term potentiation. *Nature* **360**, 70-73.

Larson, J. & Lynch, G. (1986). Induction of synaptic potentiation in hippocampus by patterned stimulation involves two events. *Science* **232**, 985-988.

Larson, J. & Lynch, G. (1988). Role of *N*-methyl-D-aspartate receptors in the induction of synaptic potentiation by burst stimulation patterned after the hippocampal theta rhythm. *Brain Res.* **441**, 111-118.

Larson, J., Wong, D. & Lynch, G. (1986). Patterned stimulation at the theta frequency is optimal for the induction of hippocampal long-term potentiation. *Brain Res.* **368**, 347-350.

Leschinger, A., Stabel, J., Igelmund, P. & Heinemann, U. (1993). Pharmacological and electrographic properties of epileptiform activity induced by elevated K^+ and lowered Ca^{2+} and Mg^{2+} concentration in rat hippocampal slices. *Exp. Brain Res.* **96**, 230-240.

Lev-Ram, V., Makings, L.R., Keitz, P.F., Kao, J.P.Y. & Tsien, R.Y. (1995). Long-term depression in cerebellar purkinke neurons results from coincidence of nitric oxide and depolarization-induced Ca^{2+} transients. *Neuron* **15**, 407-415.

Levy, W.B. & Steward, O. (1979). Synapsesas associative memory elements in the hippocampal formation. *Brain Res.* **175**, 233-245.

Levy, W.B. & Steward, O. (1983). Temporal contiguity requirements for long-term associative potentiation/depression in the hippocampus. *Neurosci.* **8**, 791-797.

Liao, D.L., Hessler, N.A. & Malinow, R. (1995). Activation of postsynaptically silent synapses during pairing-induced LTP in CA1 region of the hippocampal slice. *Nature* **375**, 400-404.

Linden, D.J. (1994). Long-term synaptic depression in the mammalian brain. *Neuron* **12**, 457-472.

Linden, D.J. & Connor, J.A. (1995). Long-term synaptic depression. *Annu. Rev. Neurosci.* **18**, 319-357.

Lisman, J. (1989). A mechanism for the Hebb and the anti-Hebb processes underlying learning and memory. *Proc. Natl. Acad. Sci.* **86**, 9574-9578.

Lisman, J. (1994). The CaM kinase II hypothesis for the storage of synaptic memory. *Trends Neurosci.* **17**, 406-412.

Lu-Yang, W., Salter, M.W. & MacDonald, J.F. (1991). Regulation of kainate receptors by cAMP-dependent protein kinase and phosphatases. *Science* **253**, 1132-1135.

Lynch, G., Dunwiddie, T.V. & Gribkoff, V.K. (1977). Heterosynaptic depression: A postsynaptic correlate of long-term potentiation. *Nature* **266**, 737-739.

Lynch, G., Larson, J., Kelso, S., Barrionuevo, G. & Schottler, F. (1983). Intracellular injections of EGTA block induction of hippocampal long-term potentiation. *Nature* **305**, 719-721.

Lynch, M.A., Errington, M.L. & Bliss, T.V.P. (1989). Nordihydroguaiaretic acid blocks the synaptic component of long-term potentiation and the associated increases in release of glutamate and arachidonate: An *in vivo* study in the dentate gyrus of the rat. *Neuroscience* **30**, 693-701.

MacDermott, A.B., Mayer, M.L., Westbrook, G.L., Smith, S.J. & Barker, J. (1986). NMDA receptor activation increases cytoplasmic calcium concentration in cultured spinal cord neurones. *Nature* **321**, 519-522.

Malenka, R.C. (1993). Long-term depression: Not so depressing after all. *Proc. Natl. Acad. Sci.* **90**, 3121-3123.

Malenka, R.C., Kauer, J.A., Perkel, D.J., Mauk, M.D., Kelly, P.T., Nicoll, R.A. & Waxham, M.N. (1989). An essential role for postsynaptic calmodulin and protein kinase activity in long-term potentiation. *Nature* **340**, 554-557.

Malenka, R.C., Kauer, J.A., Zucker, R.S. & Nicoll, R.A. (1988). Postsynaptic calcium is sufficient for potentiation of hippocampal synaptic transmission. *Science* **242**, 81-84.

Malenka, R.C., Madison, D.V. & Nicoll, R.A. (1986a). Potentiation of synaptic transmission in the hippocampus by phorbol esters. *Nature* **321**, 175-177.

Malenka R.C., Madison, D.V., Andrade, R. & Nicoll, R.A. (1986b) Phorbol esters mimic some cholinergic actions in hippocampal pyramidal neurons. *J. Neurosci.* **6**, 475-480.

Malenka, R.C. & Nicoll, R.A. (1993). NMDA-receptor-dependent synaptic plasticity: Multiple forms and mechanisms. *Trends Neurosci.* **16**, 521-527.

Malinow, R., Otmakhov, N., Blum, K.I. & Lisman, J. (1994). Visualizing hippocampal synaptic function by optical detection of Ca^{2+} entry through the *N*-methyl-D-aspartate channel. *Proc. Natl. Acad. Sci.* **91**, 8170-8174.

Manabe, T., Wyllie, D.J.A., Perkel, D.J. & Nicoll, R.A. (1993). Modulation of synaptic transmission and long-term potentiation: Effects on paired pulse facilitation and EPSC variance in the CA1 region of the hippocampus. *J. Neurophysiol.* **70**, 1451-1459.

Manzoni, O.J., Weisskopf, M.G. & Nicoll, R.A. (1994). MCPG antagonizes metabotropic glutamate receptors but not long-term potentiation in the hippocampus. *Eur. J. Neurosci.* **6**, 1050-1054.

Markram, H., Helm, P.J. & Sakmann, B. (1995). Dendritic calcium transients evoked by single back-propagating action potentials in rat neocortical pyramidal neurons. *J. Physiol.* **485**, 1-20.

Mayer, M.L. & Westbrook, G.L. (1987). Permeation and block of *N*-mehyl-D-aspartic acid receptor channels by divalent cations in mouse cultured central neurons. *J. Physiol.* **394**, 501-527.

McGlade-McCulloch, E., Yamamoto, H, Soon-Eng, T., Brickey, D.A. & Soderling, T.R. (1993). Phosphorylation and regulation of glutamate receptors by calcium/calmodulin-dependent protein kinase II. *Nature* **362**, 640-642.

McGuinness, N., Anwyl, R. & Rowan, M. (1991). Trans-ACPD enhances long-term potentiation in the hippocampus. *Eur. J. Pharmacol.* **197**, 231-232.

McNaughton, B.L., Douglas, R.M. & Goddard, G.V. (1978). Synaptic enhancement in fascia dentata: Cooperativity among coactive afferents. *Brain Res.* **157**, 277-293.

Melchers, B.P.C., Pennartz, C.M.A., Wadman, W.J. & Lopes da Silva, F.H. (1988). Quantitative correlation between tetanus-induced decreases in extracellular calcium and LTP. *Brain Res.* **454**, 1-10.

Mintz, I.M., Sabatini, B.L. & Regehr, W.G. (1995). Calcium control of transmitter release at a cerebellar synapse. *Neuron* **15**, 675-688.

Miyakawa, H., Ross, W.N., Jaffe, D., Callaway, J.C., Lasser-Ross, N., Lisman, J.E. & Johnston, D. (1992). Synaptically activated increases in Ca^{2+} concentration in hippocampal CA1 pyramidal cells are primarily due to voltage-gated Ca^{2+} channels. *Neuron* **9**, 1163-1173.

Moncada, S., Palmer, R.M.J. & Higgs, E.A. (1991). Nitric oxide: Physiology, pathophysiology and pharmacology. *Pharmacol. Rev.* **43**, 109-142.

Mott, D.D. & Lewis, D.V. (1991). Facilitation of the induction of long-term potentiation by $GABA_B$ receptors. *Science* **252**, 1718-1720.

Mulkey, R.M., Endo, S., Shenolikar, S. & Malenka, R.C. (1994). Involvement of a calcineurin/inhibitor-1 phosphatase cascade in hippocampal long-term depression. *Nature* **369**, 486-488.

Mulkey, R.M., Herron, C.E. & Malenka, R.C. (1993). An essential role for protein phosphatases in hippocampal long-term depression. *Science* **261**, 1051-1055.

Mulkey, R.M. & Malenka, R.C. (1992). Mechanisms underlying induction of homosynaptic long-term depression in area CA1 of the hippocampus. *Neuron* **9**, 967-975.

Müller, W. & Connor, J.A. (1991). Dendritic spines as individual neuronal compartments for synaptic Ca^{2+} responses. *Nature* **354**, 73-76.

Muller, D., Buchs, P.-A., Stoppini, L. & Boddeke, H. (1992) Long-term potentiation, protein kinase C, and glutamate receptors. *Molecular Neurobiol.* **5**, 277-288.

Muller, D., Hefft, S. & Figurov, A. (1995). Heterosynaptic interactions between LTP and LTD in CA1 hippocampal slices. *Neuron* **14**, 599-605.

Muller, D. & Lynch, G. (1988). Long-term potentiation differentially affects two components of synaptic responses in hippocampus. *Proc. Natl. Acad. Sci.* **85**, 9346-9350.

Neuman, R.S., Ben-Ari, Y., Gho, M. & Cherubini, E. (1988). Blockade of excitatory synaptic transmission by 6-cyano-7-nitroquinoxaline-2,3-dione (CNQX) in the hippocampus *in vitro*. *Neurosci. Lett.* **92**, 64-68.

Neveu, D. & Zucker, R.S. (1996). Long-lasting potentiation and depression without presynaptic activity. *J. Neurophysiol.* **75**, 2157-2160.

Newberry, N.R. & Nicoll, R.A. (1984). Bicuculline-resistant inhibitory postsynaptic potential in rat hippocampal pyramidal cells *in vitro*. *J. Physiol.* **348**, 239-254.

Newberry, N.R. & Nicoll, R.A. (1985). Comparison of the action of baclofen with γ-aminobutyric acid on rat hippocampal pyramidal cells *in vitro*. *J. Physiol.* **360**, 161-185.

Nicoll, R.A. & Malenka, R.C. (1995). Contrasting properties of two forms of long-term potentiation in the hippocampus. *Nature* **377**, 115-118.

Nowak, L., Bregestovski, P., Ascher, P., Hebert, A. & Prochiantz, A. (1984). Magnesium gates glutamate-activated channels in mouse central neurons. *Nature* **307**, 462-465.

Nuñez, A. & Buño, W. (1992). Intracellular effects of QX-314 and Cs^{+} in hippocampal neurons *in vivo*. *Exp. Neurol.* **115**, 266-270.

O'Connor. J.J., Rowan, M.J. & Anwyl, R. (1994). Long-asting enhancement of NMDA receptor-mediated synaptic transmission by metabotropic glutamate receptor activation. *Nature* **367**, 557-559.

O'Dell, T.J., Kandel, E.R. & Grant, S.G.N. (1991a). Long-term potentiation in the hippocampus is blocked by tyrosine kinase inhibitors. *Nature* **353**, 558-560.

O'Dell, T.J., Hawkins, R.D., Kandel, E.R. & Arancio, O. (1991b). Tests of the roles of two diffusable substances in long-term potentiation: Evidence for nitric oxide as a possible early retrograde messenger. *Proc. Natl. Acad. Sci.* **88**, 11285-11289.

O'Dell, T.J. & Kandel, E.R. (1994). Low-frequency stimulation erases LTP through an NMDA receptor-mediated activation of protein phosphatases. *Learn. Mem.* **1**, 129-139.

Oliver, M.W., Baudry, M. & Lynch, G. (1989). The protease inhibitor leupeptin interferes with the development of LTP in hippocampal slices. *Brain Res.* **505**,233-238.

O'Mara, S.M., Rowan, M.J. & Anwyl, R. (1995). Metabotropic glutamate receptor-induced homosynaptic long-term depression and depotentiation in the dentate gyrus of the rat hippocampus *in vitro*. *Neuropharmacology* **34**, 983-989.

Otani, S. & Ben-Ari, Y. (1991). Metabotropic receptor-mediated long-term potentiation in rat hippocampal slices. *Eur. J. Pharmacol.* **205**, 325-326.

Otto, T., Eichenbaum, H., Weiner, S.I. & Wilbe, C (1991). Learning related patterns of CA1 spike trains parallel stimulation parametersoptimal for inducing hippocampal long-term potentiation. *Hippocampus* **1**, 181-192.

Paulsen, O., Li, Y.-G., Hvalby, Ø., Andersen. P. & Bliss, T.V.P. (1993). Failure to induce long-term depression by an anti-correlation procedure in area CA1 of the rat hippocampal slice. *Eur. J. Neurosci.* **5**, 1241-1246.

Perkel, D.J., Petrozzino, J.J., Nicoll, R.A. & Connor, J.A. (1993). The role of Ca^{2+} entry via synaptically activated NMDA receptors in the induction of long-term potentiation. *Neuron* **11**, 817-823.

Petrozzino, J.J. & Connor, J.A. (1994). Dendritic Ca^{2+} accumulations and metabotropic glutamate receptor activation associated with an *N*-methyl-D-aspartate receptor-independent long-term potentiation in hippocampal CA1 neurons. *Hippocampus* **4**, 546-558.

Pockett, S., Brookes, N.H. & Bindman, L.J. (1990). Long-term depression at synapses in slices of rat hippocampus can be induced by bursts of postsynaptic activity. *Exp. Brain Res.* **80**, 196-200.

Pockett, S. & Lippold, OC.J. (1986). Long-term potentiation and depression in hippocampal slices. *Exp. Neurol.* **91**, 481-487.

Ranck Jr., J.B. (1973). Studies on single neurons in dorsal hippocampus formation and septum in unrestrained rats I. Behavioural correlates and firing repertoires. *Exp. Neurol.* **41**, 461-531.

Regehr, W.G. & Tank, D.W. (1990). Postsynaptic NMDA receptor-mediated calcium accumulation in hippocampal CA1 pyramidal cell dendrites. *Nature* **345**, 807-810.

Regehr, W.G. & Tank, D.W. (1992). Calcium concentration dynamics produced by synaptic activation of CA1 hippocampal pyramidal cells. *J. Neurosci.* **12**, 4202-4223.

Sah, P., Hestrin, S. & Nicoll, R.A. (1989). Tonic activation of NMDA receptors by ambient glutamate enhances excitability of neurons. *Science* **246**, 815-818.

Sastry, B.R., Chirwa, S.S., Goh, J.W., Maretic, H. & Pandanaboina, M.M. (1984). Verapamil counteracts depression but not long-lasting potentiation of the hippocampal population spike. *Life Sci.* **34**, 1075-1086.

Scanziani, M., Malenka, R.C. & Nicoll, R.A. (1996). Role of intercellular interactions in heterosynaptic long-term depression. *Nature* **380**, 446-450.

Schaer, H. (1974). Decrease in ionized calcium by bicarbonate in physiological solutions. *Pflügers Arch.* **347**, 249-254.

Schneggenburger, R., Zhou, Z., Konnerth, A. & Neher, E. (1993). Fractional contribution of calcium to the cation current through glutamate receptor channels. *Neuron* **11**, 133-143.

Schulz, P.E., Cook, E.P. & Johnston, D. (1994). Changes in paired-pulse facilitation suggest presynaptic involvement in long-term potentiation. *J. Neurosci.* **14**, 5325-5337.

Schuman, E.M. & Madison, D.V. (1991). A requirement for the intercellular messenger nitric oxide in long-term potentiation. *Science* **254**, 1503-1506.

Schuman, E.M. & Madison, D.V. (1994). Locally distributed synaptic potentiation in the hippocampus. *Science* **263**, 532-536.

Schwartzkroin, P.A. & Wester, K. (1975). Long-lasting facilitation of a synaptic potential following tetanization in the *in vitro* hippocampal slice. *Brain Res.* **89**, 107-119.

Sejnowski, T.J. (1977). Strong covariance with non-linearity interacting neurones. *J. Math. Biol.* **4**, 303-321.

Selig, D.K., Hjelmstad, G.O., Herron, C, Nicoll, R.A. & Malenka, R.C. (1995a). Independent mechanisms for long-term depression of AMPA and NMDA responses. *Neuron* **15**, 417-426.

Selig, D.K., Lee, H.-K., Bear, M.F. & Malenka, R.C. (1995b). Reexamination of the effects of MCPG on hippocampal LTP, LTD and depotentiation. *J. Neurophsiol.* **74**, 1075-1082.

Silva, A.J., Stevens, C.F., Tonegawa, S. & Wang, W. (1992a). Deficient hippocampal long-term potentiation in α-calcium-calmodulin kinase II mutant mice. *Science* **257**, 201-206.

Silva, A.J., Paylor, R., Wehner, J.M. & Tonegawa, S. (1992b). Impaired spatial learning in α-calcium-calmodulin kinase II mutant mice. *Science* **257**. 206-211.

Silver, R.A., Whitaker, M. & Bolsover, S.R. (1992). Intracellular ion imaging using fluorescent dyes: Artefacts and limits to resolution. *Pflügers Arch.* **420**, 565-602.

Skrede, K.K. & Malthe-Sorenssen, D. (1981). Increased resting and evoked release of transmitter following repetitive electrical tetanization in hippocampus: A biochemical correlate to long-lasting synaptic potentiation. *Brain Res.* **208**, 436-441.

Skrede, K.K. & Westgaard, R.H. (1971). The transverse hippocampal slice: A well-defined cortical structure maintained *in vitro*. *Brain Res.* **35**, 589-593.

Soltesz, I., Haby, M., Leresche, N. & Crunelli, V. (1988). The $GABA_B$ antagonist phaclofen inhibits the late K^+-dependent IPSP in cat and rat thalamicand hippocampal neurons. *Brain Res.* **448**, 351-354.

Spruston, N., Jaffe, D.B. & Johnston, D. (1994). Dendritic attenuation of synaptic potentials and currents: The role of passive membrane properties. *Trends Neurosci.* **17**, 161-166.

Spruston, N., Schiller, Y., Stuart, G. & Sakmann, B. (1995). Activity-dependent action potential invasion and calcium influx intohippocampal CA1 dendrites. *Science* **268**, 297-300.

Stanton, P.K. (1996). LTD, LTP and the sliding threshold for long-term synaptic plasticity. *Hippocampus* **6**, 35-42.

Stanton, P.K. & Sejnowski, T.J. (1989). Associative long-term depression in the hippocampus induced by hebbian covariance. *Nature* **339**, 215-218.

Staubli, U. & Chun, D. (1996). Factors regulating the reversibility of long-term potentiation. *J. Neurosci.* **16**, 853-860.

Staubli, U. & Lynch, G. (1987). Stable hippocampal long-term potentiation elicited by 'theta' pattern stinulation. *Brain Res.* **435**, 227-234.

Staubli, U. & Lynch, G. (1990). Stable depression of potentiated synaptic responses in the hippocampus with 1-5 Hz stimulation. *Brain Res.* **513**, 113-118.

Storm, J.F. (1987). Action potential repolarization and a fast afterhyperpolarization in rat hippocampal pyramidal cells. *J. Physiol.* **385**, 733-759.

Swope, S.L., Moss, S.J., Blackstone, C.D. & Huganir, R.L. (1992). Phosphorylation of ligand-gated ion channels: A possible mode of synaptic plasticity. *FASEB J.* **6**, 2514-2523.

Tanzi, E. (1893). I fatti e le induzioni nell'ordierna istologia del sistema nervosa. *Riv. Sper. Freniatr. Med. Leg. Alienazioni Ment.* **19**, 419-472.

Teyler, T.J., Cavus, I., Coussens, C., DiScenna, P., Grover, L., Lee, Y.P. & Little, Z. (1994). The multideterminant role of calcium in hippocampal synaptic plasticity. *Hippocampus* **4**, 623-634.

Tomasulo, R.A., Ramirez, J.J. & Steward, O. (1993). Synaptic inhibition regulates associative interactions between afferents during the induction of long-term potentiation and depression. *Proc. Natl. Acad. Sci.* **90**, 11578-11582.

Vanderwolf, C.H. (1969). Hippocampal electrical activity and voluntary movement in the rat. *Electroencephalogr. Clin. Neurophysiol.* **26**, 407-418.

Vickery, R.M. & Bindman, L.J. (1997). Long-lasting decreases of AMPA responses following postsynaptic activity in single hippocampal neurons. *Synapse* **25**, 103-106.

Volgushev, M., Voronin, L.L., Chistiakova, M. & Singer, W. (1994). Induction of LTP and LTD in visual cortex neurones by intracellular tetanization. *NeuroReport* **5**, 2069-2072.

Voronin, L.L. (1983). Long-term potentiation in the hippocampus. *Neuroscience* **10**,1051-1069.

Wagner, J.J. & Alger, B.E. (1995). GABAergic and developmental influences on homosynaptic LTD and depotentiation in rat hippocampus. *J. Neurosci.* **15**, 1577-1586.

Wagner, J.J. & Alger, B.E. (1996). Homosynaptic LTD and depotentiation: Do they differ in name only? *Hippocampus* **6**, 24-29.

Walter, E.T. & Byrne, J.H. (1985). Long-term enhancement produced by activity-dependent modulation of Aplysia sensory neurons. *J. Neurosci.* 7, 1411-1416.

Wexler, E.M. & Stanton, P.K. (1993). Priming of homosynaptic long-term depression in the hippocampus by previous synaptic activity. *NeuroReport* **4**, 591-594.

Wickens, J.R. & Abraham, W.C. (1991). The involvement of L-type calcium channels in heterosynaptic long-term depression in the hippocampus. *Neurosci. Lett.* **130**, 128-132.

Williams, J.H., Errington, M.L., Lynch, M.A. & Bliss, T.V.P. (1989). Arachidonic acid induces a long-term activity-dependent enhancement of synaptic transmission in the hippocampus. *Nature* **341**, 739-742.

Wigström, H. & Gustafsson, B. (1983). Facilitated induction of hippocampal long-lasting potentiation during blockade of inhibition. *Nature* **301**, 603-604.

Xie, X., Berger, T.W. & Barrionuevo, G. (1992). Isolated NMDA receptor-mediated synaptic responses express both LTP and LTD. *J. Neurophysiol.* **67**, 1009-1013.

Yasuda, H. & Tsumoto, T. (1996). Long-term depression in rat visual cortex is associated with a lower rise of postsynaptic calcium than long-term potentiation. *Neurosci. Res.* **24**, 265-274.

Zhang, D.X. & Levy, W.B. (1993). Bicuculline permits the induction of long-term depression by heterosynaptic, translaminar conditioning in the hippocampal dentate gyrus. *Brain Res.* **613**, 309-312.

APPENDIX 1

Calculation of $[Ca^{2+}]$ using I_{380}.

Measurements of intracellular $[Ca^{2+}]$ using Fura-2 microfluorimetry employed the following basic calibration equation:

$$[Ca^{2+}] = K_d(I_{max} - I_{380})/(I_{380} - I_{min})$$ (Grynkiewicz et al., 1985).

Where I_{max} and I_{min} are the fluorescence signal (I_{380}) at zero and saturating $[Ca^{2+}]$ respectively. I_{max} being a variable could be calculated by using the resting $[Ca^{2+}]$ as measured using the ratio method and I_{min}/I_{max} which is a measurable constant for each fluorescence system:

$$I_{max} = I_{380}([Ca^{2+}] + K_d)/\{(I_{min}/I_{max})[Ca^{2+}] + K_d\}$$

Knowing I_{max}, calcium levels using during postsynaptic depolarization could then be calculated using I_{380} measurements:

$$[Ca^{2+}] = K_d(I_{max} - I_{380})/[I_{380} - (I_{max}/I_{min})I_{max}]$$ (Silver et al., 1992).